



MONASH University

Studies on Ambulance Transport related Technologies

Sewminda Kalana Samarasinghe

A thesis submitted for the degree of *Master of Engineering Science* at
Monash University in June 2019

Department of Mechanical and Aerospace Engineering

Monash University

Clayton, Australia

Copyright notice

© Sewminda Kalana Samarasinghe (2019).

I certify that I have made all reasonable efforts to secure copyright permissions for third-party content included in this thesis and have not knowingly added copyright content to my work without the owner's permission.

Abstract

In a medical emergency, the total prehospital time, correlates with the patient's survival outcome. Therefore minimising overall emergency medical services (EMS) response time is important. Prehospital time consists of three main time intervals; ambulance response time, scene time, ambulance transport time. Another time interval observed to impact overall EMS response time was, ambulance turnaround time. The objective of this thesis therefore was to present a collection of studies aiming to minimise time delays in each of these time intervals affecting EMS response time. Firstly, we identified the electrification of ambulance powertrains as a possible solution for ambulance equipment power problem, and fuel efficiency, both of which impact ambulance turnaround time. Therefore, we studied the capability of current simulation software to explore the adoption of Hybrid Electric technology for ambulances. Next, to understand delays caused during ambulance transport, we explored the impact of disrupters and traffic calming measures on ambulance travel. Simulation data obtained from VISSIM, a microscopic traffic simulation software, was used to develop analytical relations of the ambulance response to disruptions. We expect this tool to help in formulation of traffic management strategies focusing on minimising time delays in ambulance transport. For further validation, the vehicle response to a disruption, and encountering a speed bump was then experimentally evaluated. Driving behaviour of a cargo van under the given conditions, was recorded using a drone. The speed profiles obtained, showed the deceleration and acceleration features in the influence zone expected when overcoming a speed bump or experiencing a disruption. Additionally, the van response to a disruption displayed good correlation with speed profiles generated via VISSIM simulations, providing endorsement for use of VISSIM simulation data in characterisation of ambulance response. Finally, with a focus on minimising time spent at the scene by paramedics, we sought to improve the efficacy of en-route cannulation. Here, we developed and tested a system that simulates conditions during ambulance transport to train paramedics for en-route venipuncture. The developed system also has features that makes it adoptable in the training of venipuncture procedures in a clinical skills laboratory setting.

Declaration

This thesis contains no material which has been accepted for the award of any other degree or diploma at any university or equivalent institution and that, to the best of my knowledge and belief, this thesis contains no material previously published or written by another person, except where due reference is made in the text of the thesis.

Signature:

Print Name: Sewminda Kalana Samarasinghe

Date: 04/06/2019

Publications

1. McMorran, D., Samarasinghe, S. K., Muradoglu, M., Chung, D. C. K., Williams, B., Liew, O. W., & Ng, T. W. (2018). Sensor and actuator simulation training system for en-route intravenous procedure. *Sensors Actuators A Phys.* 279, 680–687.
2. Samarasinghe, S. K., Katariya, M., Chung, D. C. K., Kuan, W.S., Leong, B.S.H., An, K. Liew, O. W., & Ng, T. W. Characterizing emergency ambulance travel response to disrupters. *Proceedings of IMechE Part H: Journal of Engineering in Medicine.* Favourable 1st Review.

Acknowledgements

I would like to thank my supervisor, Associate Professor Tuck Wah Ng, for his guidance and mentoring, also my colleagues, Dwayne Chung, Mayur Katariya, Alifa Zahidi, and Darren McMorran, for their valuable help and contributions throughout the project.

Heartfelt thanks to my parents for their unconditional support, and thank you to my sister, friends and family, especially Methma Rajamuni, Manawa Herath, and Aswin Hanifa, for their emotional support. Special thanks to my uncle, Nihal Samarasinghe for sacrificing his time to help with my studies.

Contents

Copyright notice	i
Abstract	ii
Declaration	iii
Publications	iv
Acknowledgements	v
1 Introduction	1
1.1 Background	1
1.2 Objectives	2
1.3 Outline.....	3
2 Literature Review	5
2.1 Emergency Medical Services - Ambulances.....	5
2.1.1 Ambulance Response Time	5
2.1.2 Ambulance Location Problem Models.....	6
2.1.3 Emergency Vehicle Preemption control methods.....	9
2.1.4 Effects of Traffic Calming Measures on Ambulances.....	12
2.1.5 Studies on time spent by paramedics at the scene.....	15
2.1.6 Alternative Solutions for Improving Ambulance Transport Efficiency.....	16
2.2 Hybrid Electric Vehicles for Ambulance Services	18
2.2.1 Previous studies on HEV control strategies	20
2.2.2 Methodologies developed to overcome “cycle-beating” in HEV testing	23
2.2.3 Overview of the impact of ancillary loads on HEV fuel economy	25
3 Investigations of Ambulance Transport Efficiency Using Hybrid Vehicles	28
3.1 Introduction.....	28
3.2 Simulation Systems.....	28
3.2.1 MATLAB SIMULINK Model.....	28
3.2.2 ADVISOR Simulation Tool.....	31
3.3 Comparative Verification Study	35
3.3.1 Scenario.....	35
3.3.2 Specifications of HEV Powertrains	36
3.3.3 Drive Cycles.....	38
3.4 Results & Discussion	39
3.5 Conclusions.....	44

4	Characterizing emergency ambulance travel response to disrupters	45
4.1	Introduction.....	45
4.2	Background	45
4.3	Theory.....	46
4.4	Simulation Methodology.....	49
4.5	Results & Discussion	51
4.6	Conclusions.....	56
5	UAV based measurement of vehicle travel	57
5.1	Introduction.....	57
5.2	Materials and Method	58
5.3	Results and Discussion	61
5.4	Conclusions.....	65
6	Sensor and actuator simulation training system for en-route intravenous procedure	67
6.1	Background.....	67
6.2	Simulator Kinematics.....	69
6.3	Materials and Methods.....	71
6.3.1	System Development and Evaluation	71
6.3.2	System Effects on Cannulation Performance.....	74
6.4	Results & Discussion	74
6.4.1	System Operation Evaluation.....	74
6.4.2	System Effects on Cannulation Performance.....	80
6.5	Conclusions.....	82
7	Overall Conclusions	83
	Bibliography	87

1 Introduction

1.1 Background

Emergency medical service (EMS) is a comprehensive system expected to instantly respond and provide effective emergency care to the urgent medical and surgical needs of a community. In this system, ambulances are essentially the mobile wing that reaches out to the acutely sick and injured across homes and cities. Given the time-sensitive nature of the service, reliability and timeliness of the response by the ambulance crew to an emergency is of extreme significance, since any time loss could result in a fatality. Therefore understandably, ambulance response time has been one of the key performance indicators evaluated, for improvement within the emergency services sector.

Ambulance response time incidentally forms a part of total prehospital time, which is proportional to the outcome of patient survival chances. Thus, prehospital time can be divided into three main intervals; dispatch-to-scene-arrival (response interval), time spent at the scene (scene interval), and scene-to-hospital-arrival (transfer interval). Each of these prehospital time intervals however require differing approaches for minimisation, as their flexibility towards modification vary accordingly to certain degrees. Therefore, practices in each interval need to be scrutinised in order to reveal any room for improvement.

While these main intervals of prehospital time are dissected, there appears to be a further time interval relatively less examined, which occurs after the patient is transferred to hospital emergency staff, called the ambulance turnaround time. Along with time spent on paperwork, and rest for paramedics, this interval includes time taken for replenishment of consumables (as far as this study is concerned) such as refuelling, and charging electrical equipment. In addition to the time factor, current electrical equipment charging practice, which involves running ambulance engine on idle, displays a wastage of resources citing a cost factor. Therefore, in a sense of time effectiveness, and cost efficiency, an opportunity presents itself to study the use of an alternative power source in an ambulance powertrain.

1.2 Objectives

The overall objective of the following studies is to formulate novel systems and principles that will serve to improve time and cost effectiveness of emergency ambulance services. As the nature of the service dictates, the effectiveness of it is determined by the fluidity through stages of mobile emergency medical service. This study therefore first seeks to identify gaps in existing research for improvement within all intervals of prehospital and recovery (turnaround) time, and then aims to propose analytical relationships, and innovative training systems that will help minimise overall emergency ambulance services response times in each of the intervals.

The work presented in this thesis intends to realise this overall objective through a number of relevant studies. Firstly, the viability of an alternative energy source for ambulance powertrains is proposed in relation to expediting the turnaround time intervals. More specifically, the practicality and cost-effectiveness of using of hybrid electric vehicle technology is considered. This study is expected to lay a foundation for future research on electrification of ambulance powertrains. Following this, a study was made to characterise ambulance responses to disruptions caused during travel. Subsequently, a physical approach to use unmanned aerial vehicles (UAVs) to video image process and thus depict the travel of vehicles subjected to disrupters and traffic calming measures (TCMs) is explored. These findings are meant to provide an understanding on the impacts of disrupters and TCMs on ambulance response and transfer times. The mathematical tool is expected to aid in formulating future traffic management systems aimed at reducing EMS response times. Finally, a simulator training system for en-route cannulation was developed. The aim of introducing this system is to train and encourage paramedics to adopt en-route cannulation, as this change of practice would result in time savings at the scene, and thereby in overall ambulance response times.

1.3 Outline

The structure of this thesis is arranged as follows;

- Chapter 2: A review in two parts, of existing literature on mobile Emergency Medical Services (EMS) response time, where applicable, including other types of emergency vehicles; and Hybrid Electric Vehicle (HEVs) use in EMS. The review of EMS response time explores the research conducted to date on methods to minimise ambulance response times, which includes inspecting the evolution of the ambulance location problem, emergency vehicle (EV) pre-emption methods, effects of TCMs on EVs, how time is being spent by paramedics at the scene and, how time and resources are used during ambulance recovery times. The section on HEV use in EMS reviews the current literature of the incorporation of HEV technology in mobile EMS as measures to improve cost efficiency in healthcare (including time cost) and explores room for improvement within this sector.
- Chapter 3: In this chapter, ambulance transport efficiency using HEV technology is to be investigated. The electrification of ambulances is one way to reduce fuel costs while reducing emissions provided response times during ambulance recovery intervals are not compromised. Two common software used in HEV studies was used to conduct simulations for this work. Since investigating the suitability of HEV technology for ambulances pose diverse questions as opposed commercial HEVs, the capability of the two software to study these aspects was evaluated. The findings suggest mainly that the software lacks the capacity to study the ambulance equipment power problem within a HEV architecture, extensively.
- Chapter 4: This chapter attempts to characterise interrupts faced during ambulance travel. Understanding delays caused by interruptions during ambulance travel is important towards gauging their impact on ambulance transfer times. A scenario of a disruption caused during road travel is simulated on a traffic microsimulation software (VISSIM). Based on the speed time distributions, the ambulance response to this disruption is analytically characterised. This finding is expected to help in formulating future intervention methods to minimise ambulance transfer times.
- Chapter 5: This chapter describes an approach using UAVs to record vehicle travel as it is subject to disruption and traffic calming measures. Appropriate video processing schemes

are applied to reduce data noise as well as to obtain precise tracking results. The findings here help to put context to the findings in Chapter 4.

- Chapter 6: In this chapter, a system has been developed to simulate transport in a medical emergency vehicle with the intent of assisting paramedics improve their skills in en-route cannulation. Usually paramedics perform prehospital stabilisation and administer intravenous fluid to patients at the scene. This system to help adopt en-route cannulation was proposed with the intent of minimising time spent on the scene which thereby reduces overall ambulance transfer times. The demonstrated system has features that make it amenable for incorporation into a clinical skills laboratory setting.

2 Literature Review

2.1 Emergency Medical Services - Ambulances

Emergency medical services (EMS) by definition can be identified as a whole and complete system designed to respond instantly and effectively to the medical and surgical emergencies of a community with satisfactory emergency care [1]. Out of the constituents that form an EMS system, ambulance services are attributed as a vital part, in essence, an arm of the hospital emergency department reaching out to the gravely ill and injured [2]. EMS was initially developed to help injured soldiers during the time of Napoleon and has seen only a few major advancements until the 1960s [3]. However since then, especially between 1960 and 1973 in the United States, with the convergence of many medical, historical, and social forces, the EMS system developed in a more structured manner resulting in extensive public health implications today [3].

Similarly, the ambulance services have transformed over the years. In the 21st century, the developed world is now accustomed to delighting in rapid response times from ambulance services which transfers the critically ill and injured to hospital reliably, while providing skilled resuscitation and en-route care. In comparison, during the 19th century, such services weren't prevalent and the public were required to find whatever possible means to hospital [4]. The literature providing useful background on early days of ambulance services is limited [4]. However, as with any service, development is a process, and the next section will examine the history of research attempting to improve ambulance response and transfer times.

2.1.1 Ambulance Response Time

Given the intrinsic nature of the service, the importance of the response by an ambulance service to a medical emergency being reliable and timely, is heightened by the fact that the slightest delay could result in the loss of life [5]. Especially trauma, one of the main causes of death worldwide, is a time-sensitive disease and therefore the survival outcome of patients is directly affected by prehospital time [6]–[9]. As stated by Brown et al [9], total prehospital time can be divided into three sections; the response interval, scene interval, and

transport/transfer interval. Response time interval spans from the instance the emergency medical services are notified to the point of their arrival at scene of medical emergency. Scene time consists of the time spent from arrival at the scene, up to the time EMS personnel leaves for the hospital. Finally, the transport/transfer time is the time taken from leaving the scene to the arrival at hospital [9]. Each of these prehospital time intervals require a different approach of minimisation, with some intervals being more amenable to modification [9]. Various studies have been conducted to formulate measures to minimise prehospital time at each of these stages, and the following sections will explore this literature, initially with regards to minimising response time.

2.1.2 Ambulance Location Problem Models

In 2003, Brotcorne et al [10] conducted a review of the progress of ambulance location and relocation models suggested over the preceding three decades. The study states that this period, along with experiencing extraordinary growth in computer technology, saw similar development in modelling and algorithmic sophistication, in mathematical programming solver performance, and in the extensive use of computer software at many stages of decision making. With this view, it is said that therefore, the initial models suggested were formulations of unsophisticated integer linear programming, however with time, solution techniques evolved while more realistic features were progressively introduced.

One of the earliest models addressing the static ambulance/emergency service location problem was suggested by Toregas et al [11]. The focus of this study is on emergency service facility location problem, especially regarding the maximum time or distance that separates the user from their nearest service as the critical parameter. Therefore, by setting up an upper limit on the response time or distance to a given user node, the study considers determining the minimum-cost spatial arrangement of emergency service facilities that would sufficiently serve the user area. Given if the costs determined are similar for other possible facility locations, the study then formulates an equivalent integer programming problem to minimise the number of emergency service facilities needed to meet the standards set for response time or distance for all demand points.

Another of the early models attempting to solve the ambulance location problem was suggested by Church & ReVelle [12]. This study, published 3 years after the work by Toregas et al,

provides an alternative model and attempt to address issues of the latter study. It is said that the model proposed by Toregas et al could result in a scenario where for a given number of facilities, the solution for the smallest maximal service distance could end being larger than the desired distance, which would lead to the decision maker realising an insufficiency of facilities to service the total area within its distance. This could then result in the decision maker abandoning the goal of providing total coverage, and rather attempt to locate facilities in such a way that a minimum of people would lie beyond the desired service distance [12]. Therefore, the maximal covering location problem proposed by Church & ReVelle instead suggests maximising the population coverage subject to limited ambulance availability.

As stated by Brotcorne et al [10], these two approaches in their own right are sensible. The first method can be used to help establish the correct number of ambulances to cover every demand point, and the second method to help maximise the use of the limited resources available. However the main shortcoming with this approach identified by Brotcorne et al [10] is that it ignores a few facets of real-world problems, mainly the scenario of when an ambulance is dispatched, certain demand areas are not covered anymore. Nonetheless, these early studies have provided a solid basis for the improvement of all following models [10].

Following the early static models, a number of deterministic models were developed, one of which was proposed by Shilling et al [13]. This model, called the tandem equipment allocation model, was developed to handle various types of vehicles. Even though it is naturally applied to fire companies handling two kinds of equipment, it is also relatable in the context of the ambulance location problem [10]. Later, a further expanded model to this, was developed by Marianov & ReVelle [14] which could be used to identify fire stations equipped with the two types of equipment, given that each demand area is covered sufficiently by the required number of pumper and rescue ladders. In these models too however, coverage is susceptible to being insufficient when the vehicles are occupied [10]. Furthermore, in the succeeding years, there have been studies that improves on work presented by Toregas et al, that provides better coverage while limiting the number of vehicles up to a certain threshold [15], [16].

In the following years came the probabilistic models to explain the ambulance location problem [17]–[20]. One of the first of these was proposed by Daskin [17], which made the assumption that all ambulances are independent, however had the same probability, referred to as the ‘busy fraction’ of being occupied/unable to respond to a call [10]. Two more probabilistic models were suggested by ReVelle and Hogan [18] referred to as the maximum availability location

problem (MALP I & MALP II). In these models, for a given probability, the demand area covered is looked to be maximised. Between the two models, assumptions associated with the 'busy fraction' differ. The former model assumes 'busy fraction' is same for all potential location sites, while the latter relaxes on this assumption and computes an estimate of it for each demand point [18]. Next, Ball and Lin [19] improved on the model formulated by Toregas et al [11] to present a probabilistic model called Rel-P. Following this, Mandell [20] proposed a system of two-tiers which separates basic life support units and advanced support units, and describes where these units should be located.

This is the development of the ambulance location problem up to the mid-1990s. With the nature of this problem, to ensure good coverage regularly, it was required to update relocation decisions periodically, and with short notice [10]. Therefore, with the advent of more powerful computational technologies, the ambulance location problem solving at real-time with dynamic models came to the fore. One of the first of these was proposed by Gendreau et al [21]. Along with the standard constraints on coverage and site capacity, this study accounted a few practical considerations associated with the complexion of the problem; that the same vehicles cannot be redeployed successively, round trips should not be repeated between same locations sites, and long trips between initial location point and final point should be avoided. Then at every time instance a call is registered, the ambulance relocation position is solved [10].

Peleg and Pliskin [22] too studied the possibility of reducing ambulance response time through better location of ambulances. The idea was first to observe the responses by Israeli ambulances and then present model-derived strategies to improve ambulance deployment which would thereby reduce response times. Using a Geographic Information System, the authors present a simulation model that suggests EMS could be made more effective by adopting dynamic load-responsive ambulance deployment.

In 2016, Nogueira et al [23] studied the effect of reallocating ambulances with the main assumption that optimising base locations of ambulances will lead to improved system response time. The study based in Belo Horizonte, Brazil, found that while the number of ambulances and base locations did affect EMS performance, purchasing new ambulances and initiating new bases did not particularly enhance system performance. Further, in this case study, it was observed that the time between the point of notifying EMS up to the dispatch of ambulance from the hospital was too long, and if response times were to improved, this window had high potential. Furthermore, on base distribution, it was concluded that since each base had

one basic unit, the number of ambulances could be increased at one given base by decreasing the total overall activated bases without compromising performance, as a cost-effective measure.

Nevertheless, this section aimed to provide a brief history of ambulance location problem models up to the 2010s. Therefore, at a glance, the research surrounding solving the ambulance location, or the deployment problem of improving ambulance response times appears to be rich. In parallel to this, attempts to cut down on ambulance transfer times by observing the impacts caused by roadway traffic conditions have been studied. This includes models, theories, proposed on a varying range, and the next section will explore the literature in this area.

2.1.3 Emergency Vehicle Preemption control methods

In the relatively recent times, a method to reduce emergency vehicle time travel has been brought forward in the form of traffic preemption control methods [24]–[28]. Emergency vehicles, which include fire trucks, ambulances, and police cars are usually given topmost priority and hence the right-of-way in everyday traffic. In heavily congested areas especially, emergency vehicles are at risk of facing with accidents, and experience delays in reaching a scene [29]. An option of mitigating this effect is providing right-of-way to these vehicles using preemption strategy through respective traffic signal controllers [26]. Emergency vehicle preemption (EVP) implementation at signalised intersections can provide emergency vehicles with preferential signal indications, that is, a belt of green indications along their route, thereby allowing them to reach their destination much faster [26], [29].

One of the earliest instances of using EVP to reduce EV response times was suggested by Shibuya et al [24]. Against the backdrop of increased crime rates, increased occurrences of accidents, and increasing problems with growing elderly population, this study examines the introduction EVP as per the plan of the National Police Agency of Japan in its next generation traffic management system, UTMS21. The study examines one of the subsystems within UTMS21 called FAST; a fast emergency vehicle preemption system. FAST provides highest priority to emergency vehicles within its traffic control and performs searches for optimal recommended routes for EVs. It is able to manipulate the green times, adjust this offset at each intersection and then communicate optimal route to EVs through infrared beacons placed before each intersection. After conducting verification tests, Shibuya et al [24] concluded that

through two-way infrared communication, priority signal control, and route guidance, FAST is able to provide safe and efficient EV operation and has improved response times traffic accidents and police incidents.

Following this, in 2003, Kwon et al [25] presented a real-time route-based dynamic EVP method. Using emergency vehicle data sampled from an existing network, the proposed strategy had been evaluated on the microscopic simulation software, VISSIM. Along the optimal route, this model preempts traffic signals at each intersection sequentially, which thereby would clear the traffic queue allowing the approaching EV to pass through. The authors state that the findings show with pre-determined emergency routes there was a substantial reduction in EV travel time especially in cases with relatively longer and/or complicated routes in relation to the prevalent intersection-by-intersection preemption method at the time.

Wang et al [27] too explored the EVP problem, and this was in the form of establishing an EV travel time estimation model with preemption control conditions. The study was developed over three levels of preemption control; path preemption, intersection preemption, and section pre-emption (Fig. 2-1). Based on these preemption control strategies, the authors claim to have built an accurate travel time estimation model validated over sufficient field experiment data. Additionally, a separate study conducted by Wang (1) et al [28], demonstrated the use of advanced wireless communication technology, called Cooperative Vehicle-Infrastructure System, to provide effective EVP based on real-time EV data, traffic volume and signal timing data.

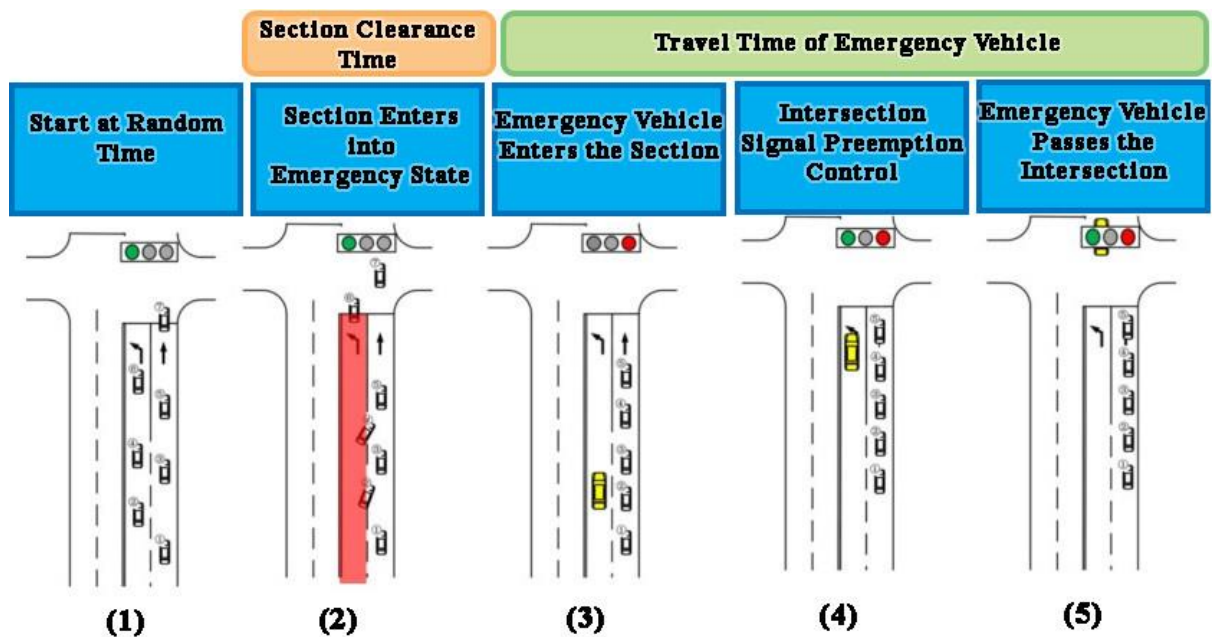


Figure 2-1: The levels of preemption control brought forward by Wang et al [27]

In early as 2000 however, Nelson & Bullock examined the effect of EVP on general traffic [30]. This work is based on a case study that investigated the impact of EVP on closely spaced arterial traffic signals on a State Route in Indiana, USA. Along this State Route, four coordinated intersections have been examined using seven preemption paths against three separate transition algorithms. While varying the number of preemption calls from one to three in the simulation, the effect of traffic volume variation has been examined including for midday and afternoon peak volumes. The findings indicated that, while a single preemption call had minimal effect, multiple preemption calls at close intervals had severe impact on travel time along the arterial.

Qin and Khan [31] too realised the impact EVP would have on general traffic and therefore presented two novel EVP control strategies that would reduce EV response time and minimise interruption caused to the rest of traffic. The first control strategy focuses on the transition of traffic signals from normal operation to EVP mode allowing the EV clear the intersection at original speed. The second control strategy, dictated by an optimal control algorithm, transitions the signal system back to normal mode through the least disruptive option for remaining traffic. Similarly, studying the impacts of EVP on general traffic, Yun et al [26] performed a comparison of different EVP methods using hardware-in-the-loop simulation, which included a VISSIM microscopic traffic simulation model, and four 170E controllers. This simulation has been evaluated by interchanging transition methods (between shortway and dwell) along with varying the transition number of cycles. This study consequently concluded that a single EVP call can cause significant disruption to remaining traffic at an intersection, however with the given controller, the shortway method outperformed the dwell method.

Therefore, as seen through this section, there has been comprehensive research conducted on preemption facilities for emergency vehicles. However similarly, the impact, or rather the disruption it causes to other road users is unavoidable. One could argue that it is a sacrifice a road user should be willing to make, especially in a life-and-death situation for a fellow citizen, which is a fair argument. Nevertheless, this still highlights the importance of exploring alternative avenues to reduce ambulance travel time, especially given that measures like EVP require development of intelligent transport systems and can only be effectively implemented when the traffic network or flow is well characterized and understood in the first place. Additionally, the infrastructure required for this, a developing country may not immediately be

capable of investing in, therefore studies on day-to-day interruptions experienced during ambulance travel need further exploring.

2.1.4 Effects of Traffic Calming Measures on Ambulances

Traffic calming, as defined by Lockwood, “is the combination of mainly physical measures that reduce the negative effects of motor vehicle use, alter driver behaviour and improve conditions for non-motorised street users” [37, p. 22]. Furthermore, according to Lockwood, Traffic calming measures (TCMs) too can be categorised as; vertical change causing (e.g. speed tables, speed bumps, speed bumps, raised intersections), lateral change causing (e.g. chicanes, offset intersections) , constrictions (islands, narrowings), narrow pavement widths, roundabouts, and related streetscaping [32]. There is no denying that traffic calming measures have been successful in achieving their main objective; i.e. reducing overall traffic speed, thereby reducing traffic accidents including fatal or serious injury accidents [33]–[35]. Given the effectiveness however, one of the main problems associated with traffic calming is that they also impact emergency vehicles and thereby result in increased response times [34]–[39]. Therefore, this section will attempt to determine the extent to which past research has studied this problem.



Figure 2-2: Common types of traffic calming measures at Monash University Clayton; (a) speed humps, (b) speed lumps/cushions

The earliest available analysis of the impact of traffic calming measures on emergency vehicle response times, is the study conducted by Atkins & Coleman [34]. These authors evaluated the Traffic Calming Program implemented for 12 years at the time, in neighbourhoods of the city of Portland, Oregon, USA. Data collection had been conducted by the relevant authorities for different types of Fire Bureau vehicles driven on roads calmed using traffic circles (roundabouts), 22-foot speed bumps, and 14-foot speed bumps. Including the type of vehicle and type of calming device, two other variables that were tested on influencing the speed at which an EV negotiates a traffic calming device were; the driver, and the desired vehicle speed. From the data, the researchers derived the impact time and the impact distance; that is the time and distance taken from the point of decelerating from a desired travel speed as the vehicle approaches a calming device, up to the point where the vehicle accelerates back to the desired speed after overcoming the calming device. Consequently, measurements on the time needed to travel the same impact distance without TCMs has been taken. The difference between these two time variables is determined to be the time delay caused by the calming device. Accordingly, their results offer quantitative data that provides a general representation of the impact of traffic calming on fire vehicle response, and is useful in future designs and plans of traffic calming projects [34].

Similarly, in 2013, Garcia et al [38] conducted a thorough investigation on impacts caused by TCMs, in this case, on ambulance response times. Speed profile data collection had been carried out by monitoring two ambulances through GPS devices for a period of 2 weeks. Furthermore, prior to analysis, these speed profiles were separated by the traffic flow type (free or restricted); type of service (i.e. whether it was an emergency transfer or a non-emergency transfer, with or without a patient); and TCM ramp gradient. Then, similar to the previous study the time delay caused by the TCM is obtained from the determined impact distance, in this study referred to as the “area of influence” [41, p. 286]. Consequently, the findings suggest considerable influence by TCMs on ambulance response time, which varied upon differences in type of traffic flow, service. However, TCM ramp slope did not have a significant correlation with response time delay. Furthermore, it was revealed in some cases ambulances were diverted more than 1 km to avoid areas with TCMs, adding delays of up to 40 seconds. Finally, the author presents a mathematical model which could predict response time based on the number of TCMs in a given route, thereby allow diversion decisions to be made more informedly [38].

Continuing on, although not entirely focused on EV response time, alternatively Ahn & Rakha [35] studied the environmental and energy impacts of traffic calming. Evaluated over a case

study, the researchers assume the aggressive accelerating after overcoming TCMs could lead to considerably higher fuel consumption and emissions, and therefore attempt to quantify this impact. Data collected for two types of vehicles (a passenger car and a sport utility vehicle) over three sites with different TCMs (roundabouts, speed bumps, speed humps, speed lumps, stop signs) was analysed. The results revealed that study's initial assumption was in fact correct, and that speed lumps and roundabouts produced highest and lowest increases in fuel consumption respectively. Finally, the most significant finding as far as the topic of ambulances are concerned was, given that high emitting vehicles produce Carbon Monoxide emissions up to 25 times greater than normal vehicles during aggressive acceleration, TCMs add to this adverse environment impact.

Additionally, there have been development of new calming devices especially with a focus on meeting emergency vehicle needs [36], [37]. Gulden & Ewing examined the speed lump as a relatively new TCM and found it to be effective in curbing residential traffic speeds, similarly to speed humps. However due to precise spaced gaps between lumps, vehicles with larger bases, buses and fire trucks, were able to pass through relatively unhindered [36]. Following this, Garcia et al [37] introduced another novel TCM, referred to as the speed kidney. The authors present the speed kidney as an alternative to speed tables and speed humps and claim the lateral shift this causes instead of the vertical shift, is more comfortable for the passengers, results in less negative environmental impacts, and has no effect on wider vehicles (buses, trucks, and emergency vehicles) as the design allows a straighter path [37].

In summary, this section provides an overlook of the relationship between EVs and TCMs. From the available resources, it would be fair to say that existing research on this area appears to be extremely limited, with Atkins & Coleman [34] and Garcia et al [38] conducting the only comprehensive studies. Furthermore, the former study focuses only on fire vehicles while the latter is the only ambulance related study. Therefore, at a glance, it can be observed that further room for exploration exists in studying the effects of TCMs on ambulances. Additionally, with regards to new calming devices, even though the authors claimed emergency vehicles were unaffected, it was noticed that the term 'emergency vehicles' was used in a general sense, and that it was in fact wider vehicles (e.g. fire trucks) that were unhindered. Therefore, the impact of TCMs on type II (shown in Fig. 2-3) and/or even type III ambulances haven't been adequately examined. Moreover, speed lumps as studied by Gulden & Ewing [36], whilst are effective TCMs and are advantageous for wider EVs, Ahn & Rakha [35] found these to be the cause of highest fuel consumption of all TCMs. Additionally, given that ambulances

(especially diesel engines) fall under high emission vehicles, the extra fuel consumption coupled with above average emission levels shows cause for concern regarding their environmental impact.



Figure 2-3: A typical Type II Ambulance; Ambulance Victoria [40]

2.1.5 Studies on time spent by paramedics at the scene

Whilst the previous subsections explored for potential gaps within the study of minimising response time, the following analysis will be of the existing literature on research regarding time spent by paramedics at the scene (scene time) and attempts to minimise this delay.

In a case study conducted by Rouse [41] to determine whether ambulance crews triage trauma patients, the findings prompted the author to conclude that excessive time is being taken up by pre-hospital stabilisation. It was suggested the additional time resulted due to administration of intravenous fluids (14 min) and this not only delayed the delivery of patients to hospital, but also lengthened the turnaround time for ambulances to respond to future calls [41]. Johnson & Guly [42] too obtained similar durations for on-scene IV insertion, and stated therefore the benefits of effective prehospital analgesia comes at a cost in the form of time.

One of the important studies as far as scene time is concerned, was conducted by Powar et al [43] in 1996. The study based in Nottinghamshire, UK, examined the patterns of deployment and use of emergency ambulance crew with special focus on crew type (paramedic or

technician), case mix, interventions undertaken, and operational times. The initial findings indicated, in accordance with previous studies [41], [44], [45], that paramedics spend more time at the scene compared to technicians. However, the key finding was that the time spent by technicians compared to non-intervening paramedics showed no considerable difference, and that it was between non-intervening and intervening paramedics the time difference was striking. This suggested that it was the carrying out of a procedure responsible for the scene time delay rather than the decision making process of whether to “scoop and run” or “stay and stabilise” [43]. Therefore, it is somewhat conclusive that to minimise scene time delays, either the on-scene procedures need to be expedited, or methods should be devised to conduct stages of procedure while on transfer.

2.1.6 Alternative Solutions for Improving Ambulance Transport Efficiency

During the analysis of preceding literature, it was observed, in addition to exploring possibilities of improving EMS efficiency/effectiveness through ambulance travel response minimisation, there were other avenues for improvement of overall ambulance response, that do not fall within the response time intervals defined by Brown et al [9]. As identified by Peleg & Pliskin [22], a fast response time is mirrored in shorter overall ambulance turnaround time as well, thereby ensuring increased availability for additional requests. Peleg & Pliskin’s definition of ambulance turnaround time includes the three time intervals defined by Brown et al (response, scene, and transfer intervals) plus the time spent by paramedics at the hospital, and the time to travel back to dispatch point [22]. However this time period between the point of paramedics arriving at hospital, to the point of ambulance again being ready for dispatch, is the period which Powar et al [43] refer to as the ‘turnaround time’ as opposed to the definition by Peleg & Pliskin of ‘overall turnaround time’. Furthermore, a number of different studies [46]–[48] presented a similar definition to Powar et al. Therefore, in this thesis, to avoid any confusion, the term ‘turnaround time’ will be used hereafter in the sense corresponding to the definition by Powar et al and others. In the past there have been a number of studies lamenting on the lack of research on this last time interval [46]–[48]. The underlying reasons, the authors state, for delays within this period, even though not clearly evident, could be the following; unexpected complications with patient transfer to hospital emergency team, sharing common

interest in patient's status, cleaning and refilling of consumables and disposables in the ambulance storage, other formalities such as documentation, or rest interval for the crew [43].

On further assessment of the aforementioned reasons, at a glance, a potential for minimising delays within the turnaround time interval therefore appears to be with the period (subinterval) of replenishment of ambulance consumables and disposables [46]. This time period is referred to as the 'recovery interval' by Cone et al [46], who also quote Maio [49] in saying that this last (recovery) subinterval has been rarely addressed in past research on prehospital care, even though it obviously impacts the overall EMS response.

In terms of restoring the ambulance back to operational standards, the ambulance communication and emergency assistance devices, which includes radios, portable suction pumps, need to be charged fully or charging continuously [50]. Therefore, according to Apodaca-Madrid & Newman, the existing practice in Denver, USA, is to keep the ambulances running at idle when waiting, as this ensures the devices will be charged when the ambulance is required to act on an emergency [50]. Similarly in Yorkshire, UK, the ambulance engine is left running waiting to respond to a call, in order to support the ambulance electrical equipment [51]. This procedure however, is coming at a cost which is becoming increasingly significant. Along with additional consumption of expensive fossil fuels, this results in adverse environmental impacts with the release of harmful emissions [50]. Williamson was able to quantify an aspect of this, finding that, an ambulance engine may be left running for 65% of a shift while waiting for a call, using up 0.9 litres of fuel per hour [51]. The study also quoted the Environment & Sustainability manager at Yorkshire Ambulance Services on this issues, "We have had many issues with diesel costs, and keeping the electric within our vehicles topped up with enough power" [57, p.12]. Additionally, regarding the ambulance equipment power problem, Cook has stated the following: "Ambulances are always short of power, all the lights, radios, and electrical medical equipment tax the traditional vehicle electrical system, typically they have two alternators and still struggle for power. A large proportion of ambulances also run inverters.." [58, p.104].

Meanwhile, due to impacts of emissions resulting from Ambulance use, and emissions accounted for by the health care sector as a whole, increasing attention has been paid to 'cleaning up' the act [53]–[55]. Health care sector is responsible 3% of all greenhouse gas (GHG) emissions in the UK [54] while this figure rises to 8% in the USA [53]. Although the per response emissions for Australian ambulances was less compared to the USA systems, the

estimated GHG emissions by Australian ambulance services were comparable to that of Australian ‘brown coal’ or ‘silver and zinc’ mining industries; therefore Brown et al suggests Australian ambulance services should strive to minimise their carbon footprint [54]. Thus, from the outlook, there appears to be three problems concerning the current use of conventional vehicles as ambulances; a cost problem, an environmental (emissions) problem, and an electrical equipment power problem. Consequently, Apodaca-Madrid & Newman suggest that “such emissions and expenses can be greatly reduced with an alternative power source that allows the vehicle to be turned off when not responding to an emergency while still maintaining critical equipment ready at all times” [56, p.1].

In the meantime, Hess & Greenberg, in a separate study, brought forward the consideration of three intervention categories to reduce EMS dependence on petroleum and vulnerability to fluctuating petroleum prices: (1) development of triage and telemedicine methods thereby reducing transportation needs; (2) using more fuel efficient vehicle models in ambulance and improving deployment strategies; and (3) switching to alternative fuels including electric vehicles (including hybrids), biodiesel, and liquefied natural gas [56]. Furthermore Brown et al suggest incorporating better fuel efficient and alternative fuel vehicles into the ambulance service fleet (combining categories 1 & 2 by Hess & Greenberg) to reduce direct ambulance services emissions [54].

2.2 Hybrid Electric Vehicles for Ambulance Services

Regarding the use of alternative fuels for ambulances, there have been a number of studies conducted to date. One such study presented a ‘Green Ambulance’, a modified ambulance which uses solar energy to power charging of electric equipment when the ambulance is waiting thereby eliminating emissions during this period [50]. Then, in 2011, Williamson suggested converting the rapid response vehicles in the Yorkshire Ambulance Services fleet to fuel cell power to address the same needs [51]. However, to the author’s best knowledge, it is evident from existing literature, that there has been insufficient attention paid to immediate or intermediary technologies, rather than incorporating relatively novel technology to ambulances. By this statement, what is meant is, exploring possibilities of electrification of Ambulance powertrains. Electric vehicles, Battery Electric Vehicles (BEVs) to be precise, and Hybrid

Electric Vehicles (HEVs) have been in the automobile industry for a significant period, and continues to be a growing sector of the automobile market. Therefore, an opportunity presents itself to study incorporating this technology for ambulances as a possible solution for petroleum dependence and equipment power problem.

A 2013 study by Baker et al [57] is one example of investigating the possible electrification of ambulance services. However, this study only looks at feasibility of introducing BEVs as smaller, compact, rapid responder vehicles of an ambulance fleets, rather than transforming the ambulances themselves. In conclusion however, the authors admit that until the performances of BEVs become comparable to conventional vehicles, the adoption of fully electric medical emergency vehicles is undesired, and expects in the next 10 years BEV technology will significantly improve whence this plan could be viable [57]. This notion regarding BEVs is prevalent within commercial automobile industry as well.

Unless there are drastic improvements in BEV batteries, the range anxiety is a factor that will consistently create doubt in the drivers and remains the main barrier for widespread approval of BEVs [58], [59]. Furthermore the adoption of BEVs depend largely on the attitude of the policy makers in formulating energy and transportation policies as the investments for the infrastructure for example, charging stations, need to be provided by these parties [59]. Therefore even given the sustainability and environment benefits of BEVs, the issues in battery technology, battery costs, and charging infrastructure remain as hurdles to be overcome [59].

Also presently, the strain added on the national grid due to the increase in energy demands to charge the new BEVs (including Plug-in HEVs (PHEVs)) entering the market makes the promotion of BEVs not as sustainable as previously thought [60]–[62]. The potential impacts of BEVs on the national grid have been overlooked in studies until recently, as it has been presumed that either the extra load is manageable with the current capacity or that the integration of BEVs will occur at a convenient pace that will allow utilities to adjust and support the current networks [60]. BEV charging, particularly if unconstrained, will significantly impact the national electric grid performance, efficiency and required capacity [61]. Addition of a considerable fleet of BEVs could lead to violation of supply/demand matching and statutory voltage limits. This also could result in power quality issues and voltage imbalance for given operating conditions [62]. Studies conducted show that designing BEV interface devices could allow the extra load to be managed and using ‘smart’ demand management strategies such as the Advanced Metering Infrastructure (AMI) can help alleviate the effects of

BEVs on the national grid [62], [63]. However despite these conclusions, it suggested that further research into effects of large-scale BEV penetration on the national grid needs to be conducted [62]–[64]. Consequently, it can be said that HEVs are not just an intermediate step towards the adoption of zero emission vehicles but a practical solution for commercialisation of low-emission vehicles [65]. Therefore HEVs will be in the highest demand, and as a result, the development of these architectures forms the priority in the advancement of the automotive industry.

On the application of HEV technology to EMS vehicles, Hawkins [66] conducted a study in 2008. However, this too focused on converting the quick response vehicle fleet, consisting of mid-size SUVs, to hybrid electric SUVs. Therefore, a study on the adoption of HEV technology for a type II ambulance remains open. The findings by Hawkins nevertheless prove important for a future study. Especially concerning the ambulance electrical equipment power problem. Hawkins fitted the study vehicle with an 110V/150W standard AC outlet to power a standard emergency light, and siren system. The draw of this additional power showed no significant strain on the vehicle, and furthermore observed the ability of the HEV to idle on battery for considerable periods (thereby decrease overall emissions) without disrupting the running lights, radios, and other equipment before the internal combustion engine switched on to recharge the batteries [66]. This therefore provides incentive to study ambulance operation with HEV technology particularly in an electrical equipment power supply sense. However, since the majority of past research on HEV dynamics analysis has been focused on passenger vehicles, the next section will explore literature within this area of study to provide a satisfactory background.

2.2.1 Previous studies on HEV control strategies

Early power management strategies have employed a fuzzy-logic-based control approach for HEVs [67], [68]. The intent of this method is to balance the power demand of the vehicle through the management of the battery, while the engine runs at its optimum region of operation. Therefore in this case the battery is used as a “load-levelling” device [69]. In Won & Langari [68] study, fuzzy logic based torque distribution control was suggested for parallel HEVs and was assessed over the Federal Test Procedure (FTP) urban drive cycle.

A more popular option to solve the optimisation problem for a power-split drivetrain HEV has been the dynamic programming (DP) technique [70]–[72]. Grizzle [70], proposed a procedure that uses deterministic dynamic programming to solve the power-split optimisation problem of a hybrid electric truck. In this case, a cost function has been defined and minimised over the Urban Dynamometer Driving Schedule for Heavy- Duty Vehicles (UDDSHDV) drive cycle. Similarly in another study [72], DP is used to converge to a global optimum for the three standard HEV powertrains; Parallel, Series, and Series-Parallel. Furthermore, a simplified model of a Toyota Prius (series-parallel) is evaluated over the UDDS drive cycle to study the impact of a cost function on fuel economy and battery state of health.

Studies have also been conducted to formulate a solution for the global optimal power distribution problem through HEV real-time control using equivalent consumption minimisation strategy (ECMS) [73]–[75]. ECMS consists of obtaining the global optimal control policy by evaluating an instantaneous cost function [74], which in this case is the total “equivalent” fuel consumption and is defined as the sum of actual fuel consumption by the internal combustion engine and the calculated equivalent fuel consumption related to the operation of the electric motor [73]. In 2004, Sciarretta et al [74], presented an ECMS-type control which used a novel technique to calculate the equivalence factor between electrical energy and fuel energy. The study was performed on Daimler-Chrysler’s prototype for the Mercedes A-Class with parallel hybrid powertrain and was evaluated on three different drive cycles; MVEG-A, ECE, and Japanese 10-15 DC. Furthermore, Rodatz et al [75], formulated a real-time optimal power control system using ECMS, but for a fuel cell/supercapacitor-powered HEV and was evaluated over the New European drive cycle (NEDS). Following these, a variant of ECMS was introduced by Musardo et al [76] named adaptive-ECMS (A-ECMS) where an on-the-fly algorithm in which the control parameters are periodically refreshed depending on the driving conditions is added for the approximation of the equivalence factor. In this study, tests have been performed on six industry regulatory drive cycles; FUDS, FHDS, ECE, EUDC, NEDC, and Japanese 10-15. To further prove the robustness of A-ECMS, it has been tested on a real driving cycle obtained during a trip in Zurich, Switzerland. Another real-time control system was derived by Delprat et al [77] from the optimal control algorithm that was based on optimal control theory. The performance was compared against ECMS while being evaluated over the CEN drive cycle and a highway drive cycle.

Different studies have explored the possibility of combining component sizing with the optimisation problem of power management [78]–[80]. A combined power management/design optimisation problem of a fuel cell/battery HEV was formulated Kim & Peng [78] and was tested over three different drive cycles; HWFET, FTP-72, and ECE-EUDC. Similarly, Assanis et al [79] suggested a design optimisation framework to obtain the best overall engine size, battery pack, and electric motor combination for minimum fuel consumption. This test was carried out using the ADVISOR vehicle simulation program for the SAE J1711 drive cycle. The prospect of joining component sizing with the control strategy too was identified by Zhang & Chen [80] and as a result proposed a multi-objective parameter optimisation using an evolutionary algorithm, NSGA-II, for a series HEV. The performance was tested on a combined UDDS and HWFET drive cycle. A similar study has been conducted by Liu et al [81] where a hybrid genetic algorithm was developed for optimisation and tested on a series HEV for a City-Hwy test procedure.

In further developments, Simulated Annealing algorithm has also been incorporated into estimation of optimal power management strategies [82], [83]. In the study by Gao & Porendla [82], two other global optimisation algorithms; DIRECT and Genetic algorithm has been used along with Simulated Annealing (SA) for design optimisation of a parallel hybrid which was modelled on Powertrain System Analysis Toolkit and tested for a combined drive cycle (FTP75 and HWFET). Chen et al [83] however applied SA algorithm to compute the engine-on power and the maximum battery current coefficient in formulating a power management method for a PHEV which was evaluated over the UDDS and HWFET drive cycles.

The study performed by Sciarretta & Guzzella [84] indicated that the fuel economy improvement achievable depends strongly on the specific HEV architecture (as the mode control logic that determines the operation of the ICE depends on the architecture) and on the driving conditions. Moreover, the control parameters could be optimised under certain driving conditions and however, may perform poorly under different conditions. It is further suggested to overcome these challenges, systematic, model-based optimisation methods using meaningful objective functions should be adopted [84]. Studies have shown that HEV fuel economy calculated from standardised drive cycles do not adequately correlate with fuel economy observed in real-world [85], [86]. In this study [85], driving patterns in real traffic conditions were simulated using a driver-road-vehicle (DRV) parameter space and also the

numerous types of customer types were taken into consideration for the simulation given the variance of driving behaviour and traffic conditions.

As observed in the studies analysed above, most of the design and controller optimisation methodologies were developed on the basis of one, or a few pre-defined drive cycles. As a result it was identified that HEV design parameters optimised for only the tested standardised drive cycle/s and were in fact not optimal for other drive cycles or the whole driving profile [85]. Single cycle optimisation can therefore lead to "cycle-beating" [69], [85]–[89].

2.2.2 Methodologies developed to overcome "cycle-beating" in HEV testing

Cycle-beating refers to achieving desired levels of performance and optimising parameters to the specifications of a given drive cycle [88]. As identified by Ntziachristos & Samaras [87], the use of legislative cycles could underestimate the emission levels due to inherent low speed dynamics of these cycle and possible cycle-beating. In Grizzle's work [70] too, that is, with the use of deterministic dynamic programming approach, it was observed that for a given driving cycle the control strategy may be optimised, however might neither be optimal nor charge sustaining under other cycles. Additional flaws of single-cycle optimisation include the disregard for variations in driving behaviour and lifetime effects such as battery degradation [90]. A study by Ekberg et al [88] examined the possibility of cycle beating for the New European Drive Cycle (NEDC), shown in Fig 2-4. Given that during tests, a deviation of ± 2 km/h and ± 1 s from the reference values of NEDC is allowed, it was found that by taking advantage of this allowance, consumption of fuel can be decreased by up to 16.56% for an automatic transmission and up to 5.90% if gear changes occur according to drive cycle specifications.

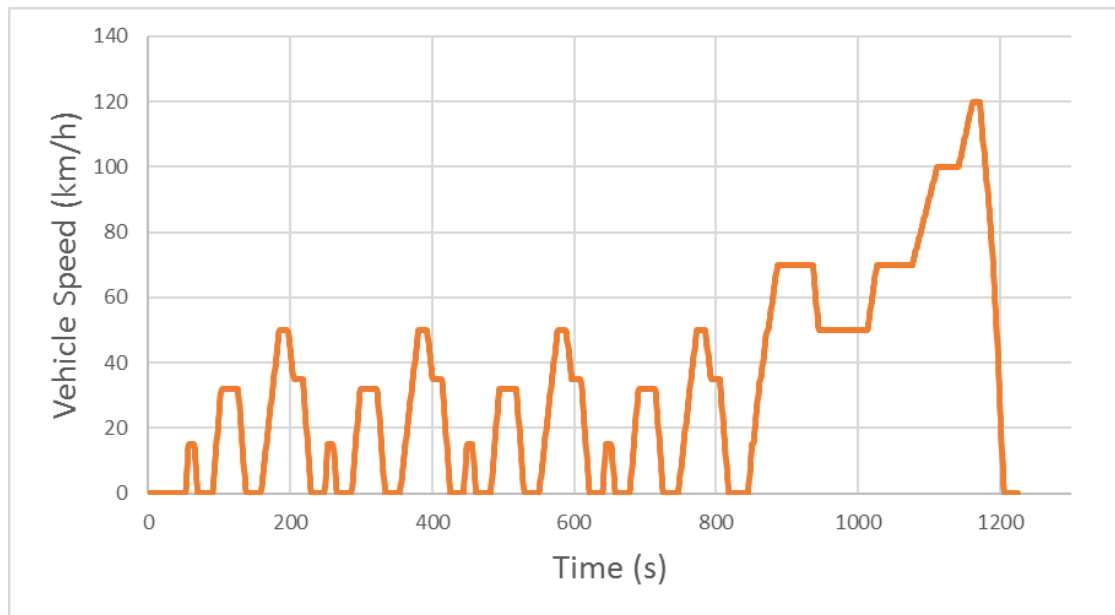


Figure 2-4: New European Drive Cycle (NEDC)

Several methods to overcome the drawbacks associated with cycle-beating have been proposed by numerous studies [69], [85]–[89]. One such method is the stochastic multi-cycle optimisation technique as proposed by Moura et al [91] where stochastic dynamic programming is used to optimise PHEV power management across a number of drive cycles. However this requires a significant amount of stochastically representative drive cycle data, that may not always be available readily [85]. In the study by Lin et al [69], a design method was developed using Markov chain modelling and stochastic dynamic programming. Instead of using a drive cycle, to characterise the future uncertainty of the power requirement dictated by the variations in driving conditions, the power demand is modelled as a Markov process. Additionally, there have been numerous methodologies suggested for drive cycle generation, most of which are focused on the aspect of emission testing. In one such study by Lin & Niemeier [92], a cycle construction approach was proposed which identified four operating modes (idle, acceleration, cruise, and deceleration) and then based on these modes of operation, the Markov model theory is used to guide the stochastic process of drive cycle construction. Then Souffran et al [93] enhanced this method with the inclusion of road gradient to the discrete Markov generation process. Another method proposed by Tazelaar et al [89] generated alternatives cycles based on the characteristics in terms of frequency spectra and speed distribution, of an existing drive cycle. With a collection of truck driving behaviour in focus, Ravey et al [94] described a stochastic methodology to generate drive cycles subject to the variations of the recorded drive cycle parameters and the increasing weight due accumulating

load. Furthermore Schwarzer & Ghorbani [85], presented a drive cycle generation tool (DCGT) that is able to generate an infinite number of drive cycles. In this method, initially, for each parameter of a recorded set of drive cycle data, the probability functions have been obtained and then these probability functions were implemented in the DCGT. Finally, a discrete cosine transform (DCT) based approach for constructing distance-based drive cycles was proposed Lin et al [86]. The entire driving route was separated into a number of segments of fixed length and then these segments were converted into a frequency sequence. Thereafter the frequency and amplitude of the generated drive cycle was adjusted to form a new cycle.

With regards to literature analysed above, the opportunity to develop a stochastic method of validating HEV control strategies using drive cycles was identified. Furthermore, regarding ambulances specifically, there lies an uncertainty whether industry legislated drive cycles actually portray driving patterns exhibited by ambulances in practice. Therefore, evaluating the suitability of hybrid electric powertrains for ambulances need to be performed over stochastic drive cycles for better understanding. An opportunity for a study to distinguish itself from the above-mentioned drive cycle obtaining methodologies, was identified to be the use of a microscopic traffic flow simulator, PTV VISSIM for example, to generate the drive cycles required for HEV testing.

2.2.3 Overview of the impact of ancillary loads on HEV fuel economy

It was documented in this chapter previously, regarding the equipment power problem faced by ambulances. This problem was raised in the context of a conventional powertrain. Therefore, electrification of an ambulance powertrain especially should be undertaken after a thorough study of the impact of ancillary loads on power management especially due to the extra number of equipment in an ambulance compared to a general passenger car and the equipment being powered by the battery as opposed to an alternator. If the engine is required to be run for longer to charge the battery due its depletion by equipment power demand, then the conversion of powertrain becomes counterproductive. However since there is a lack of research into this relationship concerning ambulances, it would be useful to explore literature on impact of ancillary loads on fuel economy of passenger HEVs to gain better understanding of the problem.



Figure 2-5: Example of the interior of a general Type II Ambulance with the equipment available in focus [95]

With regards to fuel economy testing in automobiles, the effect of ancillary loads like the air-conditioning (A/C) system, the body electrical system, and the engine thermal management system, on fuel consumption has been previously studied [96]–[98]. However, the A/C system comparatively demands a higher amount of power, and therefore becomes a burden, especially for battery electric vehicles, due to the limited battery storage [99]. Out of these, the A/C system being highest contributor to total ancillary load fuel consumption, promising opportunities for fuel economy improvement has gained the attention of researchers [100].

An automobile A/C system plays an important role in automotive systems because it does not merely provide thermal comfort for the passenger but also improves road safety as this reduces driver fatigue [99]. The main purpose of an A/C system is to preserve the vehicle cabin temperature and humidity at comfortable levels for the occupants. However, another important purpose served is the recirculation of cabin air and the prevention of cabin atmosphere stagnating, due to CO₂ build up from the passengers, volatile organic compounds, and other foreign particulate matter [98]. The actual consumption of the A/C system depend on a number of factors such as climate, season, time of day, vehicle type and colour, outdoor/indoor parking, type of passenger clothing, the occupant level of activity, trip duration, vehicle speed, and

personal preference [96]. According to [101], the A/C system accounts for around 30% of the Miles per Gallon expenditure in a conventional vehicle. Furthermore, for EVs, the energy required by the A/C loads can reduce the EV range by nearly 40% [96].

Farrington & Rugh [96] too studied the impact of accessory load on the parallel HEV fuel economy. Based on a few assumptions, the maximum electrical load resulting from A/C was taken to be 3kW. The fuel economy for an initial accessory load of 500W was measured for four EPA certified drive cycles, FUDS, HWFET, SC03, and US06. The change in fuel economy was then calculated in increments of 1000W ancillary load and compared against the initially obtained reference value. The reduction in fuel economy was observed to be nearly 40% on average over the different cycles. However, this study only states, for all simulated cycles, the HEV model started and ended at the same battery SOC to within 0.5% and has neglected the electricity cost in the fuel economy. Hence, from an overview there seems room for further investigations into impact of A/C systems on HEVs specifically, due to this system being the largest power consumer. However, whether this would prove the same in the case of an ambulance needs to be determined.

3 Investigations of Ambulance Transport Efficiency Using Hybrid Vehicles

3.1 Introduction

The electrification of ambulance powertrains could provide a sustainable solution to the ambulance equipment power problem. This will also reduce time required to recharge equipment, as well as decrease the frequency of refuelling required for the ambulance, thereby reducing overall ambulance turnaround time. Therefore, the ability to simulate the operation of hybrid vehicles will be crucial to determine its usefulness as ambulances. In this chapter we will first review the simulation systems that are available. This will be based on looking at their ability to encompass the control, mechanical, and electrical system characteristics. Following this, we will conduct performance comparison tests to verify their suitability for future use in studying characteristics of ambulances.

3.2 Simulation Systems

3.2.1 MATLAB SIMULINK Model

The first simulation model to be evaluated in this chapter, is a series-parallel hybrid electric passenger car, modelled on MATLAB Simulink. This HEV model (Fig. 3-1), designed by Steve Miller, at The MathWorks [102], comprises of, a control system with several proportional integral controllers and mode logic programmed as state flow; the mechanical system that includes the internal combustion engine (ICE), the power-split mechanism and other vehicle dynamics; the electrical system which consists of the battery, synchronous motor, generator, and the DC-DC convertor.

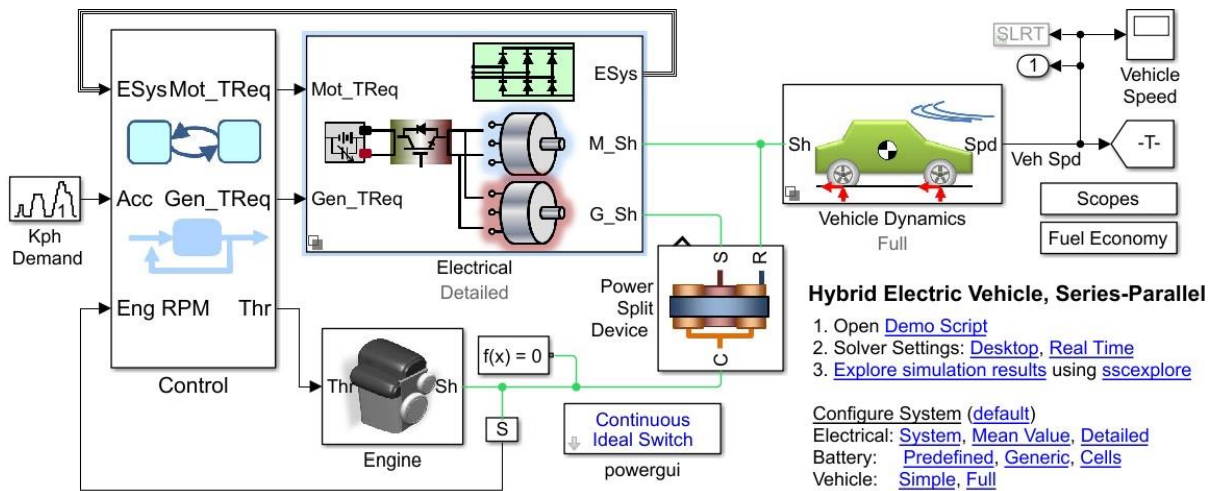


Figure 3-1: MATLAB Simulink model of series-parallel hybrid electric vehicle [102]

3.2.1.1 Control System

The simplified mode logic implemented in the control system of this model is shown in Fig. 3-2, and operates as follows.

The vehicle begins operation at Start_mode. It initially operates on the electric drivetrain purely, where the electric motor propels the vehicle and then if required, the generator acts as the starter motor to start the engine in this mode. When the ICE surpasses a specified threshold, the vehicle enters normal mode where the ICE partially propels the vehicle and charges the battery. During acceleration (Accelerate_mode), the motor output is increased, and the generator is disabled so as the total torque produced by the ICE is used to satisfy the increase in torque demand. When the vehicle is in cruise mode, the generator may charge the battery depending on the battery state-of-charge (SOC). The mode logic includes transitions to re-enter Accelerate_mode/Start_mode. In the case of brakes being applied, the vehicle enters Brake_mode, where the motor operates as a generator to recharge the battery during regenerative braking. To summarise, the mode logic takes the vehicle speed, brake input, battery SOC%, and engine speed as inputs, identifies the state of vehicle operation, and either enables or disables the motor, the generator, or the engine accordingly.

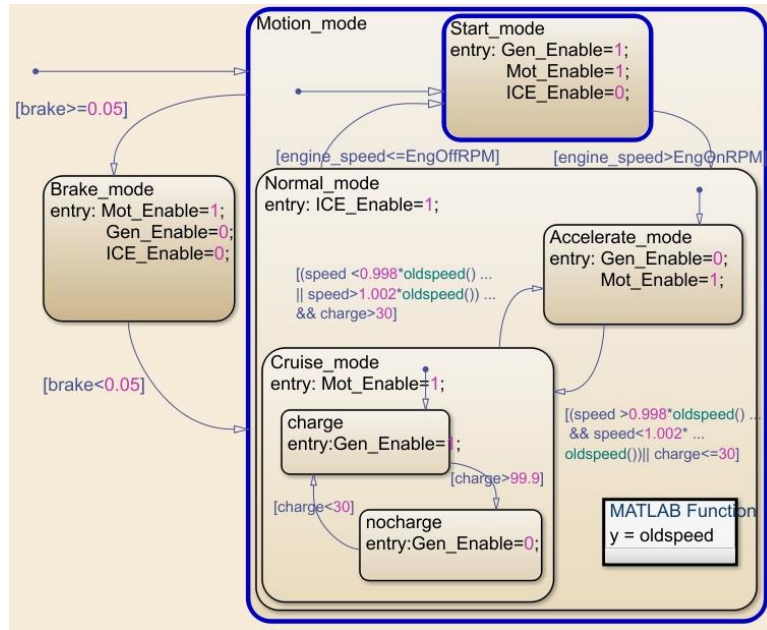


Figure 3-2: Control system of the MATLAB Simulink HEV model [102]

3.2.1.2 Mechanical System

The engine is modelled as a lookup-table which relates engine speed to available power. The engine speed controller inputs the throttle signal to the engine. Mechanical links connect the engine to the rest of the drivetrain. The power-split device is modelled as a planetary gear using the gear libraries in Simulink. The carrier of this planetary gear is connected to the engine, the ring connects to the rear differential and the electrical motor, and the sun connects to the generator. The full vehicle model includes the tire models and the longitudinal dynamics. The tire model includes the steady-state and transient dynamics and longitudinal dynamics used are the parameters that affect the fuel economy studies.

3.2.1.3 Electrical System

In the system level analysis, the motor and generator are modelled using data sheet parameters (for e.g. torque-current relationships) to simulate faster and include torque independent, dependent losses. The detailed variant, shown in Fig. 3-3, models the entire three-phase electrical network and includes switching dynamics. The balance of the trade-off between model fidelity and simulation speed is vital for efficient development, therefore in this study, the system level variant is used, in order to match ADVISOR in model fidelity.

The DC-DC converter in the electrical networks boosts the voltage of the battery to the required 500 V on the DC network. This voltage is used to drive the synchronous motor. In the system level variant, the DC-DC converter is modelled using Simscape, basically by setting the power from the battery equal to the power transmitted to the bus, and the power lost to load dependent losses. The current through the load dependent losses is used to calculate the temperature of the DC-DC converter. The temperature of the DC-DC converter is fed back to the controller to affect the mode logic of the system accordingly. In the detailed variant, the power electronics of the DC-DC converter is included.

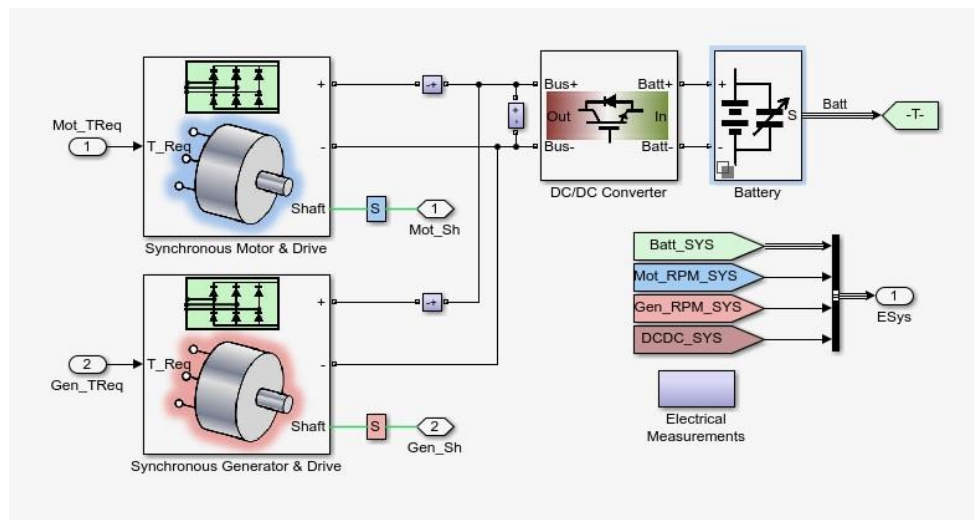


Fig. 3-3: Electrical system of the MATLAB Simulink HEV model [102]

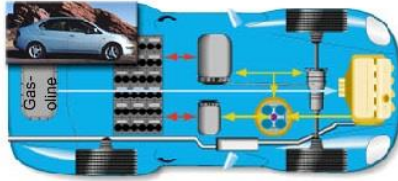
3.2.2 ADVISOR Simulation Tool

On the requirement of the U.S. Department of Energy (DOE) the Advanced Vehicle Simulator (ADVISOR) was first developed in 1994 to aid in developing HEV technology at the National Renewable Energy Laboratory (NREL) in conjunction with industry partnerships including General Motors, Ford, DaimlerChrysler [103]. ADVISOR is also written in the MATLAB/Simulink software environment. In addition to HEVs, ADVISOR can simulate conventional, advanced, light duty and heavy-duty vehicles, including fuel cell vehicles. The three graphical user interfaces (GUIs) of ADVISOR shown in Fig. 3-4, allows the user to evaluate iteratively the effects of vehicle parameters and different drive cycles on the vehicle

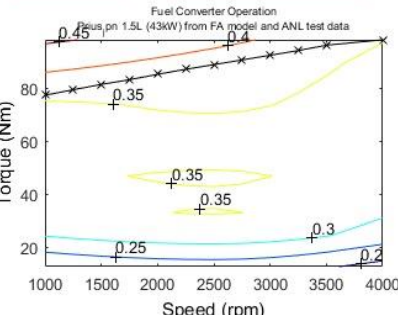
dynamics, performance, emissions and fuel economy [103]. The first GUI screen in ADVISOR is the vehicle input screen (Fig. 3-4(a)), followed by the simulation parameters setup screen (Fig. 3-4(b)), and finally the results screen (Fig. 3-4(c)). The vehicle input screen allows the user to construct a vehicle of choice with the options provided from a number of drop-down menus. These options of pre-defined vehicle parts, even though limited, provides the user the alternative to formulate custom parts by editing properties of each pre-defined part. In the next screen, the user mainly selects the drive cycle over which the vehicle performance is to be evaluated. It is also at this stage that the user would define parameters for variables if a parametric study were to be conducted. Finally, the results screen displays the output plots of time-dependent variables, maximum of four simultaneously, and the user is able to select from a drop-down menu a variety of performance indicators.

ADVISOR, in its iterative calculation method, combines a backward/forward approach [104]. In a forward approach, the user inputs like throttle position and braking, are dictated by a desired speed-based driver model. This information is then used in calculations of drivetrain dynamics such as torque and energy demand, from where, through the engine, the process continues to the transmission and then finally to the wheels where the resulting tractive force at tire/road interface is calculated [104]. However, with regards to scope of this study, that is, in comparison with the SIMULINK model, it is the backward-facing approach of ADVISOR that is directly relevant. Therefore, similar to the SIMULINK model, the backward approach is guided by the required vehicle speed obtained through a simulated drive cycle. Based on this, the required speed and torque of drivetrain components to meet the desired vehicle speed accounting for inertial forces, is calculated. In contrast to the forward approach, the process then continues to calculations at the tire/road interface, from there over to the drivetrain, finishing with the energy source, the internal combustion engine for a conventional vehicle [104].

Vehicle Input



Component: fuel_converter | Plot Selection: fc_efficiency



Load File: PRIUS_JPN_defaults_in | Auto-Size

Drivetrain Config: prius_jpn

Component	version	type	max pwr	peak eff	mass (kg)
Vehicle	?	VEH_PRIUS_JPN			918
Fuel Converter	ic	si	41	0.37	132
Exhaust Aftertreat	?	EX_SI			#of mod V nom 11
Energy Storage	rint	nimh	40	308	40
Energy Storage 2	?	ess 2 options			
Motor	?	MC_PRIUS_JPN	50	0.91	57
Motor 2	?	motor 2 options			
Starter	?	starter options			
Generator	reg	reg	31	0.84	33
Transmission	pg...	pgcvt		0	0
Transmission 2	?	trans 2 options			
Clutch/Torq. Conv.	?	clutch/torque converte...			
Torque Coupling	?	TC_DUMMY			
Wheel/Axle	Crr	Crr			0
Accessory	Co...	Const			
Acc Electrical	?	acc elec options			
Powertrain Control	pri...	pg			

front wheel drive | rear wheel drive | four wheel drive ?

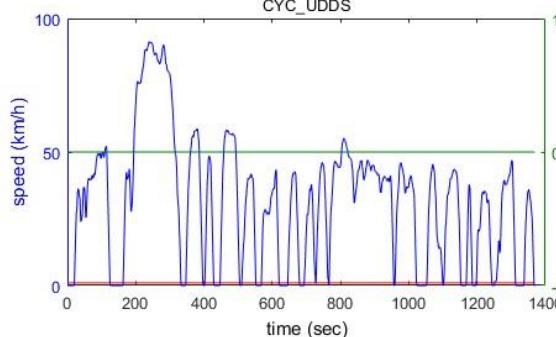
View Block Diagram: BD_PRIUS_JPN

Variable List:
 Component: fuel_converter | Edit Var.
 Variables: fc_acc_mass | 32.8986

Cargo: 9 | Calculated Mass: 1200 | override mass: 1200

Buttons: Save, Help, Back, Continue

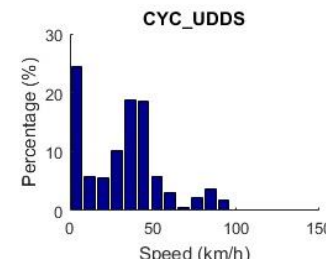
(a) ADVISOR Vehicle Input Screen



Speed/Elevation vs. Time

Statistics:

time:	1369 s
distance:	11.99 km
max speed:	91.25 km/h
avg speed:	31.51 km/h
max accel:	1.48 m/s^2
max decel:	-1.48 m/s^2
avg accel:	0.5 m/s^2
avg decel:	-0.58 m/s^2
idle time:	259 s
no. of stops:	17
max up grade:	0 %
avg up grade:	0 %
max dn grade:	0 %
avg dn grade:	0 %



Drive Cycle: CYC_UDDS

Trip Builder

Time Step: 1 | # of cycles: 1

SOC Correction | Cycle Filter

Initial Conditions

Constant Road Grade | Interactive Simulation

Multiple Cycles: none

Test Procedure: TEST_CITY_HWY

Acceleration Test | Accel Options

Gradeability Test | Grade Options

Parametric Study: # of variables: 1

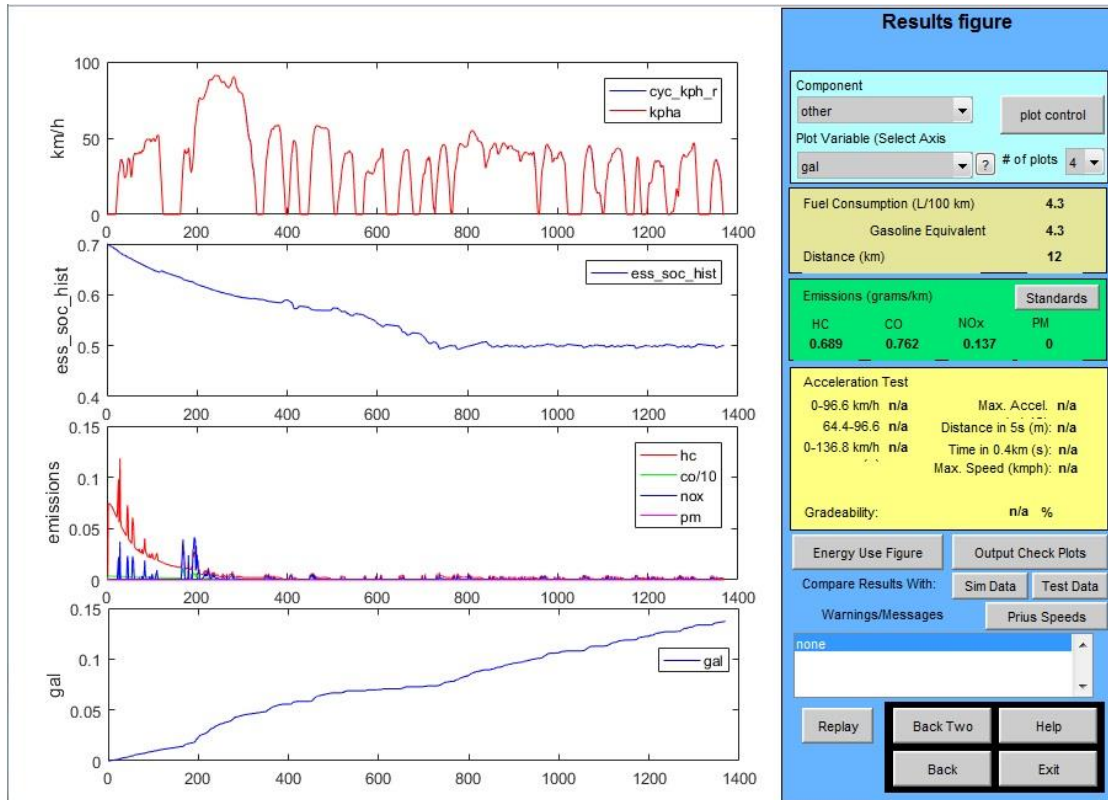
Variable	Low	High	# Pts
veh_mass	1200	1600	3
veh_CD	0.3	0.5	3
veh_FA	1.746	3.746	3

Save Runs | Prefix: cp | Dir: C:\Users\kskam5\Do

Elec. Aux. Loads

Buttons: Load Sim. Setup, Optimize cs vars, Save, Help, Back, RUN

(b) ADVISOR Simulation Parameters Setup Screen



(c) ADVISOR Results Screen

Figure 3-4: GUIs of ADVISOR

3.3 Comparative Verification Study

3.3.1 Scenario

Given the scope for a study on incorporating HEV technology to an ambulance, the building of a comprehensive simulation model poses the question as to which simulation environment would best suit the purpose. ADVISOR being the more extensively used vehicle simulation software provides the dependable option. However, building a distinct model as the MATLAB Simulink Model, provides the alternative option to customise the model to match components and accessories of an ambulance more closely. That is, even though ADVISOR provides model customisation through options provided for each vehicle input within the software, and allows the properties of these input options to be further edited; the number of vehicle input options itself is limited. For example, accessory load data for a given vehicle model, in terms of mechanical, and electrical accessory power, is inputted to ADVISOR as one value for total power. Given the model fidelity and simulation speed of ADVISOR, this generalisation is reasonable when studying passenger vehicle models intended for mass production, where the range of accessories is standard. However, this is not suitable when studying special purpose vehicles, especially Ambulances. Due to the extra number of auxiliary components associated with an ambulance, the equipment power problem faced by ambulances is well documented by previous studies [51], [52]. Since alternators that directly power electrical equipment are not available in HEVs, and the total electrical power demand has to be supplied by the HEV battery, the impact of each auxiliary component (e.g. air conditioning system, ventilators, defibrillators) on the energy storage system, will need to be studied. Therefore, building of a distinct MATLAB Simulink model provides the option to incorporate designs of every auxiliary component to the overall model, and thereby study the ambulance equipment power problem by parameterising power requirements of each component. Furthermore, using a customised model on a platform as prevalent as MATLAB, allows for easy integration with other software. For example, a traffic microsimulation software such as PTV VISSIM, which links to MATLAB via its Component Object Model (COM) interface, can be used to further enhance HEV powertrain study, especially in the case of an ambulance. Vehicle simulations are typically evaluated against legislated drive cycles. However, whether these legislated drive cycles accurately emulate driving patterns displayed by ambulances is questionable. Moreover,

legislated drive cycles can be prone to cycle-beating techniques being employed by manufacturers [105]. Therefore, VISSIM can be used to simulate traffic scenarios experienced by ambulances, by which drive cycles can be generated. Consequently, by importing this data into MATLAB, the Simulink model can be evaluated. Thus, using a distinct Simulink model allows the possibility to build a further robust simulation tool for HEV powertrain study.

Irrespective of this possibility however, the Simulink model remains yet to be validated as a competent simulation model to be used in HEV studies. Therefore, given ADVISOR being a proven simulation program in automotive research in the preceding two decades, a comparison of performance of the Simulink model against ADVISOR may provide a form of validation to the model, and thereby deliver a clearer indication of the robustness of using a customised Simulink model for ambulance powertrain architecture studies.

Additionally, ADVISOR allows the user to manually vary parameters albeit there being only limited choice of components, and therefore provides the opportunity to approximately model a hybrid electric powertrain with ambulance specifications. Consequently, this requires ambulance specifications to be defined. Furthermore, this section would also help explore any limitations associated with ADVISOR in studying this particular scenario.

3.3.2 Specifications of HEV Powertrains

The Simulink model parameters defined by Steve Miller, based on industry datasheets and lookup tables, were matched closely as possible in the ADVISOR simulated model, in order to provide reasonable consistency for the comparisons. The series-parallel HEV modelled in MATLAB Simulink, was replicated on ADVISOR, for the purposes of this study, by editing the properties for the Toyota PRIUS (Japan) made available by the software. The Toyota PRIUS was chosen as it is the only HEV model available on ADVISOR with a planetary gear power-split device, similar to the Simulink model. Table 4-1 shows the specifications defined for each simulation model.

Table 3-1: Specifications of HEV components for each simulation model

		Simulink Model	ADVISOR
Gross Vehicle Mass (kg)		1200	1200
Engine		Modelled using same lookup table. Max. power (kW) = 41 Max. speed (RPM) = 4000	
Generator		Modelled using same lookup table. Max. power (kW) = 31 Max. torque (Nm) = 160	
		N/A	Efficiency (%) = 84
Traction Motor	Max. power (kW)	50	
	Max. speed (RPM)	6000	
	Max. torque (Nm)	400	
	Efficiency (%)	91	
Energy Storage System	Battery type	NiMH	
	Nominal voltage (V)	288	
	Rated capacity (Ah)	6.5	
Planetary gear ratio (Ring to Sun)		2.6	
Final drive ratio		-	3.93

3.3.3 Drive Cycles

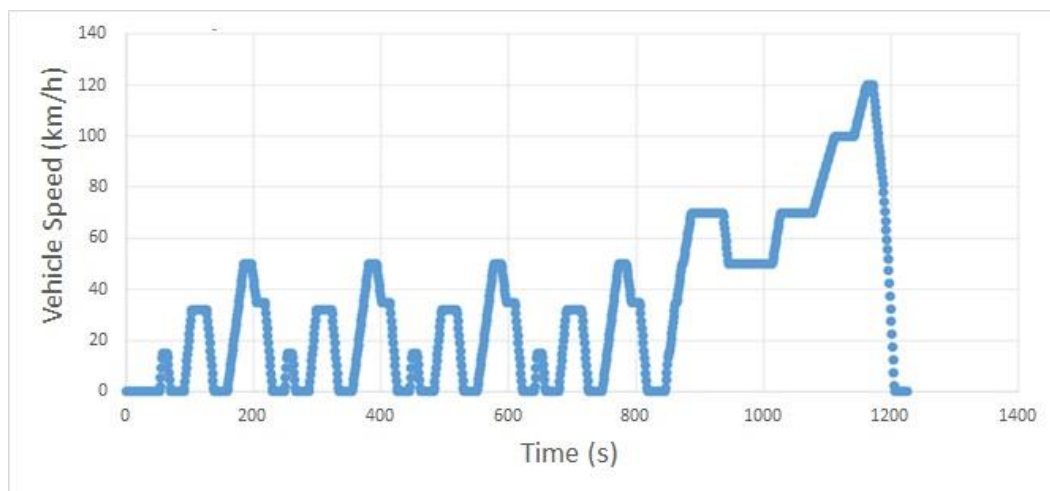
Once the parameters for ADVISOR and SIMULINK models were set, the drive cycles to be evaluated against were chosen to be the following;

- New European Drive Cycle (NEDC)
- Urban Dynamometer Driving Schedule (UDDS)
- Highway Fuel Economy Test Driving Schedule (HWFET)

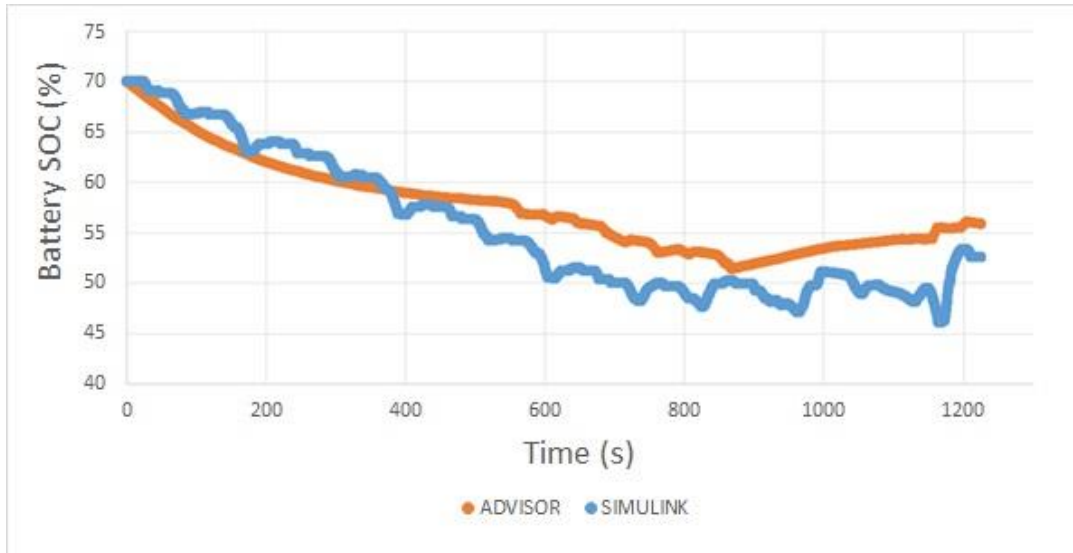
First, the European type-approval drive cycle, NEDC, also known as ECE+EUDC, which is a combination of an urban (ECE) and extra urban (EUDC) drive cycle [106], was chosen. Being one of the first legislated drive cycles, developed initially in the 80s, NEDC was last updated in 1997 [107]. Researchers therefore have argued that NEDC was outdated as it does not portray real-world driving with many segments of constant-velocity and constant-acceleration (along with precise gear-shift schedule), which allows manufacturers to apply cycle-beating techniques more easily [88], [105]. As a result EU legislators have replaced NEDC by Worldwide Harmonised Light Vehicle Test Procedure (WLTP) as of September 2017 up to 2019 [108]. However, NEDC will be still used in this study as merely a variable to compare performance of the two simulation models, and to provide variety to the driving profile. UDDS drive cycle was selected as it provides a more real-world like urban driving experience with aggressive accelerations and stop-starts. UDDS is also one of the few globally legislated chassis-dynamometer cycles for heavy-duty vehicles [109], which in turn would be an appropriate drive test for an (medium-duty) ambulance. Finally, HWFET was chosen to represent highway driving conditions which includes no stops in the drive cycle until the finish, and therefore adds another dimension to the drive profile.

3.4 Results & Discussion

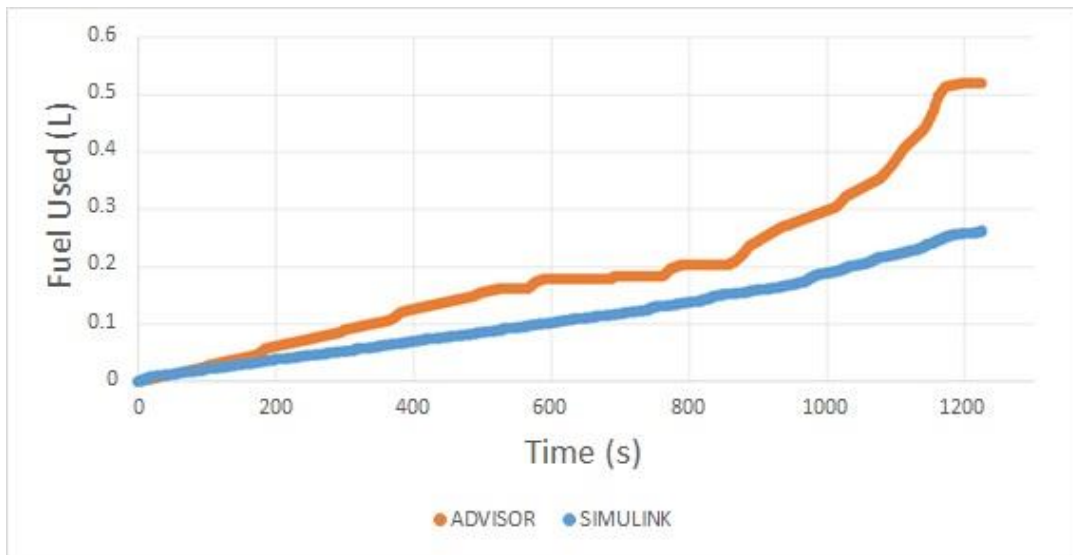
Figures below present data obtained from the simulations performed on both the Simulink model, and ADVISOR, for three stipulated drive cycles, NEDC, UDDS, and HWFET. Two important factors to be considered in assessing the simulation performances are the Battery State-of-Charge (SOC) % and Fuel used data. These indicators are the main performance outcomes that are optimised in an HEV vehicle as they directly reflect the operation of the two energy sources of a HEV, the (electrical) energy storage system (ESS), and the internal combustion engine. When the NEDC drive cycle was applied, the results indicated from Fig. 3-5, show that the Battery SOC and Fuel used in both simulation software show reasonably good correlation. The Simulink Model appeared to drain its battery more but used less fuel in return (see Figs. 3-5(a) & (b)). This behaviour seems consistent when energy conservation is considered, as one energy source is depleted more, the other ought to be conserved more. The reason for the Simulink model to consume less fuel could be attributed to how the powertrain control parameters are optimized to do so under this condition.



(a) *New European Drive Cycle (NEDC)*



(b) Battery State-of-Charge % history for the 2 simulation models over the NEDC

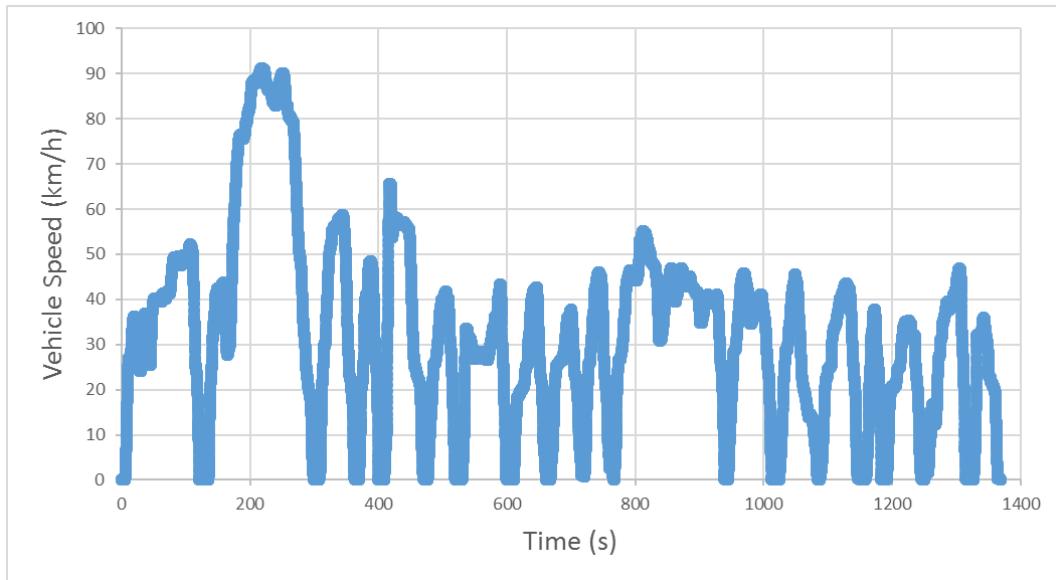


(c) Fuel used for the 2 simulation models over the NEDC

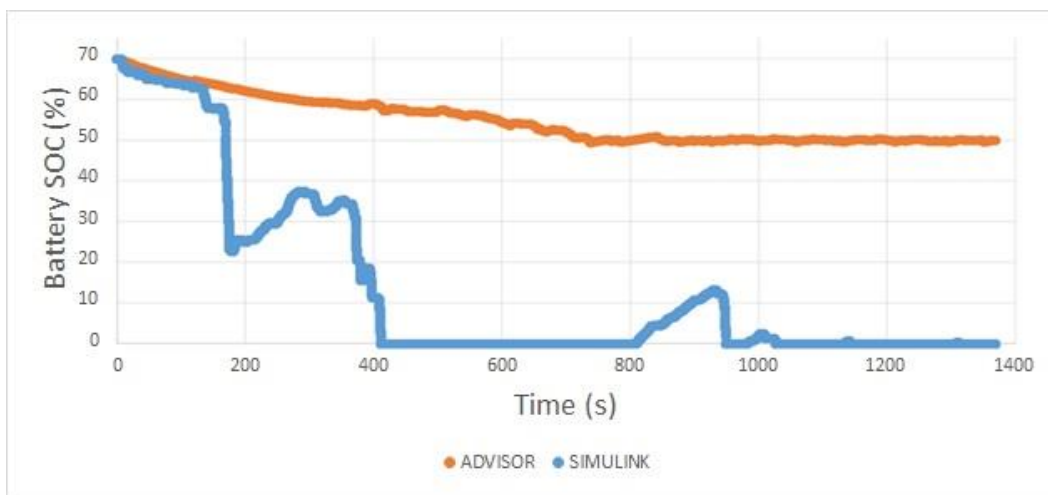
Figure 3-5: Simulation results for Simulink and ADVISOR models for NEDC

The results from using the UDDS drive cycle offers significantly different results in terms of the Battery State-of-Charge (SOC) % and Fuel used data. Compared to NEDC results, for UDDS, the solver for Simulink battery model appears to generate rather dubious results (see Fig. 3-6(b)). While the NEDC drive cycle entirely consists of sections of constant accelerations and constant speeds, the UDDS drive cycle elicits relatively more aggressive driving with rapid accelerations and sudden braking. It therefore remains to be seen if the solver is suitable to be simulated for drive cycles of the type of UDDS. Interestingly, similar battery SOC% performance was observed when yet another drive cycle (MANHATTAN) was applied (Fig. 3-7(b)).

It is also noteworthy that the Simulink model allows the battery drain to zero with the UDDS drive cycle (see Fig. 3-6(b)). The mode logic of the model attempts to maintain a minimum SOC of 30%, however it is not being applied as specific parameters in the simulation. It appears then that some higher order settings are introduced that are outside the control of users using the software.



(a) *Urban Dynamometer Driving Schedule (UDDS)*

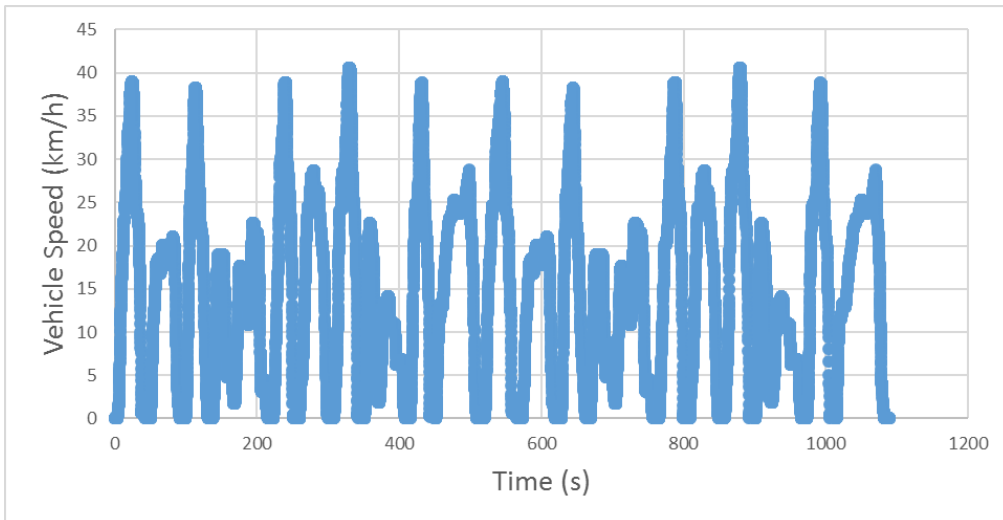


(b) *Battery State-of-Charge % history for the 2 simulation models over the UDDS*

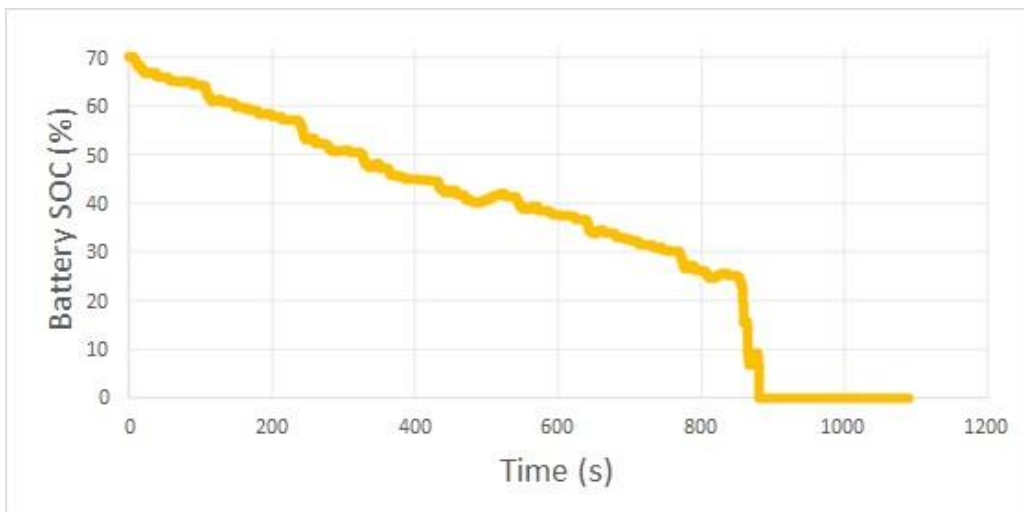


(c) Fuel used for the 2 simulation models over the UDDS

Figure 3-6: Simulation results for Simulink and ADVISOR models for UDDS



(a) Manhattan Drive Cycle

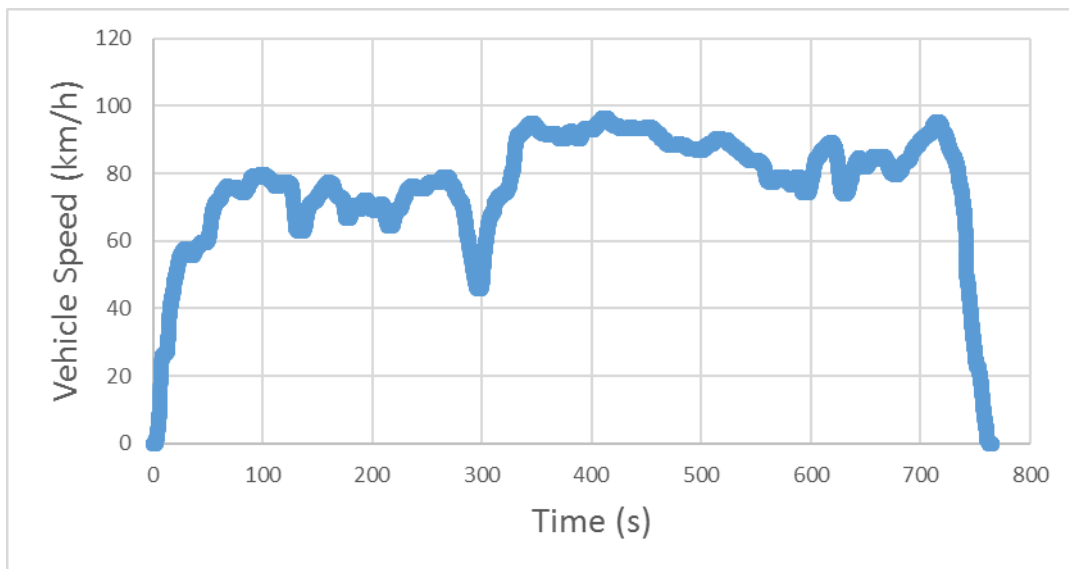


(b) Battery State-of-Charge % history for the Simulink model over the Manhattan DC

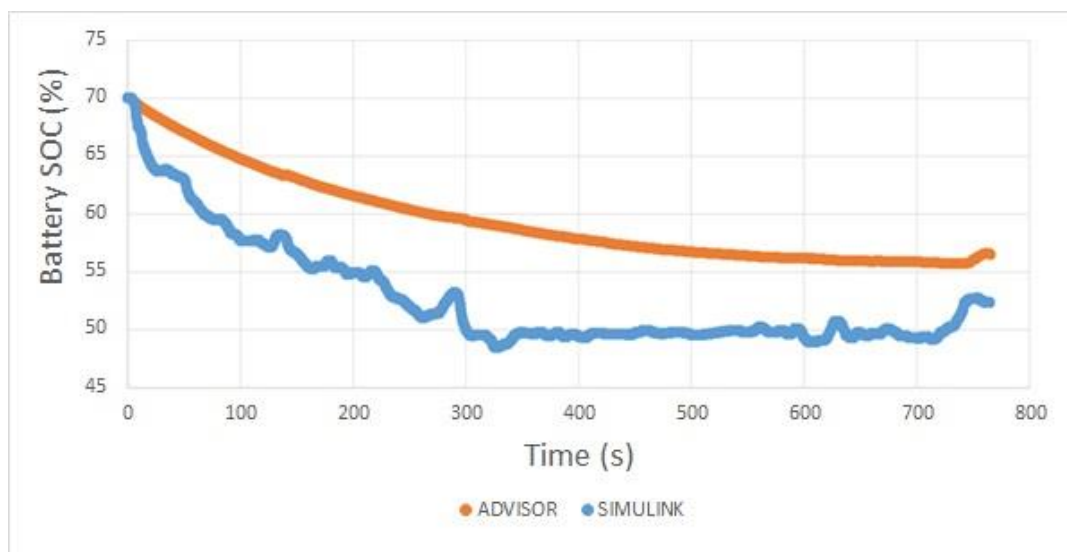
Figure 3-7: Simulink model simulation results for the Manhattan drive cycle

In the case of the HWFET drive cycle, the Battery State-of-Charge (SOC) % correlates well for both software (Fig. 3-8(b)). However, the fuel used data for the 2 software was vastly different compared to the NEDC drive cycle. In particular, the difference for NEDC between the SOC% of the batteries and fuel used were 3.29% and 0.258 litres respectively, while the corresponding figures for HWFET were 4.18% and 0.380 litres.

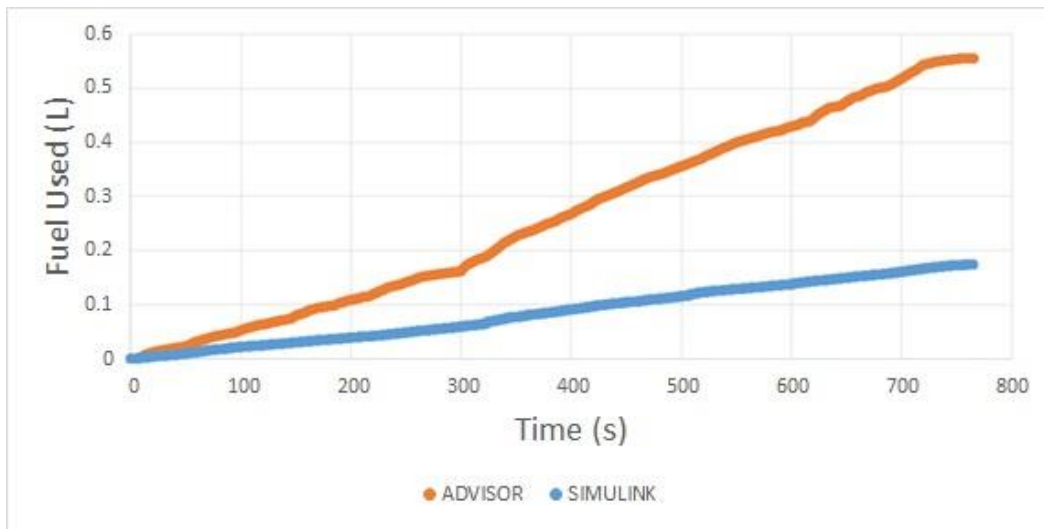
One possibility for this discrepancy is that the Simulink model might have been optimised to perform well for older legislated drive cycles such as the NEDC. This drive cycle has not been in use since September 2017. Alternatively, it may indicate the manner in which the solver operates in the Simulink model that is causing the irregularities. Notwithstanding the instability of the Simulink model makes it too dubious for use in HEV studies.



(a) Highway Fuel Economy Test Driving Schedule (HWFET)



(b) Battery State-of-Charge % history for the 2 simulation models over the HWFET



(c) Fuel used for the 2 simulation models over the HWFET

Figure 3-8: Simulation results for Simulink and ADVISOR models for HWFET

3.5 Conclusions

The MATLAB Simulink Model and ADVISOR have been evaluated to learn the suitability of the software to study the feasibility of incorporating hybrid electric powertrains to ambulances. The MATLAB Simulink Model only yields logical results under the NEDC drive cycle. The exact cause for its inability to produce the same with the UDDS, Manhattan, and HWFET drive cycles is difficult to uncover due to the complex manner in which the algorithm is configured.

While ADVISOR delivers logical distributions of Battery State-of-Charge (SOC) % and fuel use data, its closed form makes it difficult to be incorporated into traffic simulation software like VISSIM. Furthermore, ADVISOR lacks the provisions to extensively study the ambulance equipment power problem. Nevertheless, the Battery State-of-Charge distributions can still help to guide decisions on whether to adopt hybrid vehicles as ambulances. It is noteworthy that the availability of electrical power in ambulances is vital in order to maintain operation of key instrumentation like ventilators and defibrillators when they are needed.

4 Characterizing emergency ambulance travel response to disrupters

4.1 Introduction

Understanding the delays caused during emergency ambulance travel is important, in order to formulate effective intervention methods. When exploring types of delays caused within ambulance transfer times, a certain aspect overlooked by researchers are delays caused during non-light-and-siren (NLAS) ambulance travel. These delays add to the overall turnaround time of ambulances. Therefore, in this chapter first, possible interrupts caused during NLAS ambulance travel are identified. Then the ambulance response to these interruptions are analytically characterised, which will prove important in devising future remedial measures to minimise overall ambulance transport and turnaround times.

4.2 Background

Emergency medical services are generally not subject to road traffic regulations when light-and-siren (LAS) transfer protocols are applied in emergency situations. LAS protocols are used on the premise that total ambulance transport time (dispatch-to-scene-arrival interval and scene-to-hospital-arrival interval) is significantly reduced and that timely transport of patients to definitive care will result in better clinical outcomes. In support of these suppositions, the use of LAS has been demonstrated to result in significant time saving in both urban and rural settings [110], [111]. Furthermore, increase in transport time as a function of distance travelled was also associated with increased mortality in a generalized study of life threatening morbidities excluding out-of-hospital cardiac arrest cases [112], [113]. The case against the use of LAS in rendering emergency services relates to mounting evidence of risks of injuries and fatalities to emergency medical services personnel, patients and the public as a result of ambulance collisions [114]. Exposure of emergency medical services personnel to high-noise levels from the sirens (typically in the range of 100 dB) presents significant discomfort as well as risks of occupational hearing loss [115], [116]. Importantly, significant differences in heart rate, blood pressure, cortisol, somatotropin, adrenocorticotrophic hormone, epinephrine,

norepinephrine, and lactate have also been found between participants taken on ambulance rides with or without LAS [117].

Emergency transportation, especially without warnings with the use of LAS, can be affected by the presence of travel disruptors. This may occur when a pedestrian attempts to cross the road, or when a car in an adjacent lane moves into the same lane the ambulance is travelling on. While sounding a horn in such situations may provide the necessary warning to abrogate these actions, the ambulance will still need to slow down and then accelerate back to its intended travel speed, resulting in an increase in travel time. In this work, a multi-modal traffic flow simulation software VISSIM (PTV Group, Karlsruhe, Germany) will be used to generate the condition where an ambulance travelling on a two-lane road encounters a stationary vehicle that attempts to move into its lane. Based on the speed-time distributions obtained, analytical relations to characterize this condition are devised. These relations, which are far easier to use compared to conducting traffic flow simulations repetitively, will in turn guide future efforts to devise the appropriate traffic interventions needed.

4.3 Theory

Speed control and reduction measures, or sometimes known as calming measures, is a known aspect of traffic management [118]. Devices such as speed bumps and speed raised medians are most commonly implemented due to their cost effectiveness. The speed profile of a vehicle under calming measures assumes a deceleration followed by acceleration characteristic (see Fig. 4-1) which together makes up the influence zone [119]. The speed profile of an ambulance vehicle subjected to a disruption is expected to follow a similar characteristic.

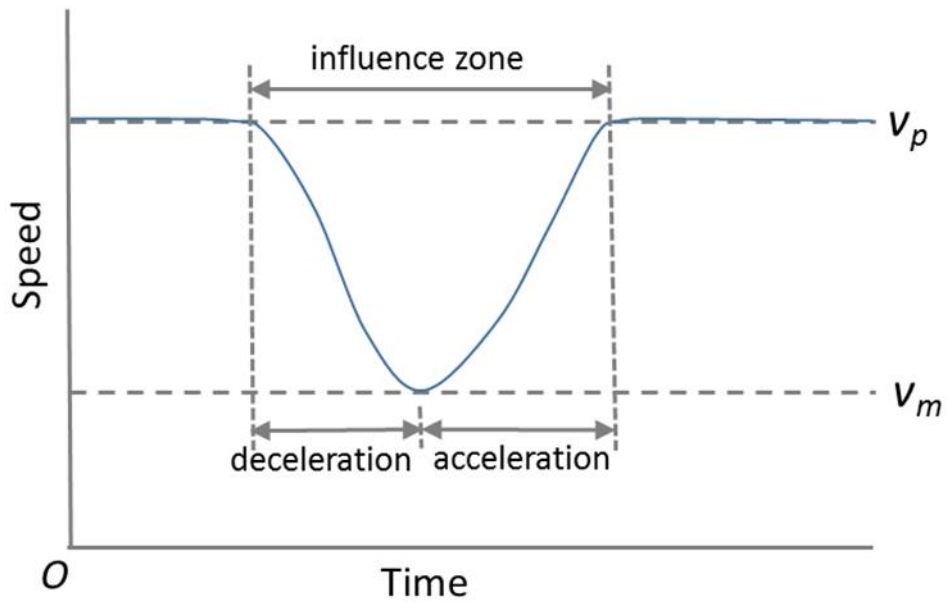


Figure 4-2: Depiction of the expected speed-time profile of a vehicle undergoing traffic calming or an ambulance subjected to disruption, which has deceleration and acceleration zones that make up the influence zone. In the process, the vehicle has its travel speed v_t reduced to a minimum speed of v_m

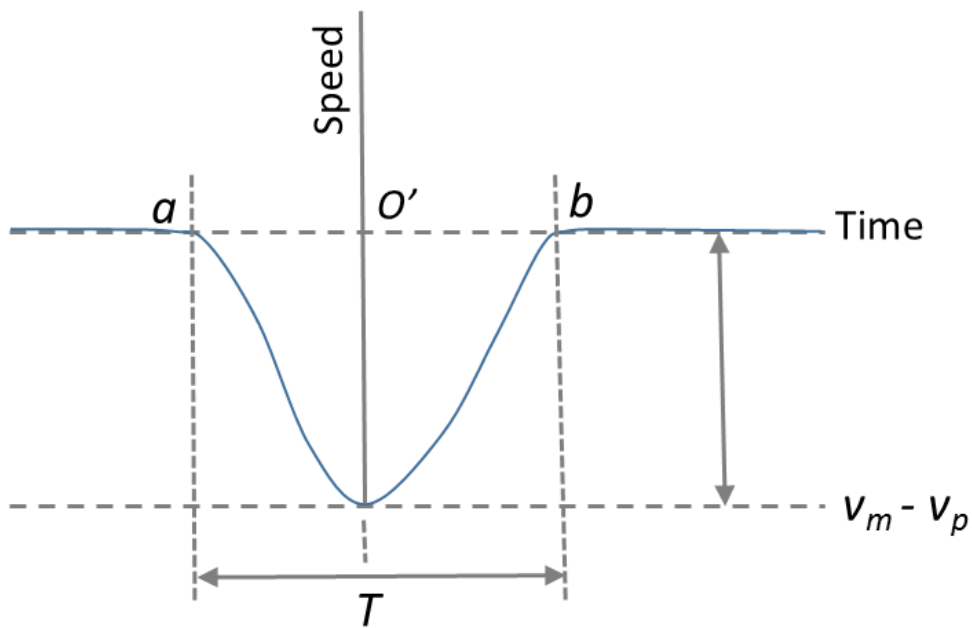


Figure 4-1: On locating the minimum in the curve in Fig. 4-1, it is possible to use it to shift the speed and time axes to coincide with a new origin O' . This altered curve allows scaling correspondence, distance lost due to disruption, as well as analytical depiction of the process using polynomials to be conducted

For every planned travel speed v_p , the distance between the ambulance and disruptor d will alter the speed profile as shown in Fig. 4-1. It is possible, however, that the shape of the speed profile remains unchanged. If this is the case, it will be possible to devise an analytical depiction by deriving a general polynomial function. To verify this, the first step will be to use the minimum speed in the profile (which is the easiest to determine) as a pivot point. From this, it will be possible to shift the origin O of the speed and time axis in Fig. 4-1 to a new origin O' in Fig. 4-2. Suppose that the polynomial based on the shortest distance for disruption is d_o . From the altered speed-time profile (as in Fig. 4-2), the method of least squares allows the variance between the values from the polynomial and the expected values from a dataset to be estimated. In doing so, it will be possible to find the coefficients of the polynomial regression (a_0, \dots, a_k) by solving the following system of linear equations

$$\begin{bmatrix} N & \cdots & \sum_{i=1}^N x_i^k \\ \vdots & \ddots & \vdots \\ \sum_{i=1}^N x_i^k & \cdots & \sum_{i=1}^N x_i^{2k} \end{bmatrix} \begin{bmatrix} a_0 \\ \vdots \\ a_k \end{bmatrix} = \begin{bmatrix} \sum_{i=1}^N y_i \\ \vdots \\ \sum_{i=1}^N x_i^k y_i \end{bmatrix} \quad (1)$$

Once the polynomial constants are obtained, the use of the Generalized Reduced Gradient (GRG) algorithm will permit the values of a and b of the curve in Fig. 4-2 to be determined by solving to zero. The GRG handles both equality and inequality constraints. Inequality constraints are converted to equalities by the use of slack variables, in which

$$g(X) = 0 \text{ where } X = \{x_1, \dots, x_n\} \quad (2a)$$

$$g(X) + x_{n+1} = 0 \quad (2b)$$

This then converts the unconstrained problem into a constrained one, whereby through an iterative process of searching, if S^q is the search direction and α is the step size, then

$$\bar{x}_{q+1} = \bar{x}_q + \alpha S^q \quad (3)$$

Gradient information is used to arrive at a solution by finding the steepest decent. This approach has been shown to be robust [120]. It is noteworthy that the area under the curve in Fig. 4-2 equates to the lag in distance experienced by the vehicle when it encounters the disruption. This area is determined by integrating the polynomial between the bounds of a and b .

The ability to scale is determined by comparing these with values associated with the shortest distance for disruption d_o . There are two ways to scale the velocity-time profiles at any other

disruption distance d to the velocity-time profile at d_o . In the first instance, only the velocity magnitude is scaled. Hence, the values of $(v_m - v_p)$ are modified using the time variable t according to a scaling factor K such that

$$(v_m - v_p)'(t) = K[v_m(t) - v_p(t)] \quad (4)$$

In the second approach, both the time variable t and values of $(v_m - v_p)$ are modified according to the scaling factor K such that

$$t' = tK \quad (5a)$$

$$(v_m - v_p)'(t') = K[v_m(t') - v_p(t')] \quad (5b)$$

Using the appropriate value of K , the values in Eq. (4) or (5b) should correspond well with all values of $(v_m - v_p)$ under the disruption distance d_o .

4.4 Simulation Methodology

A microscale simulation environment (via VISSIM) was used in this study to assist in the evaluation of the proposed method. In the scenario where a moving ambulance is subjected to a disruption, the simulation was set up to portray the situation where a stationary vehicle in an adjacent lane on the left attempts to move into the lane of an ambulance travelling at constant speed. It is then programmed to abort this lane changing manoeuvre midway, and returns to its original lane, under the assumption that the oncoming ambulance has applied its horn to warn of its presence. The environment created was that of a section of a two-lane road with standstill traffic on the left-hand lane, which includes a designated disruptor vehicle, and the right-hand lane is free of any other traffic, to allow the ambulance to maintain a constant speed (see Fig. 4-3). The link parameters are initially set such that vehicles on the left lane are blocked from changing into the right lane. In addition, the ambulance is required to travel on the right-hand lane at all times, to provide consistency to the model. Due to the limited number of vehicle

classes available on the software, the ambulance is depicted as a heavy goods vehicle (HGV) since it most closely matches the size and weight of a typical ambulance in Australia.

While the simulation is modelled within the VISSIM environment, the scenario is implemented in MATLAB (MathWorks, Natick, MA) through the VISSIM Component Object Model (COM) interface. The COM interface allows the user to manipulate the attributes to various objects in VISSIM during the simulation to enable the user to model the desired circumstances [121]. The attributes of the objects that are to be managed included, timing the introduction of the ambulance, and timing the attempted lane change of the designated disruptor vehicle. The simulation was run for a certain period first until the traffic on the left-hand lane is built up to a halt. The ambulance is then added to the simulation at the start of the link, on the right-hand lane, at a planned constant speed v_p using the relevant COM commands. While the ambulance is in motion, the designated disruptor vehicle is made to move on to the right-hand lane at a predetermined distance d ahead of the ambulance, and then moved back into the left lane (its original lane) within a duration of 0.6 seconds. This value was selected to reflect the general conditions of driver responses to auditory signals [122]. Two planned travel speeds (40 and 50 km/h) were interrogated in order to adhere to the general guidelines given to ambulances travelling under such traffic conditions. At both speeds, the simulation queried for data for values of $d = 5\text{m}, 7.5\text{m}, 10\text{m}, 12.5\text{m}, 15\text{m}, 17.5\text{m}, 20\text{m}, 22.5\text{m},$ and 25m .

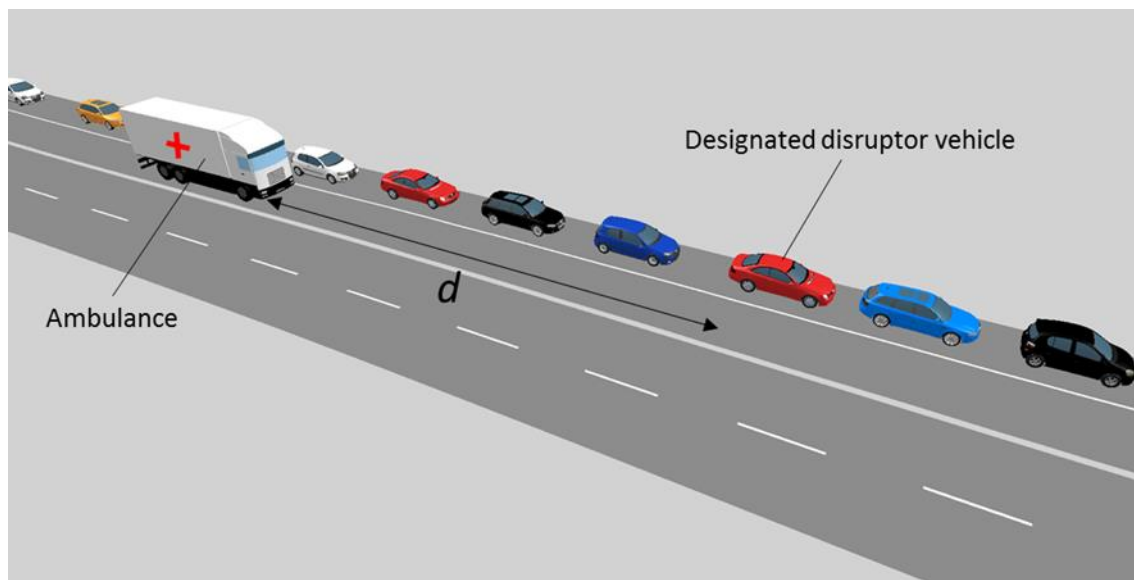


Figure 4-3: Simulation (using VISSIM) of an ambulance on one lane subjected to a designated stationary vehicle located a distance d ahead that turns out briefly.

4.5 Results & Discussion

The speed-time profiles planned travel speeds (40 and 50 km/h) at various values of d are given in Fig. 4-4. They show the general characteristic given in Fig. 4-2 but with some differences. It is clear in all cases that the deceleration phase occurred over a shorter period than the acceleration phase which is unlike the case of vehicles encountering calming measures, in which both phases are typically equally long [119]. This can be explained by the former lacking signboards that herald a speed hump or speed raised median, which then forces the driver to apply reactionary responses for speed adjustment. During the deceleration phase, it can also be seen that the time taken for the vehicle to slow down from the planned travel speed to the minimum speed is about the same. This again demonstrates a reactionary response in action. Finally, there was a minimum distance (5 m), in which values lower than this would indicate a collision. In studies of such nature, the post encroachment time (PET) is a parameter that is often used and refers to the time difference between two vehicles that passes a common spatial zone. The minimum distance found here translates to the time headway to incursion that coincides with the PET having zero values [123]. These characteristics provide indication that the simulation tool is able to replicate the conditions in real life well.

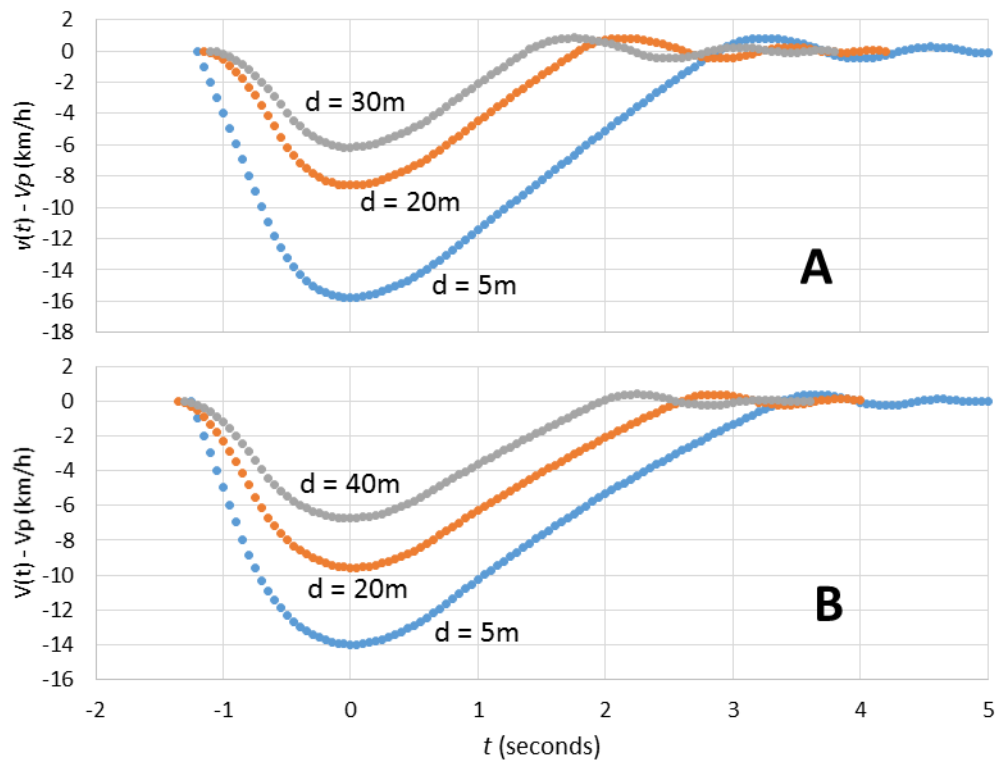


Figure 4-4: Plots of $v(t) - v_p$ against time (taken with reference to when minimum speed occurred) for (A) $v_p = 40$ km/h, and (B) $v_p = 50$ km/h at various values of d (distance between ambulance and disrupter).

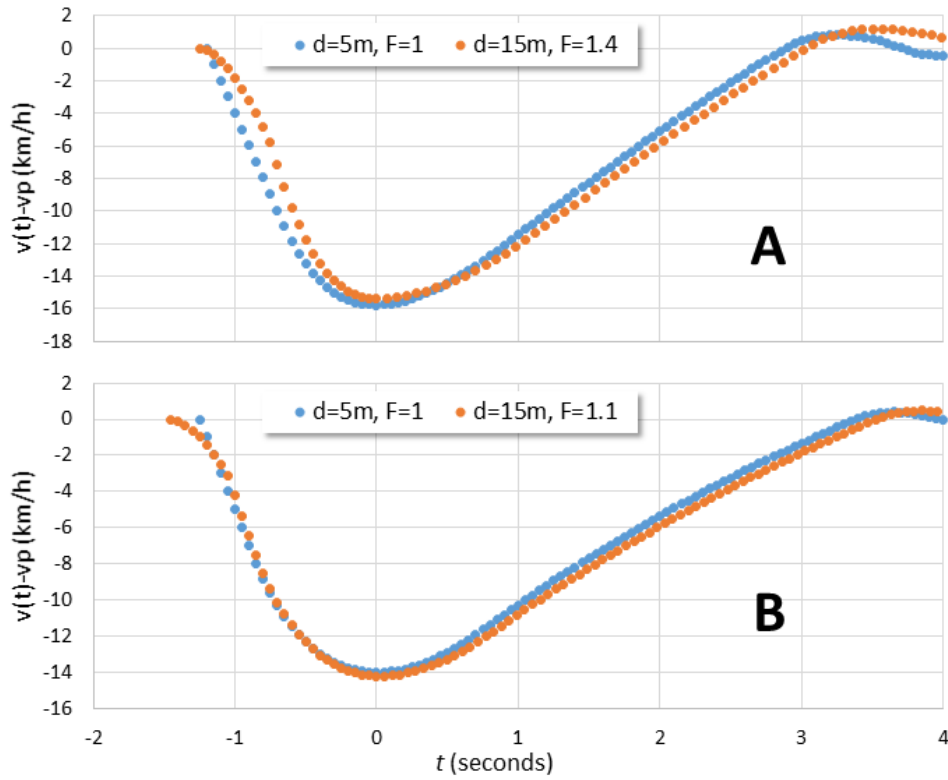


Figure 4-6: Plots of $v(t) - v_p$ against time (taken with reference to when minimum speed occurred) for (A) $v_p = 40$ km/h, and (B) $v_p = 50$ km/h at $d_0 = 5$ m. The plots of $v(t) - v_p$ against time with $d = 15$ m when modified using $F = 1.4$ ($v_p = 40$ km/h) and $F = 1.1$ ($v_p = 50$ km/h) using the proposed scaling method provided good correlation.

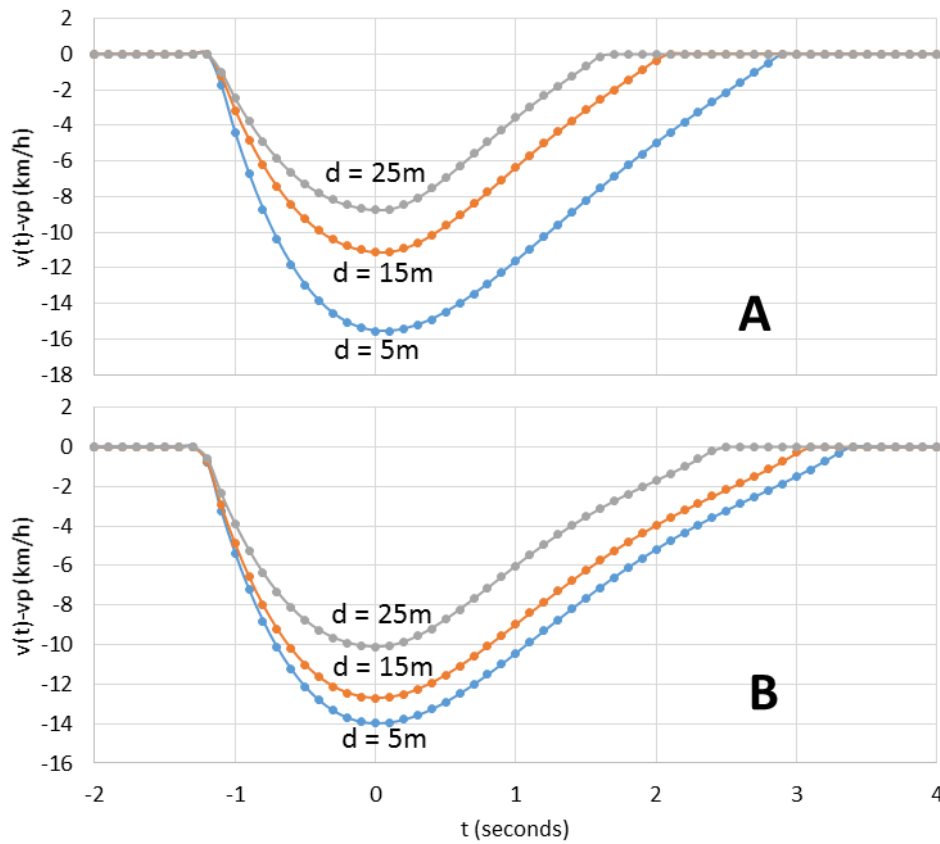


Figure 4-5: Plots of $v(t) - v_p$ against time recreated using the analytical function involving polynomials in Eq. (7) for (A) $v_p = 40$ km/h, and (B) $v_p = 50$ km/h for various values of d .

	$v_p = 40 \text{ km/h}$	$v_p = 50 \text{ km/h}$
d	F	F
10.0	1.02	1.05
12.5	1.20	1.07
15.0	1.40	1.1
17.5	1.69	1.34
20.0	1.72	1.36
22.5	1.75	1.37
25.0	1.78	1.38

Table 4-1: Tabulation of the best fit scaling values of F for $v_p = 40 \text{ km/h}$, and $v_p = 50 \text{ km/h}$ at various values of d to match with the plots of $v(t) - v_p$ at $d_o = 5\text{m}$.

The plots in Figs. 4-4A and B indicate different scaling characteristics for $t < 0$ and $t > 0$. In the former, only the values of $(v_m - v_p)$ needed to be scaled while both t and $(v_m - v_p)$ should be scaled in the latter. In other words, Eq. (4) is applicable when $t < 0$ and Eqs. (5A and B) can be applied when $t > 0$. This scaling approach provides good correlation results as seen in Fig. 4-5. Table 1 presents the best fit scaling values of F at various values of d to match with the plots of $v(t) - v_p$ at $d_o = 5\text{m}$ for the cases in which $v_p = 40 \text{ km/h}$, and $v_p = 50 \text{ km/h}$. With these values it is then possible to apply analytical relations based on polynomials to generate $v(t) - v_p$ against time to account for the disruptions without any further need to use VISSIM simulations.

The plots of $v(t) - v_p$ at $d_o = 5\text{m}$, have been found to be adequately described using polynomials of the fourth power such that

$$(v_m - v_p)(t) = a_4 t^4 + a_3 t^3 + a_2 t^2 + a_1 t + a_0 \quad (6)$$

It has been found that with $v_p = 40 \text{ km/h}$, $a_4 = 0.3611$, $a_3 = -2.7774$, $a_2 = 7.161$, $a_1 = -0.8218$, $a_0 = -15.548$; while with $v_p = 50 \text{ km/h}$, $a_4 = 0.2981$, $a_3 = -2.3345$, $a_2 = 5.767$, $a_1 = -0.1854$, $a_0 = -13.971$. Using these polynomial constants, the velocity-time profiles for various values of K (to account for varying values of d) for $v_p = 40 \text{ km/h}$ and $v_p = 50 \text{ km/h}$ can be created using

$$\begin{aligned} (v_m - v_p)(t) &= (a_4 t^4 + a_3 t^3 + a_2 t^2 + a_1 t + a_0)/K & t \leq 0 \ \& \ (v_m - v_p) < 0 \\ (v_m - v_p)(t') &= (a_4 t'^4 + a_3 t'^3 + a_2 t'^2 + a_1 t' + a_0)/K & t > 0 \ \& \ (v_m - v_p) < 0 \\ (v_m - v_p)(t) &= 0 & \text{otherwise} \end{aligned} \quad (7)$$

where $t' = Kt$. Fig. 4-7 presents the results of the analytical generation with polynomials, which show good correlation with the results in Fig. 4-4 obtained with VISSIM simulation. This confirms the ability to obviate using VISSIM simulations to obtain information on the disruptions.

In order to find the time delay caused by disruption (which has important significance in emergency ambulance transport), it will be necessary to first find the area under the velocity-time curve. This requires establishing the bounds a and b (Fig. 4-2) that make up the influence zone. With the constants of the analytical fourth power polynomial functions determined, these bounds can be established using the GRG algorithm outlined earlier. With $d = 5\text{m}$, the values of a and b are -1.159 s and 2.883 s respectively for $v_p = 40\text{ km/h}$, and -1.229 s and 2.883 s for $v_p = 50\text{ km/h}$. At other values of d (until 25 m), the values of a are unchanged to that at $d = 5\text{m}$, while b is simply found by dividing the value at $d = 5\text{m}$ by K . Once a and b are established, the area under the curve (representing distance D due to slowdown from disruption) can be determined using

$$D = \int_a^0 (v_m - v_p) dt + \int_0^b (v_m - v_p) dt' \quad (8)$$

The slowdown in time due to the disruption T can then be found using

$$T = Dv_p \quad (8)$$

The results shown in Fig. 4-7 indicate that time delays were generally higher with $v_p = 40\text{ km/h}$. This is a logical outcome, as the ambulance would be travelling at a slower speed to start off with and the reduction in speeds tended to be the same (Fig. 4-4) for the same value of d . The time delay from closer disruptions (i.e. $d = 5\text{m}$) was much higher at $v_p = 40\text{ km/h}$ than at $v_p = 50\text{ km/h}$. With disruptions that are located increasingly further away, these differences reduced. At $d = 15\text{m}$, these differences were almost non-existent.

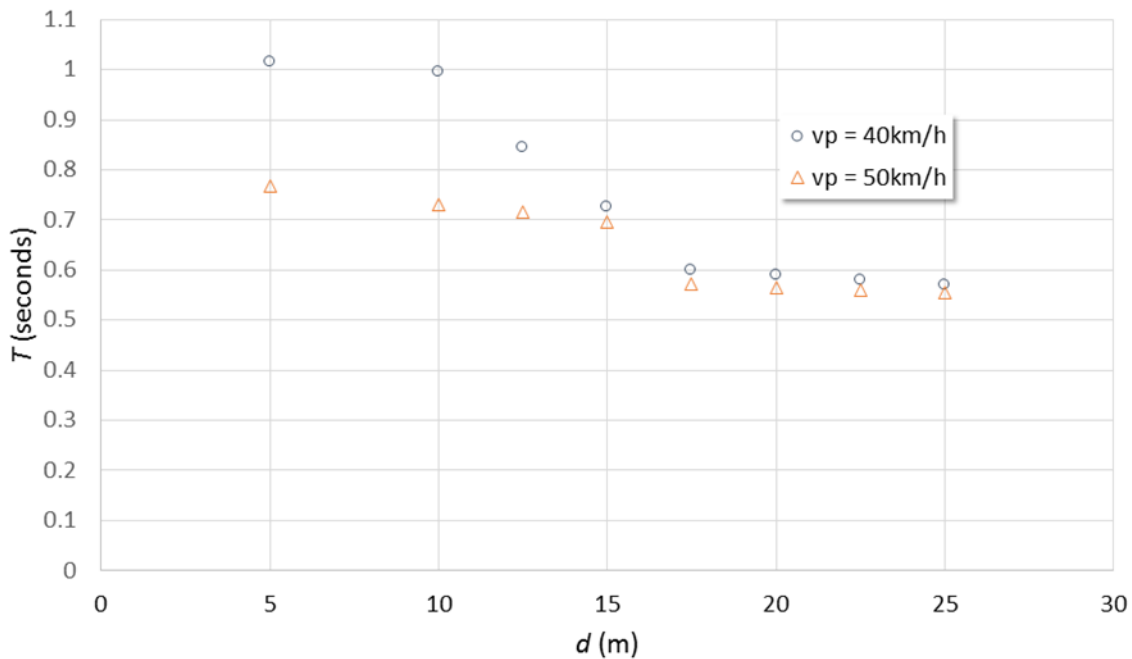


Figure 4-7: Plots of time delays (T) with disruptors located various distances d for $v_p = 40$ km/h, and $v_p = 50$ km/h

It is important to note that the values in Fig. 4-7 represent the time delay resulting from one disruption event. In the course of ambulance dispatch to scene arrival and departure from scene to hospital, numerous disruption events could occur along the way, leading to significant losses in time which can be determined by a simple summing up step. Clearly, an ability to reduce the number of disruption events is crucial to capitalize on hastened ambulance travel in metropolitan areas. This is a crucial point to consider when planning to introduce pre-emptive measures, through redirection of traffic for instance, as a remedy. If the ambulance is directed to use alternative stretches of road that is shorter in distance, but has heavy vehicle and pedestrian traffic, the increase in possible disruptions will negate the benefits presumed. Disruption events can be reduced through the use of LAS but with the attendant problems as previously mentioned. It is also noteworthy that the level of sound itself is not necessarily the only factor involved. Studies have shown that the ability of road users to localize alarm sources quickly while driving or walking plays an important role. It has been established that the binaural cues that represent the difference in arrival time and level of the sound between the two ears: the inter-aural time difference (ITD) and the inter-aural level difference (ILD), is responsible for decoding the direction of arrival of the sound [124], and this can lead to greater challenges for the elderly to respond to LAS [125]. There is also potential usefulness in incorporating physical responses related to disruptions in simulation training of emergency

medical service personnel [126] or in the design of devices to reduce sudden movement to patients [127].

4.6 Conclusions

It has been found here that VISSIM simulations provided realistic depictions of velocity-time characteristics of ambulances responding to disruptions. They have similarities and differences to vehicles responding to traffic calming conditions. The analytical relations involving the use of fourth power polynomials makes it possible to develop a generalized means of accounting for time delays associated with these disrupters without the need to run the simulations each time. This tool will help in exploring solutions for minimising ambulance transfer time delays, and the formulation of strategies for traffic management needed to cope with the increasing demand for emergency ambulance transportation in the future.

Work in this chapter has been included in Samarasinghe, S. K. et al. Characterizing emergency ambulance travel response to disrupters. Proceedings of IMechE Part H: Journal of Engineering in Medicine. Favourable 1st Review.

5 UAV based measurement of vehicle travel

5.1 Introduction

With the ever-increasing challenges of managing traffic volume and congestion, researchers have continually been exploring the use of intelligent traffic management systems [128]. The importance of quick and accurate traffic data collection therefore is further highlighted to ensure efficient operation of traffic management systems. Furthermore, consequent analysis of traffic data has been vital to the development of microscopic and macroscopic traffic simulation models [128]. However, traffic data collection especially for longer spans of roadway, has been difficult due to a combination of the process being labour-intensive and requiring large permanent infrastructure [129].

One of the promising approaches hence recently being used in traffic data collection and traffic flow studies are Unmanned Aerial Vehicles (UAVs) [130], [131]. UAVs, more commonly referred to as drones, are mobile imaging systems that provide high resolution data airborne, useful in traffic flow studies [130]. With the ability to cover expansive areas in quick time [128], drones have the advantage of mobility and are extremely cost-effective compared to traditional methods of traffic monitoring, such as induction loops, microwave sensors, and fixed surveillance video camera systems [132]. Cost savings can further be achieved as all equipment of a UAV is reusable owing to requirements of the given purpose [133]. Additionally, UAV maintenance can be carried out off-site causing no congestion in traffic [132]. Their mobility means the ability offer reconnaissance and rapid assessment of a site of an emergency, where no fixed traditional methods of monitoring are installed, or is inaccessible for humans [134], [135]. Therefore, considering the encouraging potential of UAVs in future traffic related studies, in this chapter we use this novel technology for data acquisition in the presented work.

Studies have indicated that vehicle speed and speeding is at the core of the road safety problem and is a major contributor to fatal accidents [136], [137]. Measures such as traffic calming are widely taken to be an effective approach in vehicle speed management and therefore able to reduce road fatalities. Yet, it is necessary to note that traffic calming measures can result in greater fuel consumption and exhaust gas emission [35], [138], [139]. Furthermore, traffic calming can have significant impacts on ambulance transport times [38], an increase of which

is associated with increased mortality in a generalized study of life threatening morbidities [113].

Traffic calming measures (TCMs) can be carried out using means such as speed cameras [140], speed limits [141], and speed alerting devices [142]. However, the impact of these types of TCMs on ambulance travel may be minimal. Speed bumps on the other hand, the most common physical traffic calming interventions used in urban areas, may impact ambulance travel significantly. They are essentially abrupt raised areas on the road which is jarring to motorists and thus serve as deterrents to using high travel speeds. Speed bumps are a cost effective method to reduce vehicle speeds and the reduction of motor vehicle collisions [143]. A number of studies investigating the impact of TCMs (including speed bumps) on emergency vehicles have been conducted [34]–[39]. Garcia et al [38] found that in some cases ambulances were diverted more than 1 km to avoid areas with TCMs, adding delays of up to 40 seconds. Therefore, characterising an ambulance response to a TCM such as a speed bump may help understand the delays expected on a given route. Incorporating the findings from the previous chapter on ambulance response to disrupters, this new information may be used in formulation of traffic management strategies to minimise delays in ambulance transfer times.

5.2 Materials and Method

The two scenarios to be experimented was an instance of ambulance encountering a speedbump (scenario 1), and an instance of ambulance experiencing a disruption while cruising at constant velocity (scenario 2). The experiments were conducted at locations of 37°54'02.8"S, 145°07'51.6"E and 37°54'16.6"S, 145°07'55.6"E (both located within an industrial precinct) respectively. A stretch of straight road with a single speed bump along the route was deemed suitable for the first scenario. The length of this stretch was such that the vehicle is able to reach a desired velocity of travel before encountering the speed bump, and accelerate back up to the initial speed after overcoming the speed bump. A different location without TCMs, a section of straight road of sufficient length that would allow the vehicle to reach constant velocity, and then accelerate to same velocity after experiencing a disruption, was chosen for the second scenario. In this scenario, one of three participants standing adjacent to the road was randomly asked to raise a flag to simulate a disruption to the vehicle driver. All tests were

conducted on weekends and at a time where vehicle travel in the vicinity was at its absolute minimum.

Due to the difficulty of arranging for an ambulance, a cargo delivery van was used in the experiment as its specifications and drivability would reliably compare to a vehicle model used for a type II ambulance. The vehicle used, was a 2019 Toyota HiAce SLWB (Diesel) which compares to the Mercedes-Benz Sprinter used by the Ambulance Service of New South Wales [144] (Fig. 5-1). The drone used to obtain high quality video footage of the vehicle movement, was a DJI Phantom 4 Pro (Fig. 5-2). Two images taken from the video recordings for two scenarios can be seen in Fig 5-3.



Figure 5-1: (a) The 2019 Toyota HiAce SLWB (Diesel), the vehicle model used in the experiment [145]; (b) a modified Mercedes-Benz Sprinter that forms a part of the type II ambulance fleet at Ambulance Services of NSW [146].



Figure 5-2: The Quadcopter, DJI Phantom 4 Pro used to obtain aerial video recordings of vehicle movement [147].

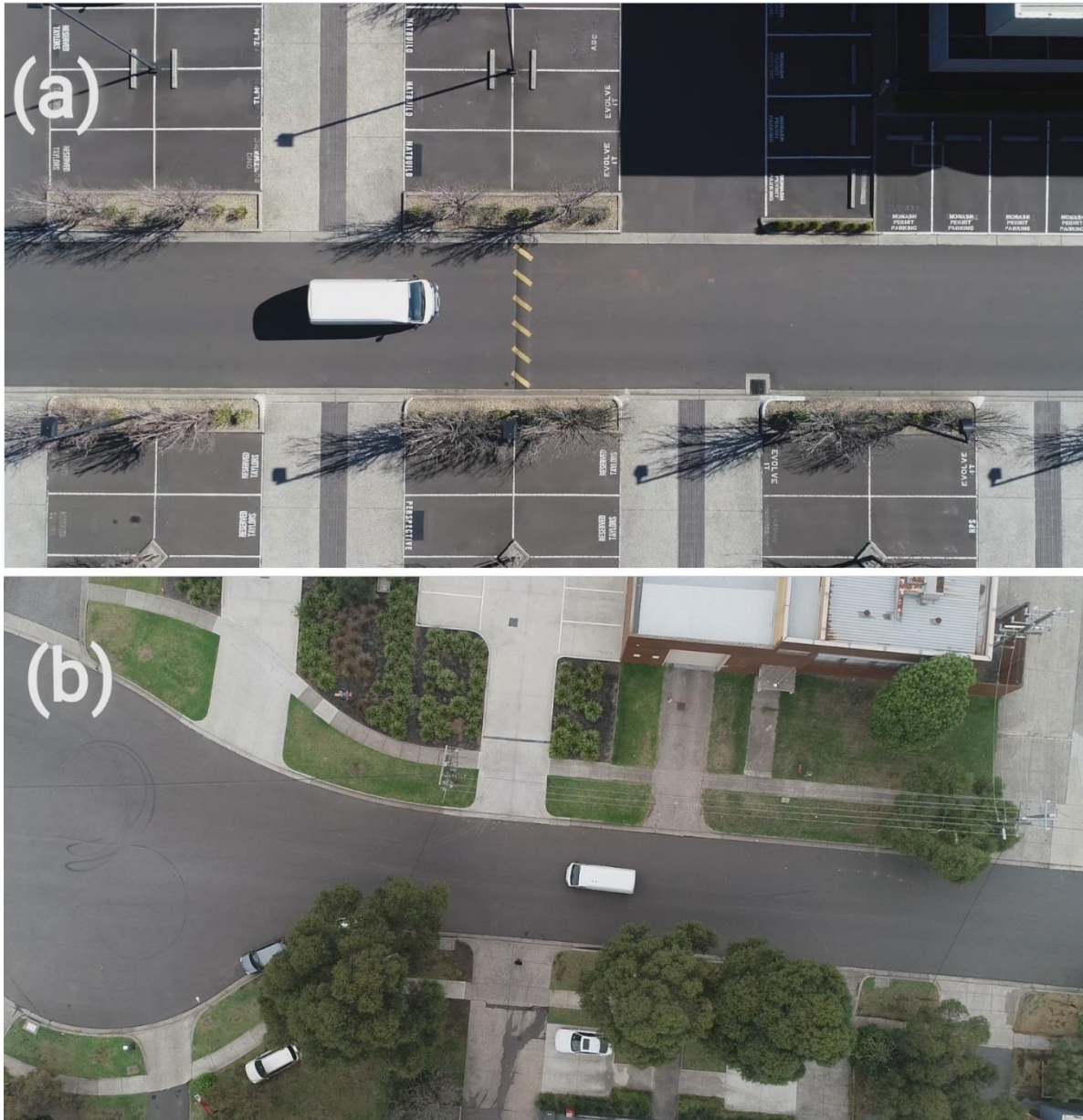


Figure 5-3: Aerial images recorded with the drone of the test vehicle (a) negotiating a speed bump, and (b) experiencing a disruption.

A video analysis and modelling software, Tracker, developed by Open Source Physics was used for processing video recordings. Based on pre-measured locations at the recorded scenes, the scaling aspects relating pixel size (in the image) to actual distance was established. The tool was then used to measure the van position from frame to frame by tracking a designated point on the van (Fig. 5-4). The instantaneous speed of the van was then calculated using the positional data, and the time between each frame. These calculated values were then used to obtain speed-time distributions of the van for each vehicle trip in both scenarios.

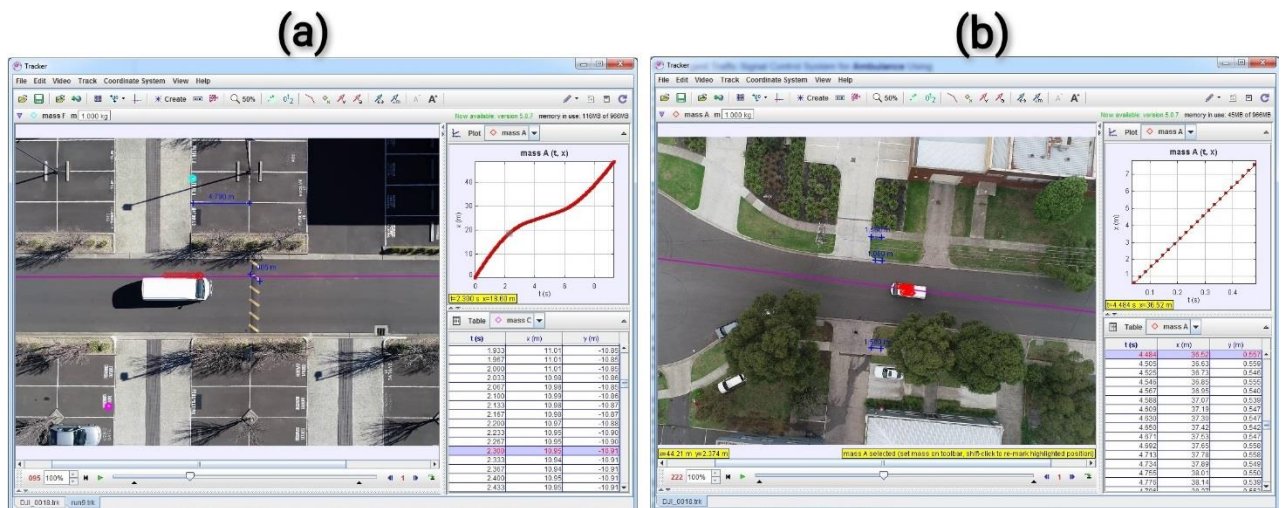


Figure 5-4: Video footage acquired from UAV, being processed to obtain positional data for the van on Tracker, a video analysis and modelling software.

5.3 Results and Discussion

Examples of two speed-time distributions obtained from raw video processed data, for each scenario is shown in Fig. 5-5. Similar to in chapter 4, the distributions obtained were adjusted to a new origin, by shifting speed and time axes based on the planned travel speed v_p , and median time value or time value at minimum speed (minimum value is not always the median due to scattering of data points). This altered curve allows scaling correspondence, distance lost due to braking, as well as analytical depiction of the process for better comparison. The adjusted curves for the two speed-time distributions in Fig. 5-5 for each scenario, is shown in Fig. 5-6.

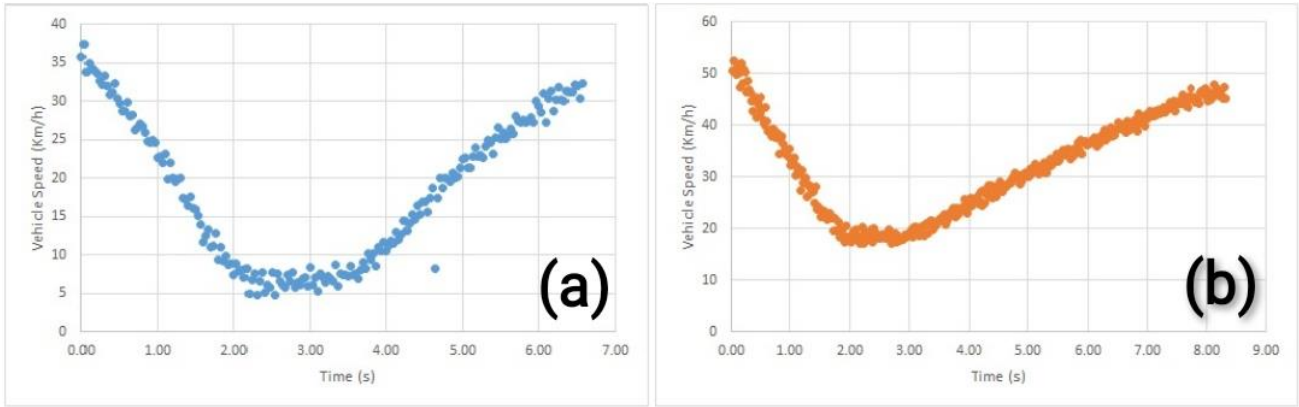


Figure 5-5: An example of a speed-time distribution obtained from video processed data for; (a) van overcoming a speed bump, (b) van experiencing a disruption.

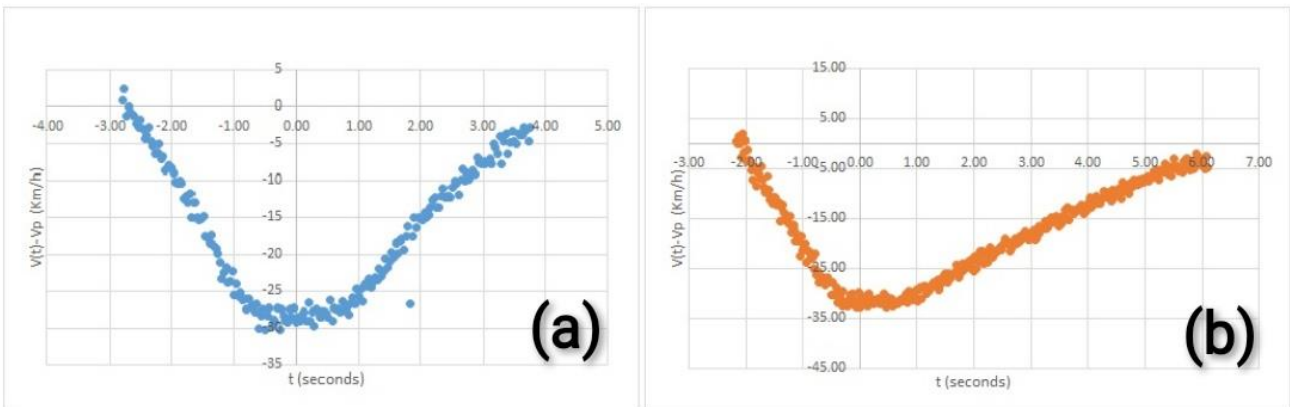


Figure 5-6: The altered curves for respective speed-time distributions shown in Fig. 5-5.

To derive data with good fidelity, the drone was required to be kept at a fixed hovering position. However, this necessitated attaining a sufficient field of view in order to capture the motion of the vehicle as it negotiated through the traffic calming and disruption measures. The lowered levels of magnification engenders inaccuracy when determining the speed profiles. In addition, errors arose due to flight instability of the drone during hovering (due to wind, rotor vibration, etc.) and inherent image noise. Therefore, in spite of over ten video recordings being obtained for each scenario performed at a given travel speed, the five best (with least noise) speed-time distributions were altered as in Fig. 5-6, and then were used obtain an overall average curve for each scenario.

Fig. 5-7 shows the averaged curve obtained for scenario 1, the van negotiating a speed bump. The curve exhibits good correlation with the expected behaviour of a speed profile encountering a vertical change causing traffic calming measure, especially a speed bump [119].

The influence zone displays the near symmetrical characteristics of the braking and acceleration areas as noticeable in Fig. 4-1, which could be associated to the driver's prior knowledge of the obstacle, as opposed to a speed profile observed for scenario 2. Fig. 5-8 shows the averaged curve for the van experiencing an unexpected disruption (scenario 2). It can be observed that the shape of the curve matches reasonably to the speed profiles obtained via VISSIM simulations in chapter 4. This therefore indicates the feasibility of analytically characterising the ambulance response to a disruption, using data obtained from VISSIM simulations. The difference noticeable between the experimentally obtained data, and the VISSIM simulations however, is the deceleration for the replicated experiment, is higher than that for the VISSIM simulation. This can be attributed to the VISSIM simulation being defined a set duration for the disruption (0.6 seconds), while the disruption (simulated by a flag raised by a participant) duration for the experiment was relatively more difficult to gauge with this variable being dictated by the driver's understanding, indicating the human factor in the results.

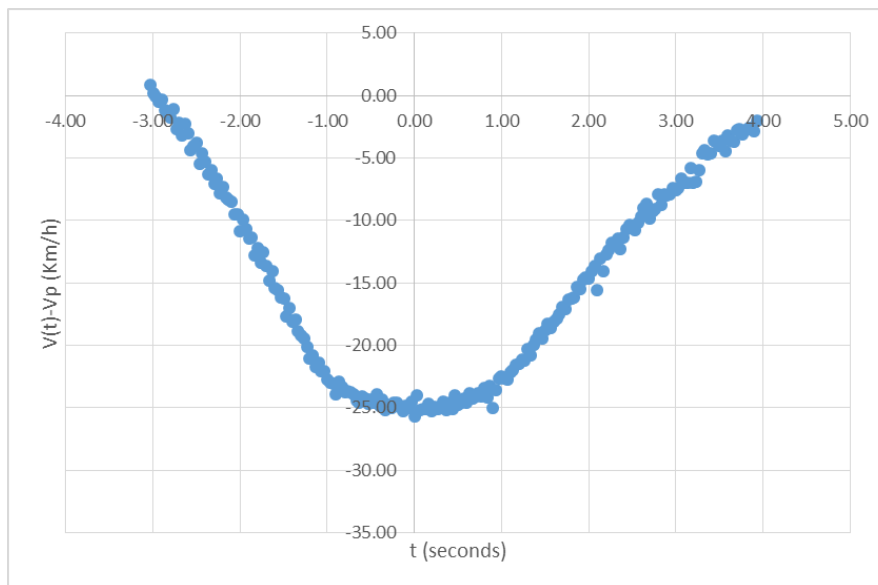


Figure 5-7: The averaged curve for the vehicle response overcoming a speed bump, generated using the five best speed-time distributions obtained from UAV video footage.

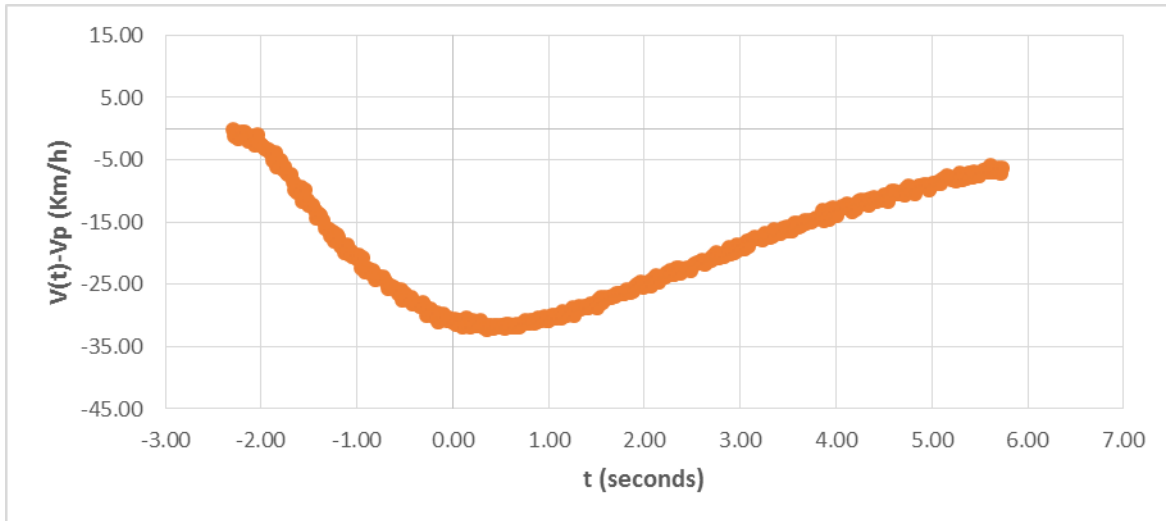


Figure 5-8: The averaged curve for the vehicle response experiencing a disruption.

Despite the averaged curves showing good correlation with the hypothesized and resulting speed profiles presented in chapter 4; as mentioned previously, only a limited amount of data was used to generate the averaged curves, and a considerably large dataset was discarded due to errors caused by flight instability and inherent image noise. Therefore admittedly, the shortage of usable data, and the excess of noisy data does not permit verification of the parameters used in the theoretical formulation. This is illustrated in the relatively large spread of the velocity profiles obtained in Figs. 5-9A and B. Nevertheless, the differentiated characteristics when the vehicle encounters a traffic calming device and disruption are still evident. Therefore, we envisage that improvements made to the accuracy of video data recording in terms of the hardware and software applied [148], significant undertakings in their own right, may assist in fine tuning these parameters.

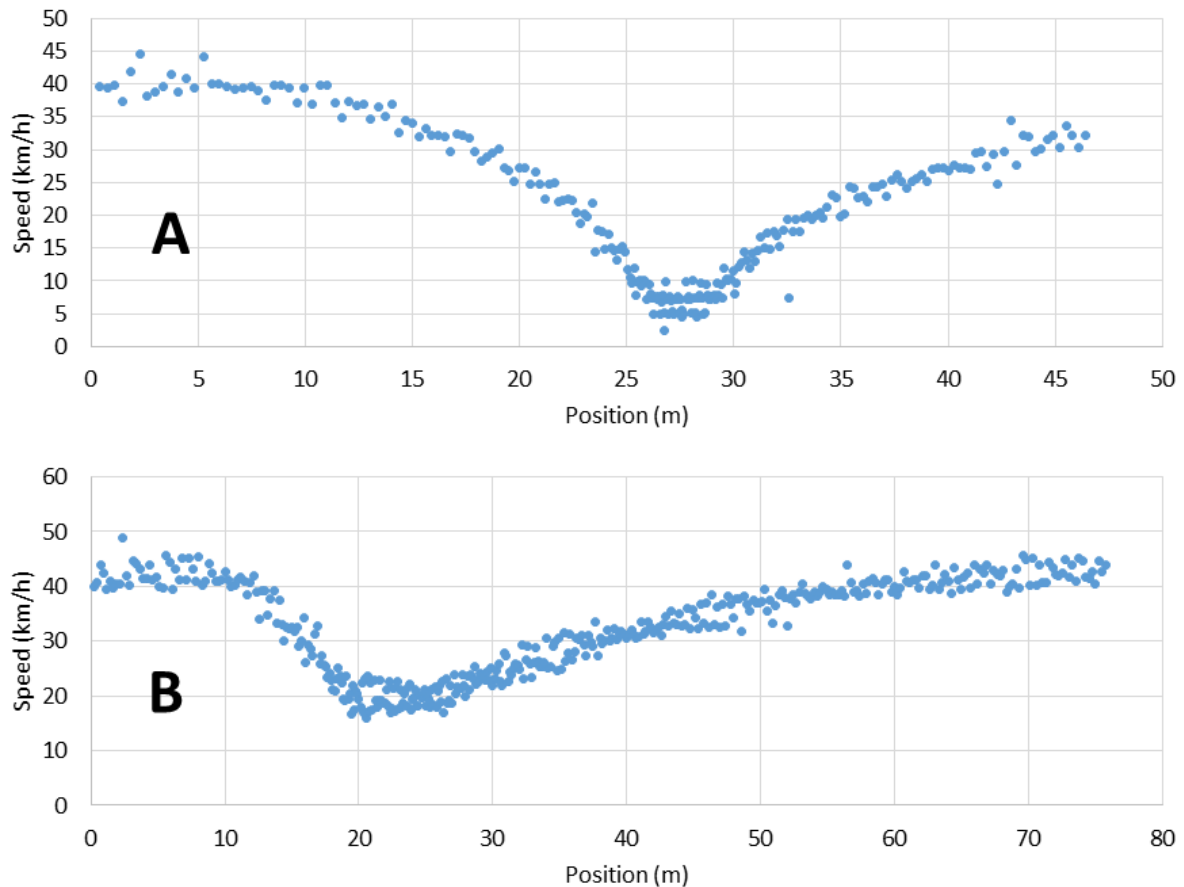


Figure 5-9: Speed profiles obtained from experimental video data of the test vehicle (A) negotiating a speed bump, and (B) undergoing a disruption. The initial travel speed was 40 km/h in both cases

5.4 Conclusions

The findings suggest that UAV have great potential in data acquisition for traffic flow and traffic management related studies. Under ideal weather conditions (especially wind speed), UAV video footage provided satisfactory data usable in the analysis of this study. The speed-time distributions obtained from video recordings for the two scenarios replicated, clearly showed the differentiable characteristics evident with when the vehicle encounters a speed bump, and when experiencing a disruption. Furthermore, the vehicle response to a disruption in this study displays good correlation with the ambulance response to a disrupter obtained through VISSIM simulations presented in the previous chapter. Therefore, this endorses the viability of using analytical relations generated from VISSIM simulation data in understanding delays that could arise with ambulance response times due to disruptions.

In spite of this however, it was observed that the usable data was few and far between with a large portion of the dataset being noisy. The errors were noticed to be caused by factors such as drone flight instability (due to wind, rotor vibration, etc.), inaccuracy surrounding the requirement of high magnification of footage, and inherent image noise. Nevertheless, we expect future improvements made to UAV technology, in terms of video recording stability, along with video processing software, may help fine tune these parameters.

Work presented in this chapter was mainly conducted by S.K. Samarasinghe, with contributions from M. Katariya, supervised by Associate Professor Tuck Wah Ng. Furthermore, the contribution of Nihal Samarasinghe in facilitating the controlled experiment on vehicle tracking is also appreciated. Parts of this chapter have been included in Samarasinghe, S. K. et al. Characterizing emergency ambulance travel response to disrupters. Proceedings of IMechE Part H: Journal of Engineering in Medicine. Favourable 1st Review

6 Sensor and actuator simulation training system for en-route intravenous procedure

6.1 Background

Trauma cases, although not dominant, form a significant portion of all calls for ambulance services, with over 40% of ambulance transfers being attributed to trauma related emergencies [149], [150]. Early venous access in trauma patients to permit the administration of fluids, or if necessary drugs such as anaesthetic, analgesic, and resuscitation agents is vital to improving survival outcomes [151]. The placement of a venous line is likely to be technically easier in the early stages of shock, before any hypovolaemia has progressed. It also prevents compensatory mechanisms from having the opportunity to cause any peripheral vasoconstriction. While early successful cannulation will save time when the patient arrives at the hospital, repeated and unsuccessful attempts, or the use of a cannula with the wrong gauge will be detrimental [152]. Apart from the introduction of intravenous fluids, the transfer time to the hospital is also another important factor affecting the positive outcomes for patients [8], [9]. If paramedics spent longer periods at the scene trying to administer pre-hospital fluid, this will cause a further delay in transfer, which then subjects the paramedic to scrutiny [42], [43]. One way to balance the benefits of gaining pre-hospital venous access without the risk of lengthening transfer times is to attempt cannulation en-route. While there is strong support for this approach [153], [154], there are attendant health and safety implications at play such as needle stick injuries [155]. The confidence level and skill of the paramedic in carrying this out effectively is a crucial factor for success.

Clinical skills laboratories have been widely acknowledged to be effective in providing a safe and protected environment where the learner can perform the procedures and rehearse competency skills in a simulated setting prior to execution in real situations [156]. A recent study has found that skills laboratory training enabled students to perform intravenous cannulation more rapidly, accurately and professionally than bedside teaching [157]. The use of trainer or manikin models is an indispensable feature in these programs [158]. To date, there has yet to be any training system reported that is able to furnish simulation exercises that mimic the transport conditions experienced by paramedics while attempting en-route intravenous therapies. The discomfort experienced in emergency transport vehicle rides has been widely

recognized to adversely affect the well-being of patients [159]. It is thus reasonable to assume that paramedics executing intravenous procedures under turbulent conditions may have their performances similarly impaired. Hence, the incorporation of training modalities that provide simulated motion environments for honing paramedic skills would be advantageous.

A well working simulation system will typically require the seamless integration of relevant technologies, as evidenced in recent reports of those advanced on other aspects of medicine and healthcare [160], [161]. It is noteworthy that numerous studies have been made to replicate the characteristics of vibration using electrodynamic shakers to understand their consequences during transport [162], [163]. The inputs introduced are mostly derived from generalized readings of vibration obtained via sampling studies in various scenarios [164], [165]. Yet, the levels of vibration can vary significantly according to a variety of factors, which include the route taken, vehicle used, expertise of the driver, and the level of urgency of the transport. The ability to attain full monitoring of the transport conditions in the vehicle itself, not just in the spatial but also temporal sense, and to physically impose these conditions in a controlled manner provides arguably the most realistic simulation possible. The monitoring approach is inherently different to incorporating embedded sensors on pavements which can provide highly accurate information but only at specific locations [166]. Logically it will be prohibitively expensive to introduce embedded sensors along all the routes that emergency vehicles can take.

Sensor technology has progressed at a phenomenal pace in the last decade due to progress in microelectromechanical systems (MEMS). This has resulted in a myriad of miniature and inexpensive transducers that can now be incorporated into generic devices such as smartphones. Smartphone sensing is an exciting field that is now being routinely adopted in a wide range of applications [167], [168]. Another area that has contributed positively towards sensor technology is in the proliferation of small micro-controllers such as the Arduino. This has also resulted in a myriad of applications which can now be tackled in a compact and cost-effective manner [169]–[171]. It is widely accepted that actuators which are configured to provide 6 degree of freedom (DOF) are arguably able to replicate motion realistically. Such functionally efficient control systems have a long history of applications in the development of simulators used in the automotive and aerospace industry [172].

In this work, we created a simulator system that utilizes MEMS-based sensors incorporated in smartphones or interfaced with an Arduino micro-controller to collect vibration and impact data during actual transport. This data is then relayed to a 6 DOF mechanical simulator that is

designed and developed to accurately replicate field spatial and temporal motions. This system was then tested to evaluate its performance. A preliminary study on how this system affects the cannulation performance of six volunteer participants will also be conducted.

6.2 Simulator Kinematics

The 6 DOF simulator developed is based on the use of revolute and spherical joints (Fig. 6-1). The base and platform origins are defined by the respective orthogonal Cartesian coordinates x, y, z and x', y', z' . Since the base is stationary, the platform origin has three displacement components with respect to the base. However, it will be more convenient to convert this to three rotations about the origin of the base; ψ (yaw) about the z -axis, θ (pitch) about the y -axis, and φ (roll) about the x -axis. The transformation matrix R that relates the coordinates on the base to that of the platform via

$$\begin{bmatrix} x \\ y \\ z \end{bmatrix} = R \begin{bmatrix} x' \\ y' \\ z' \end{bmatrix} \quad (1)$$

This matrix is the product of the respective yaw $R(\psi)$, pitch $R(\theta)$, and roll $R(\varphi)$ matrices, such that

$$\begin{aligned} R &= R(\psi) \cdot R(\theta) \cdot R(\varphi) \\ &= \begin{pmatrix} \cos \psi & -\sin \psi & 0 \\ \sin \psi & \cos \psi & 0 \\ 0 & 0 & 1 \end{pmatrix} \cdot \begin{pmatrix} \cos \theta & 0 & \sin \theta \\ 0 & 1 & 0 \\ -\sin \theta & 0 & \cos \theta \end{pmatrix} \cdot \begin{pmatrix} 1 & 0 & 0 \\ 0 & \cos \varphi & -\sin \varphi \\ 0 & \sin \varphi & \cos \varphi \end{pmatrix} \\ &= \begin{pmatrix} \cos \psi \cos \theta & -\sin \psi \cos \varphi + \cos \psi \sin \theta \sin \varphi & \sin \psi \sin \varphi + \cos \psi \sin \theta \cos \varphi \\ \sin \psi \cos \theta & \cos \psi \cos \varphi + \sin \psi \sin \theta \sin \varphi & -\cos \psi \sin \varphi + \sin \psi \sin \theta \cos \varphi \\ -\sin \theta & \cos \theta \sin \varphi & \cos \theta \cos \varphi \end{pmatrix} \quad (2) \end{aligned}$$

Let us suppose that joints on the base B_i and platform P_i are considered (see Fig. 6-2(a)). T is the translation vector that gives the positional linear displacement of the origin of the platform O' from the origin of the base O . If b_i is the translation vector of O to B_i , and p_i is the translation vector of O' to P_i , then the vector l_i from B_i to P_i can be expressed as

$$l_i = T + (R \cdot p_i) - b_i \quad (3)$$

Further calculation is needed in order to find the rotations needed at revolute joint B_i (see Fig. 6-2(b)). Naturally, the length of arms $B_i A_i$ and $A_i P_i$ are fixed. At B_i , suppose that β is the rotational angle from the x -axis, and α the rotational angle from the x - y plane. If the coordinates of B_i and A_i are (x_B, y_B, z_B) and (x_A, y_A, z_A) respectively, they are related to each other via

$$\begin{aligned} x_A &= a \cos \alpha \cos \beta + x_B \\ y_A &= a \cos \alpha \sin \beta + y_B \\ z_A &= a \sin \alpha + z_B \end{aligned} \quad (4)$$

where a is the fixed length between B_i and A_i . If the distance between A_i and P_i is s , applying Pythagoras theorem gives us

$$\begin{aligned} a^2 &= (x_A - x_B)^2 + (y_A - y_B)^2 + (z_A - z_B)^2 \\ s^2 &= (x_P - x_A)^2 + (y_P - y_A)^2 + (z_P - z_A)^2 \\ l^2 &= (x_P - x_B)^2 + (y_P - y_B)^2 + (z_P - z_B)^2 \end{aligned} \quad (5)$$

Since the coordinates of B_i are known, the coordinates of B_i and P_i as well as l can also be established. For any translation, yaw, pitch, and roll of the platform relative to the base, it will be possible to establish l_i from Eq. (3) and thus the coordinates of P_i from Eq. (5). Since β is known, it will be possible to determine α and thus the rotation of the arm that is connected to the motor at B_i .

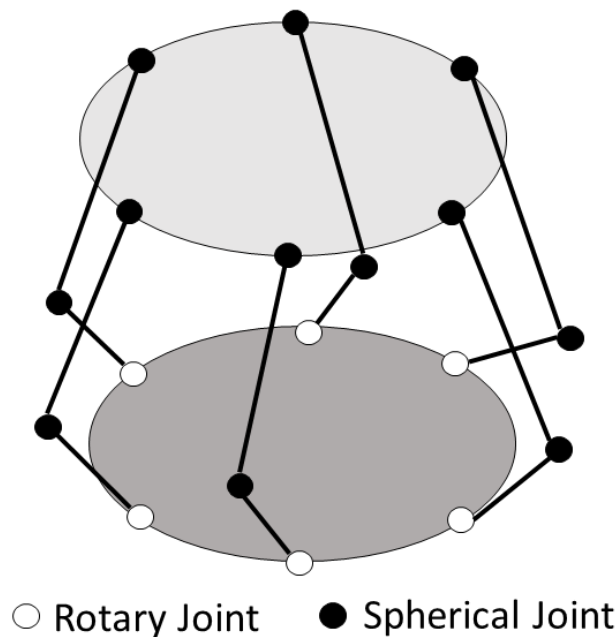


Figure 6-1: Schematic depiction of the 6 degree of freedom simulator which comprises 6 rotary and 12 spherical joints

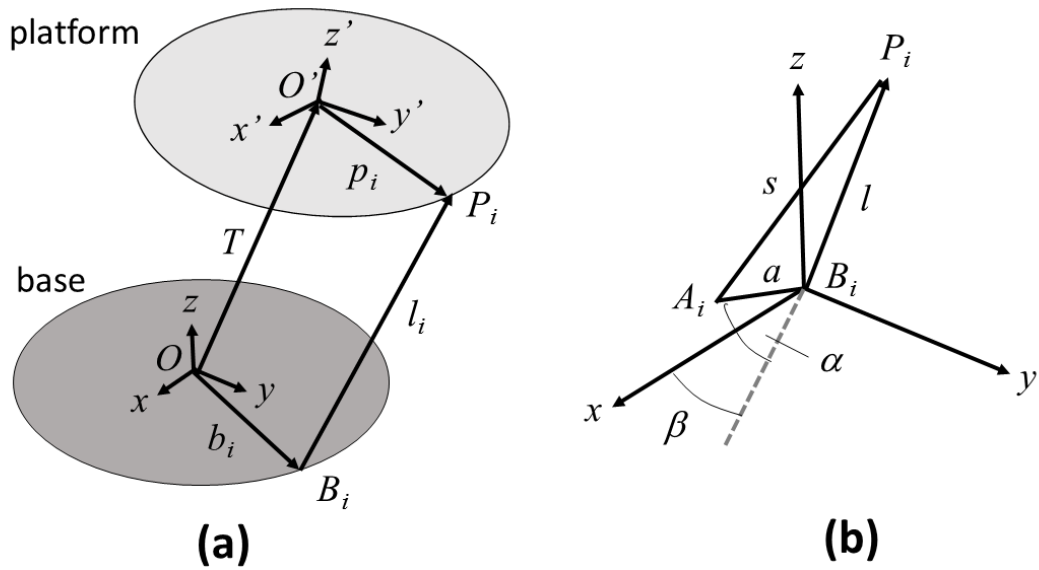


Figure 6-2: Depiction of (a) the vectors connecting points O and B_i on the base, and points O' and P_i on the platform, as well as the 3D positional depiction (b) of the links between B_i , P_i , and A_i . Since a and s , are fixed, the parameter to be determined is the angle α .

6.3 Materials and Methods

6.3.1 System Development and Evaluation

For micro-computer sensor recording, an inertial measurement unit (IMU) was used (LSM9DS0, ST Microelectronics). It is a system-in-package featuring a 3D digital linear acceleration sensor, a 3D digital angular rate sensor, and a 3D digital magnetic sensor. It has a linear acceleration full scale of $\pm 2g/\pm 4g/\pm 6g/\pm 8g/\pm 16g$, a magnetic field full scale of $\pm 2/\pm 4/\pm 8/\pm 12$ Gauss and an angular rate of $\pm 245/\pm 500/\pm 2000$ dps. The LSM9DS0 has an I2C serial bus interface that supports standard and fast mode data transmission (100 kHz and 400 kHz) and an SPI serial standard interface. It can be configured to generate interrupt signals on dedicated pins, and the thresholds as well as timing of interrupt generators are programmable. The IMU signals were fed into an ATmega328P single board microcontroller (Arduino Uno). It has 14 digital input/output pins (of which 6 can be used as PWM outputs), 6 analog inputs, a 16 MHz quartz crystal, a USB connection, a power jack, an ICSP header and a reset button.

It operates under a voltage of 5V and has a clock speed of 16 MHz. The device is highly compact with dimensions of 68.6 mm (length) by 53.4 mm (width), and weighing 25 g.

For smartphone sensing, readings were recorded using a custom designed Android application. The smartphone used was a Samsung Galaxy SIII. The application was programmed to record data from the in-built sensors into a text file to the external memory. The application logs data from the inbuilt accelerometer (LSM330DLC 3-Axis, ST Microelectronics). The LSM330DLC is a system-in-package featuring a 3D digital accelerometer and a 3D digital gyroscope. It has a dynamically user-selectable full-scale acceleration range of ± 2 g/ ± 4 g/ ± 8 g/ ± 16 g and angular rate of ± 250 / ± 500 / ± 2000 deg/sec. The application was able to log data at a maximum frequency of 100 Hz.

The 6 DOF motion simulator developed is based on the design shown in Fig. 6-1. Six servomotors (Hitec, HS-422) were used to serve as revolute joints as well as to drive arms of $a = 40$ mm (see Fig. 6-2(b)). Spherical joints were used to link the ends of this arm to rods in which $s = 175$ mm. The base and platform were made of aluminum in order to provide rigidity while limiting weight. The servomotors are controlled using an AMC1280USB motion controller board which receives instruction from 6-DOF BFF Motion Driver software via USB. The program performs the necessary kinematics to determine the required angles for each servomotor to produce the desired platform position.

Figs. 6-3(a) and 6-3(b) show the breakout board comprising the inertial measurement unit and the Samsung Galaxy SIII smartphone respectively that was used to collect the vibration and impact data from the field. This was done by attaching either of them on the dashboard of a vehicle (see Fig. 6-3(c)) travelling along poorly maintained roads. The x-axis was oriented along the direction of travel, while the z-axis was in the direction of gravitational action. The data collected was then used to drive the six servomotors on the 6 DOF simulator developed (see Fig. 6-3(d)) such that its platform replicated the motion experienced on the dashboard of the vehicle. In order to establish that this was achieved, data was collected from another breakout board with an IMU sensor attached to the bottom surface of the platform.

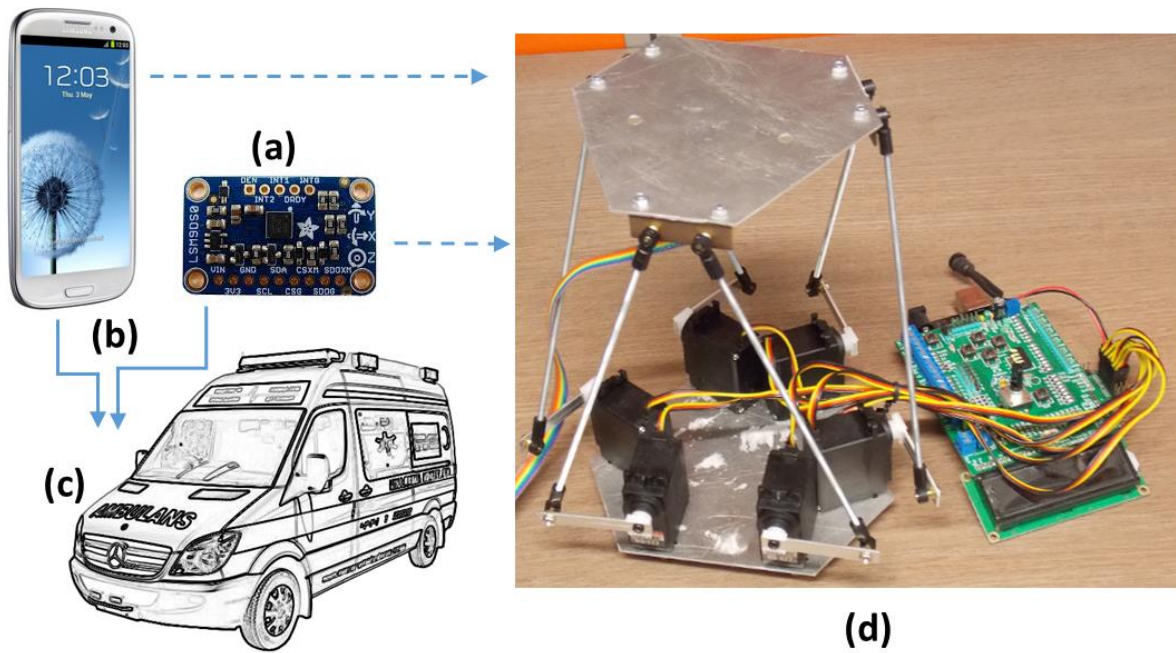


Figure 6-3: The simulator system that comprises either an LSM9DS0 inertial measurement unit breakout board (a), or a Samsung Galaxy SIII smartphone utilizing the in-built LSM330DLC chip (b), placed on the dashboard of a vehicle (c) to obtain accelerometer data. This data can then be fed into the 6 DOF simulator (with AMC1280USB motion controller board shown on the right) (d) to replicate the same movements encountered during vehicle travel.

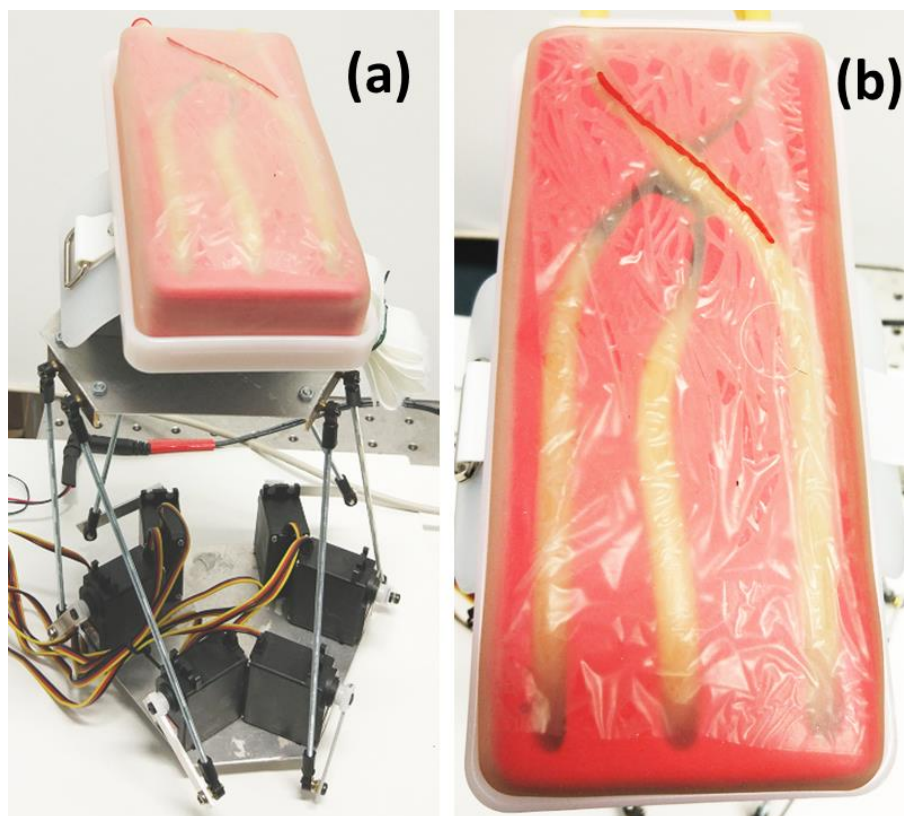


Figure 6-4: The venepuncture trainer attached to the platform of the 6 DOF simulator (a). A red line indicates the centre region of the "vein" on the trainer (b), in which a needle inserted into it is assumed to be optimal.

6.3.2 System Effects on Cannulation Performance

A venipuncture trainer (Venatech IV trainer) was attached firmly on the platform of the 6 DOF simulator (see Fig. 6-4(a)). During the performance tests, participants were required to insert a winged infusion set (Terumo, 21G x 0.75 inches) into the artificial vein a total of 7 times without and with the simulator running. The center location of the “vein” of the trainer is marked (see Fig. 6-4(b)) and insertion of the needle into this location is assumed to be optimal. The number of times in which the needle punctures into the center of the vein, into the vein but not at its center, and missing the vein altogether were recorded and tallied. The duration taken for each insertion attempt was also measured using recorded video footages.

A total of six volunteer participants were involved in the performance evaluation exercise. One of the participants is a registered nurse with twenty-two years working experience and had the qualifications to administer intravenous therapies to de-facto patients. The remaining participants did not have any prior experience and were given a short session on the basics of cannulation before conducting the exercise.

6.4 Results & Discussion

6.4.1 System Operation Evaluation

Fig. 6-5 presents typical accelerometer data obtained with vehicle transport using the IMU sensor board as it was placed inside a vehicle travelling over some rough terrain. The larger magnitude of the z-axis sensor is due to it registering the gravitational acceleration as well. The traces show that there were certain instances in which large fluctuations were present. These variations, of up to ± 0.4 g and ± 0.2 g in the x and y, as well as z axis respectively, meant that there would be substantial discomfort in the vehicle during transport.

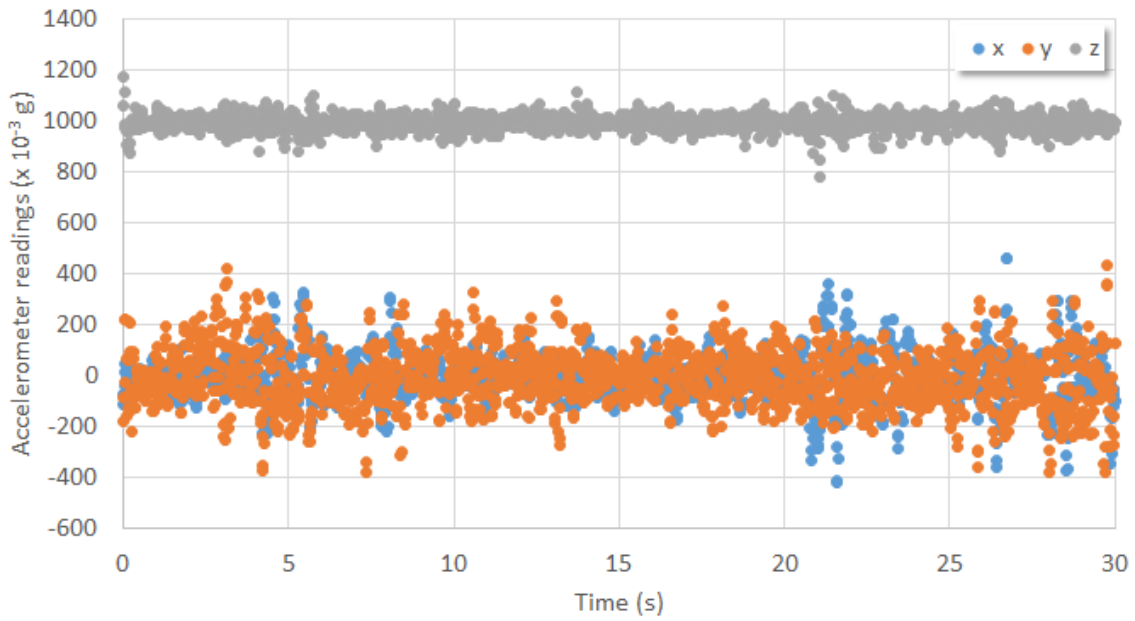


Figure 6-5: Sample accelerometer data obtained with vehicle transport using the LSM9DS0 inertial measurement unit breakout board. The roughness of the terrain is evident from the strong fluctuations within the 30-seconds recording of the travel.

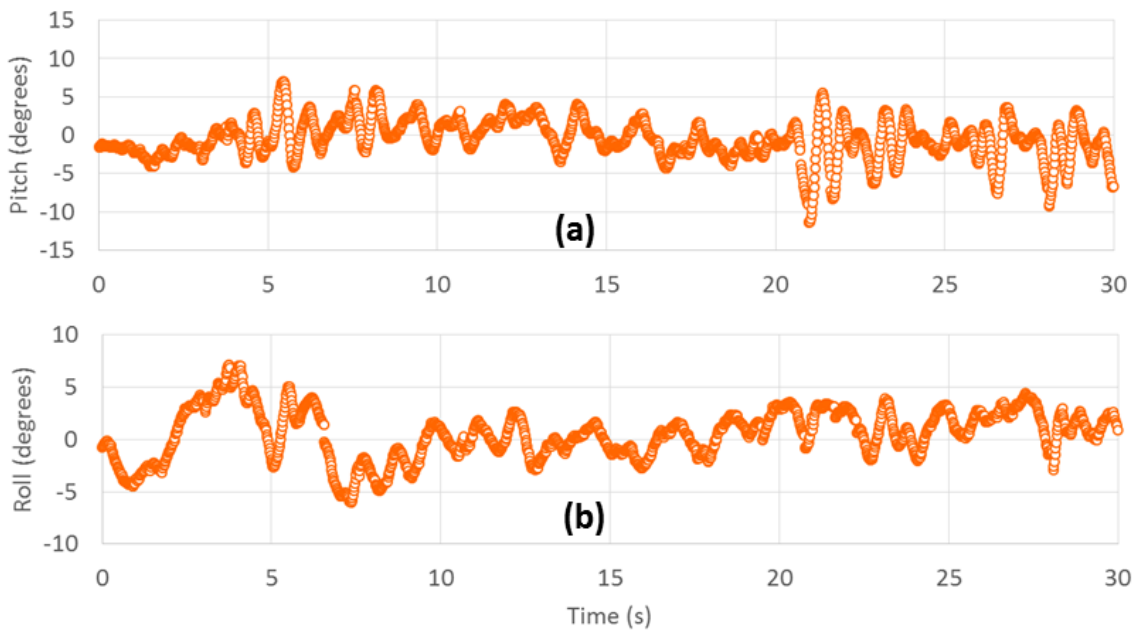


Figure 6-6: The pitching (a) and rolling (b) of the 6 DOF simulator platform used to replicate the pitching and rolling trends in Fig. 6.

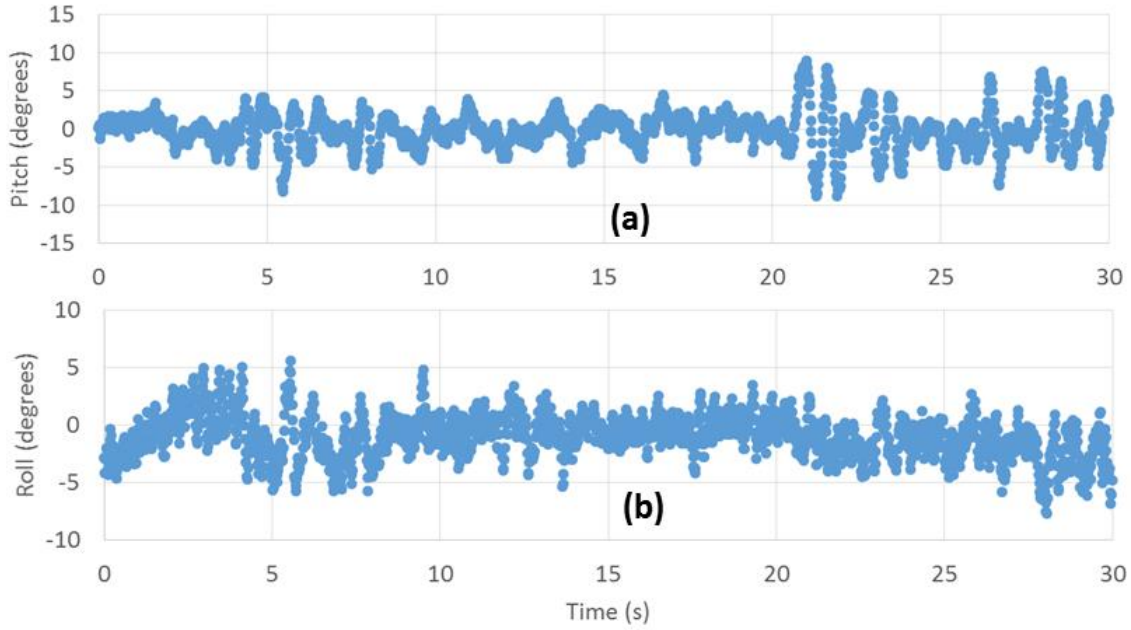


Figure 6-7: Calculations of the pitching (a) and rolling (b) of the vehicle's dashboard from the acceleration data in Fig. 5.

Based on the acceleration values in Fig. 6-5, calculations of the degree of pitching and rolling on the dashboard of the vehicle (where the sensor was placed) gave the distributions shown in Fig. 6-6. The degrees of fluctuation ($\pm 10^\circ$ in pitching, $\pm 7.5^\circ$ in rolling) reinforce the earlier contention of discomfort. When this data was fed into the simulator system, the pitching and rolling distributions of the platform (recorded using another sensor board located at its bottom) are that given in Fig. 6-7. In order to compare these values in a quantitative manner, a normalized differencing metric S_d was introduced at each time point t for the pitch and roll signals detected on the vehicle S_v and the platform S_p

$$S_d(t) = \frac{S_p(t) - S_v(t)}{S_p(t) + S_v(t)} \quad (6)$$

The distributions of S_d this, given in Fig. 6-8 for pitching (a) and for rolling (b), reveal a large majority of signal points centered around the zero value within the time period sampled. This imputes general good correlation between the distributions in Figs. 6-5 and 6-6. The extent or error lies predominantly in the outlier points which is the natural outcome in view of differences in the movement and recording responses of the simulator platform and sensor respectively. The outlier points can be identified using the Grubb's test [27] in which the test statistic can be determined from

$$G = \frac{S_d(t) - \langle S_d \rangle}{\sigma(S_d)}$$

$$G = \frac{\langle S_d \rangle - S_d(t)}{\sigma(S_d)} \quad (7)$$

whereby $\langle S_d \rangle$ and $\sigma(S_d)$ are the mean and standard deviation respectively of the distribution. In a two-tailed test, outliers are then identified when for a t -distribution and $N - 2$ degrees of freedom and significance level of α

$$G > \frac{N-1}{\sqrt{N}} \sqrt{\frac{t^2_{\alpha/(2N), N-2}}{N-2 + t^2_{\alpha/(2N), N-2}}} \quad (8)$$

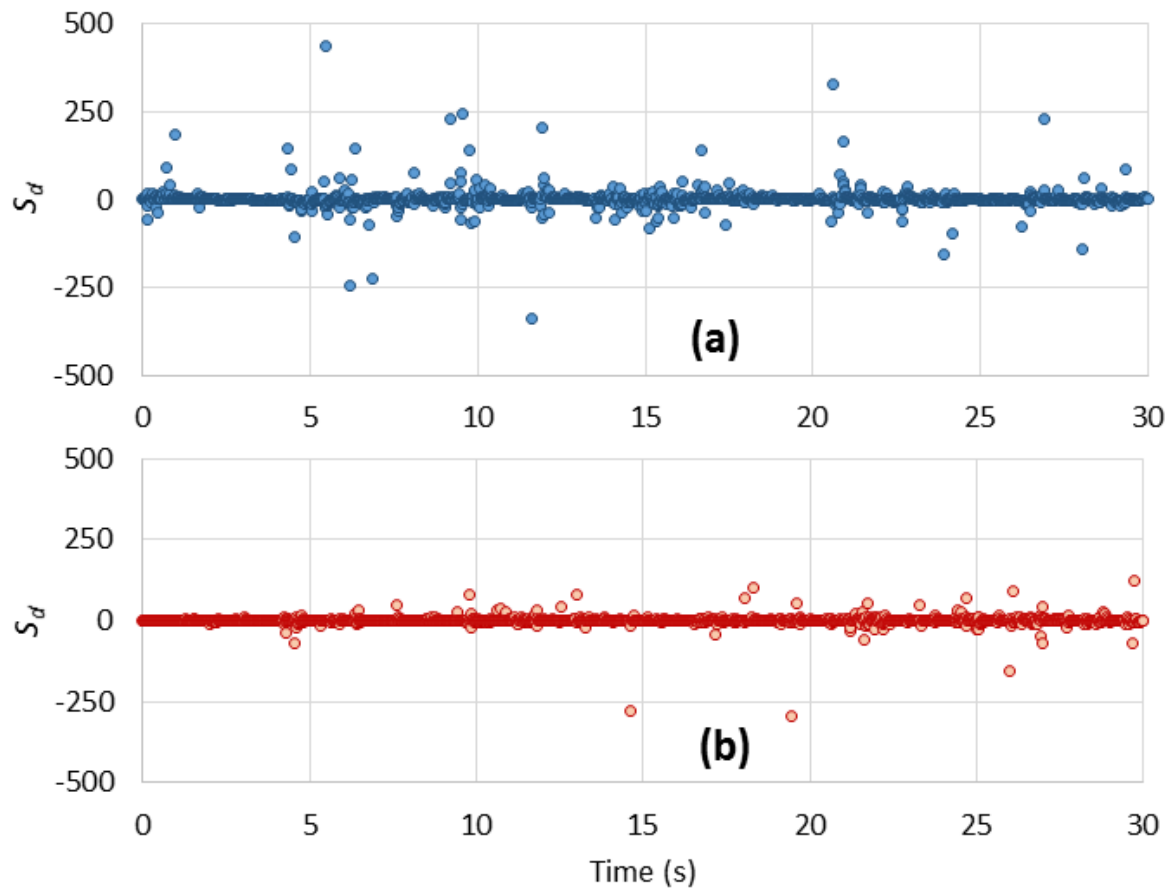


Figure 6-8: Plots of the normalized differencing metric distribution calculated to compare the results in Figs. 6 and 7 under (a) pitching, and (b) rolling.

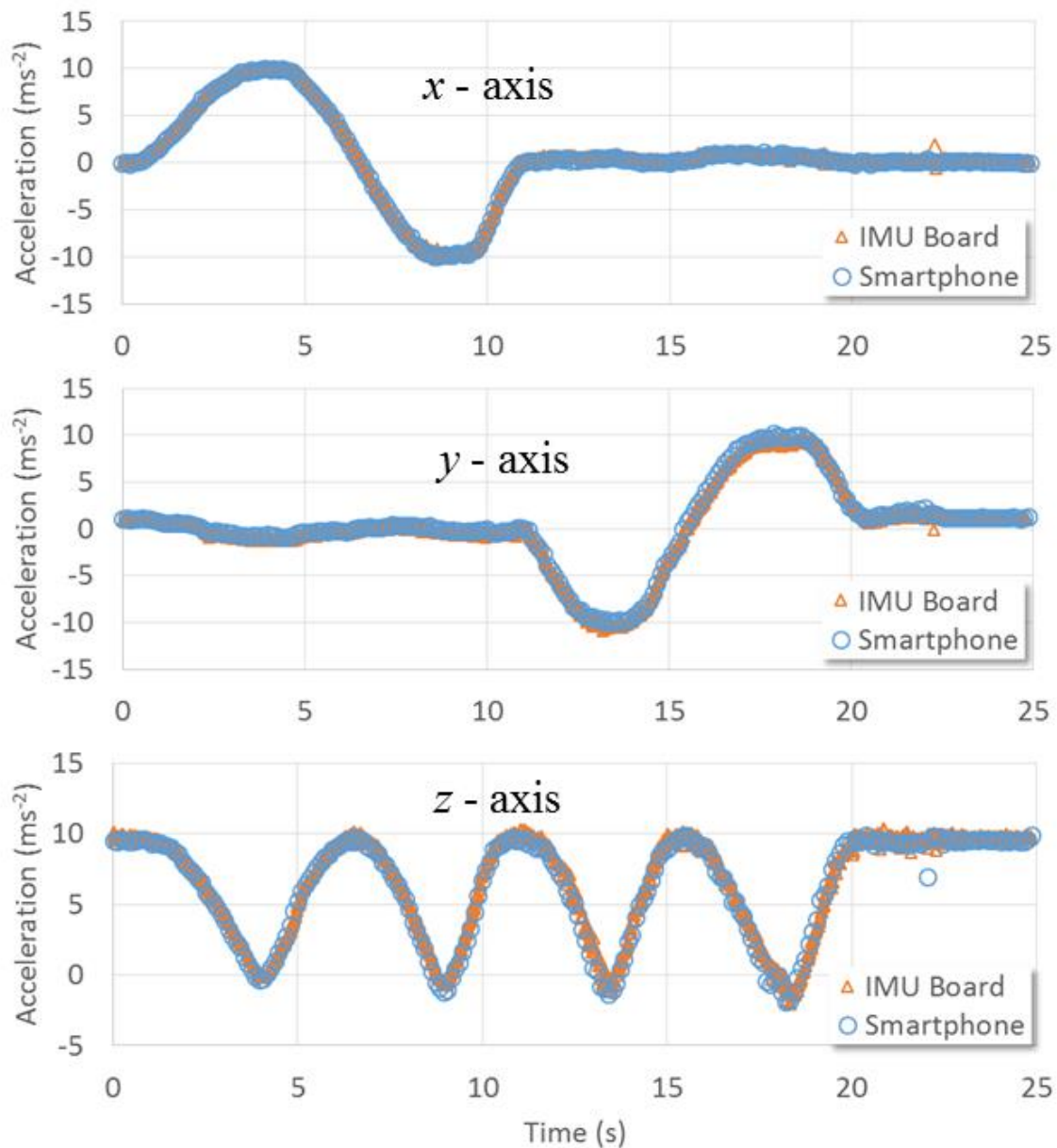


Figure 6-9: Acceleration measurements obtained from the inertial measurement unit breakout board and smartphone placed on a platform and subjected to identical perturbation at frequencies < 100 Hz. The close correlation of acceleration in the x , y and z axes showed that either device could be used to obtain comparable measurements when placed inside a vehicle.

Based on this criterion, we have found the percentage of outlier points to be 1.1% with pitching, and 0.8% with rolling. Despite these small values, we expect that the incorporation of better electronic processing schemes should allow for these outlier points to be totally eliminated. These results indicate that there is capacity of the system to provide good replication of the transport conditions in the vehicle.

At this stage, most smartphone models offer sampling rates in the order of 20 – 300 Hz as opposed to the 16 MHz sampling rate possible with the IMU sensor board. Hence, the ability to record high frequency transport perturbations with the smartphone is currently limited. Such a limitation may not play a significant role in transport situations where lower frequency perturbations are dominant. Fig. 6-9 provides acceleration measurements using the IMU sensor board and smartphone (with 100 Hz sampling rate) as both were placed on a platform and subjected to identical lower frequency perturbations. It is clear that the measurements are highly correlated. A typical Samsung Galaxy SIII smartphone retails for US\$225 as opposed to the IMU sensor board (and Arduino processor) that is available for US\$50. It is conceivable that the smartphone may already be available to a user, but the counterargument is that it may be needed for communication during the time when data is collected. It is also noteworthy that the lower frequency sensing limitations in current smartphones may soon be overcome when newer versions of IMUs, such as the LSM6DS3 by STMicroelectronics which features a 1.6 kHz sampling rate, begin to be adopted by smartphone manufacturers. However, the decision to incorporate higher sampling rate IMUs into smartphones is determined more by power consumption rather than data processing considerations.

In the construction and fabrication of the 6 DOF simulator, it was important to ensure that the length of the arms and links were accurate to achieve good reproduction of motion. In addition, we found that the poor tightening of parts together can cause significant chattering of the simulator when operated at certain speeds. This likely corresponded to the onset of matching between the driving and mechanical system frequencies. Using this system, we also note that it may be possible to evaluate the performances of spillage or vibration ameliorating devices during transport [173]. The cost of the simulator with its controller was estimated to be US\$800. The load that could be placed on the platform developed was approximately 3 kg. This setup is easily scalable using correspondingly larger motors and component parts. Overall, we have demonstrated an inexpensive but effective system that enables the extent of vibration and impact to be monitored during transport and then replicated in a motion simulator.

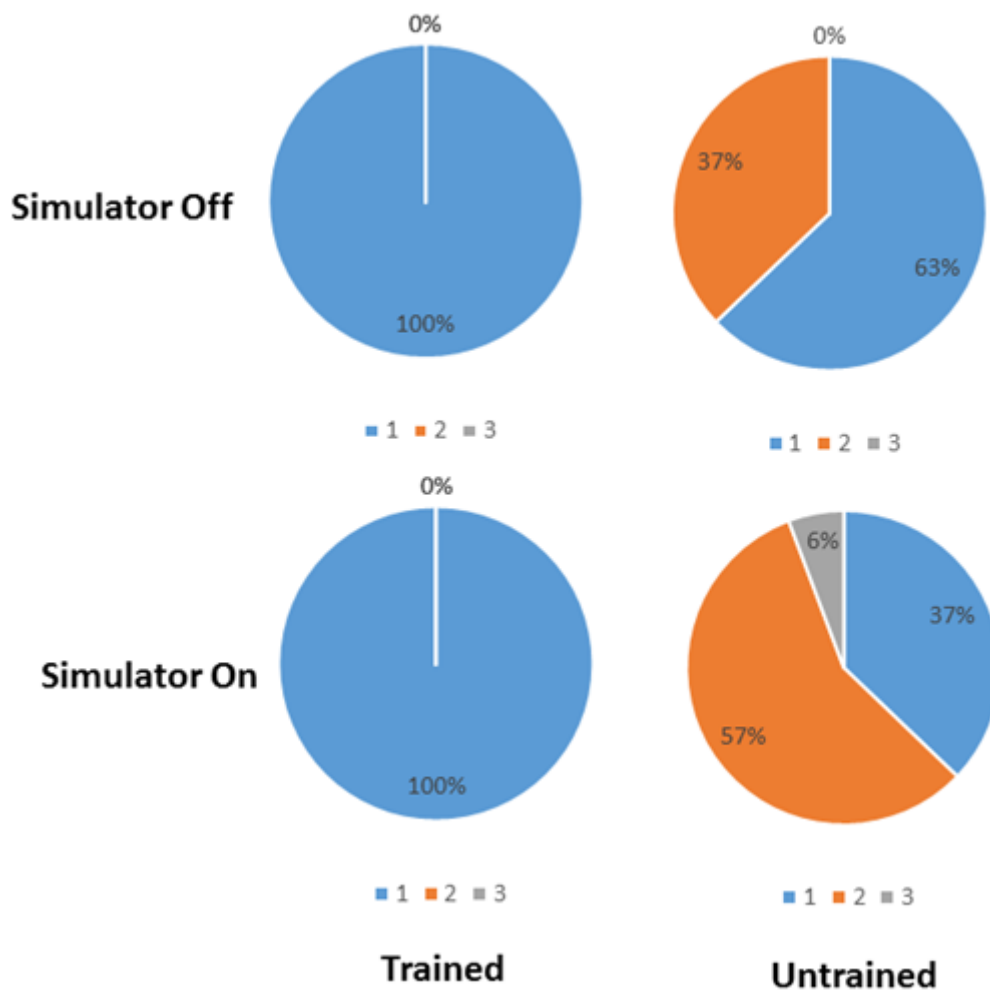


Figure 6-10: Pie charts showing the percentage of attempts where the needle was inserted into the center of the vein (1), the vein but not at the center (2), and completely missing the “vein” of the trainer (3), recorded with the simulator switched on and off. The simulated venous access was performed by one skilled participant (registered nurse) and five unskilled participants with no prior experience in cannulation.

6.4.2 System Effects on Cannulation Performance

From the pie-charts depicting the positioning results given in Fig. 6-10, the ability of the trained participant (nurse) in accessing the venipuncture needle position site correctly was clearly better than the other participants. In fact, there was no deterioration in this aspect even when the simulator was switched on. This was not the case with the other untrained participants. These results implied that prevailing skill and ongoing practice are important attributes in retaining the ability to perform the venous access procedures correctly notwithstanding any

unfavorable environments that are encountered. While there was no impairment in the ability of the trained participant to set the venipuncture position correctly with the simulator switched on, the time taken to do so was longer (see Fig. 6-11). What is also apparent is that this performance deterioration seems to be affected more by low frequency movements. This lends to the suitability of using the smartphone which has sensing range limited to 100 Hz. The other untrained participants, interestingly, did not take any significant additional time to do so. This may be attributed to them approaching the exercise merely as a physical task to complete without considering, as a trained practitioner would, the potential discomfort (and pain) to real patients arising from an unsuccessful venipuncture procedure [174].

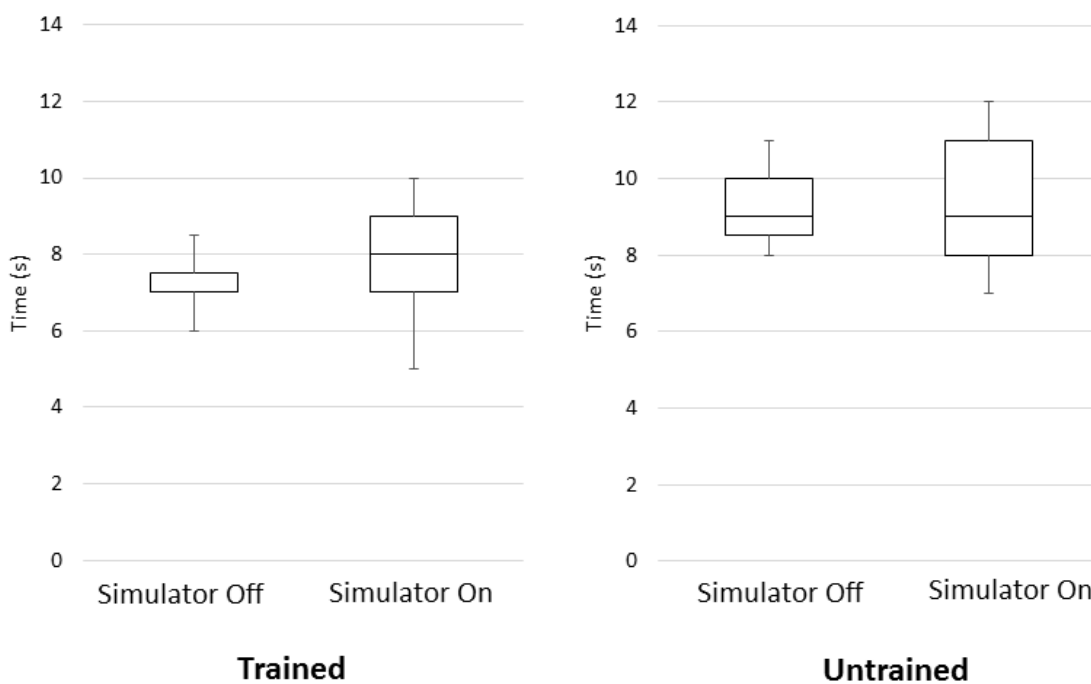


Figure 6-11: Box plots of the average time taken from seven attempts by the same six participants to perform the venipuncture procedure on the trainer with the simulator switched on and off.

It should be noted that the learning of motor skills is dependent on four factors: observational practice, the learner’s focus of attention, feedback, and self-controlled practice [175]. The last aspect typically gives rise to a dose-response relationship wherein with a rising number of repetitions, increasingly superior performances can be attained until a plateau is reached [176]. The preliminary study here was not designed to reveal this. Furthermore, due to constraints regarding availability, a real-life paramedic could not be involved in the experiment, which would have added better context to the results. Therefore, it is envisaged that a follow-on

comprehensive study conducted with a more targeted cohort of participants will provide the data needed to address this issue more definitively. The architecture of this system portends extension to the training of other pre-hospital procedures that are done en-route [177]–[179]. Applications of the simulator described here may also be extended to sharpening training for flight paramedics where the performance of more complex lifesaving skill sets such as endotracheal intubation and needle chest decompression may be necessary in the pre-hospital trauma setting.

6.5 Conclusions

A system to simulate conditions during transport in the context of en-route venipuncture initiation was developed and tested. The IMU sensor board used was found to reveal acceleration fluctuations up to ± 0.4 g and ± 0.2 g in the x and y, as well as z axis on a vehicle during typical transport. This translated to swings in pitching and rolling of $\pm 10^\circ$ and $\pm 7.5^\circ$ respectively. When these distributions were input into the 6 DOF motion simulator, it was found that good replications in pitching and rolling of the platform could be achieved. The lack of some detail in the replications were attributed to the limited movement and recording responses of the platform and sensor respectively. Tests conducted found that acceleration measurements using the IMU sensor board and smartphone, when both were placed on a platform and subjected to identical lower frequency perturbations (< 100 Hz), were highly correlated. In the preliminary test with participants, it was found that the simulated vibration affected the performances of participants trained and untrained in venipuncture procedures. There is therefore potential for developing this tool further to enhance the training of venipuncture procedures in a clinical skills laboratory setting. The architecture of the system lends itself to the necessary reconfigurations and modifications to meet the requirements in extended applications, that could prove vital to minimizing time spent by paramedics on the scene, thereby reduce overall ambulance transfer time delays.

Material from this chapter have been included in McMorran, D., Samarasinghe, S. K. et al. (2018). Sensor and actuator simulation training system for en-route intravenous procedure. *Sensors Actuators A Phys.* 279, 680–687.

7 Overall Conclusions

The studies conducted throughout this thesis sought to formulate novel theories and systems that will serve to improve time and cost effectiveness of emergency ambulance services. The opening section of the thesis was dedicated to perform a review of literature on current theory and applications used and proposed to improve emergency medical service response times. This review included studying the evolution of the ambulance location problem, emergency vehicle (EV) pre-emption methods, the effects of TCMs on EVs, the use of time by paramedics at the scene and, and the use of time and resources during ambulance recovery times. Furthermore, the use of HEV technology in mobile EMS as measures to improve cost efficiency in healthcare (including the time cost) was reviewed.

Based on the findings from this review, it was observed that in addition to the potential for improvements within the stages of prehospital time, there was a post-hospital time interval relatively neglected, that however still affects overall emergency medical service response time. This interval is the time period between the point of paramedics arriving at hospital, to the point of ambulance again being ready for dispatch. While this interval, includes time for formalities such as documentation, rest for paramedics, cleaning and replenishment of ambulance consumables (including refuelling) and disposables, it was further noticed the ambulance engine was run at idle for considerable periods (including while waiting on-call) to ensure that ambulance electrical equipment is sufficiently charged. Therefore, considering the inefficient use of fuel, emission problems associated with it, and the ambulance equipment power problem, we suggested the adoption of an alternative power source to make ambulance operation more cost effective. Given practicality and feasibility considerations, especially regarding equipment power problem, adopting HEV powertrains for ambulance was suggested.

Consequently, the need to evaluate the feasibility of HEV powertrains in ambulances arose. Given the additional dynamics to be studied in this case, compared to commercial passenger HEVs, the capability of simulation software however, to perform a thorough analysis was required to be evaluated. Therefore in Chapter 3, we conducted a comparison verification study of two automotive simulation software; a MATLAB Simulink model, and the popular ADVISOR tool. The MATLAB Simulink Model only yielded logical results under the NEDC drive cycle. The exact cause for its inability to produce the same with the UDDS, Manhattan, and HWFET drive cycles was difficult to uncover due to the complex manner in which the

algorithm is configured. While ADVISOR delivered logical distributions of Battery State-of-Charge (SOC) % and fuel use data, its closed form makes it difficult to be incorporated into a traffic simulation software like VISSIM, which could help prevent optimising the models for legislated drive cycles. Furthermore, it was observed that both software, especially ADVISOR, were limited in terms of functionality, due to which, the ambulance equipment problem in the context of a hybrid-electric powered ambulance could not be studied. Therefore, it is envisaged, a more comprehensive study on applicability of HEV powertrains for ambulances with the equipment power problem in focus, will be performed in the future. Nevertheless, the Battery State-of-Charge distributions is still expected to guide decisions on whether to adopt HEV technology for ambulances. It is noteworthy that the availability of electrical power in ambulances is vital in order to maintain operation of key instrumentation like ventilators and defibrillators when they are needed.

In chapter 4, with a focus on contributing towards work on minimising time losses during ambulance response and transfer time intervals, we attempt to understand delays caused due to disruptions during ambulance travel. A scenario of a disruption caused during road travel, where a disruptor vehicle attempts to move into the ambulance's lane of travel, thereby interrupting ambulance's progress, is simulated on PTV VISSIM, a traffic microsimulation software. It was observed that VISSIM simulations provided realistic depictions of velocity-time characteristics of ambulances responding to disruptions. Based on the velocity-time distributions, the ambulance response to this disruption was analytically characterised. Using the analytical relations involving the use of fourth power polynomials, a generalized means of accounting for time delays associated with these disrupters was developed, replacing the need for further simulations. We expect the tool to help in the formulation of strategies for traffic management especially with emergency vehicles in focus, thereby minimise ambulance transfer time delays.

Subsequently, in chapter 5, we explored an approach to use UAVs to record vehicle travel as it is subjected to a disruption, and is required to overcome a speed bump. Due to the inconvenience caused to local EMS by arranging an ambulance for experiments, a cargo delivery van was used instead, chosen to relate closely to specifications and drivability requirements of a vehicle model used for a type II ambulance. On retrieving the video footage from the UAV, necessary video processing techniques were applied and the vehicle speed-time

distributions were obtained. A large portion of the data was found to be noisy due to errors caused by drone flight instability, inaccuracies related to magnification of footage, and inherent image noise. Therefore, the noisy data was deemed unsuitable for verification of the parameters to be used in theoretical formulation. The usable data however was illustrated the deceleration and acceleration features in the influence zone expected in a speed profile of vehicle negotiating a speed bump. Furthermore, the vehicle response to a disruption from the experiment correlated with the ambulance response to a disrupter obtained through VISSIM simulations, presented in chapter 4, suggesting the viability of using simulation data to analytically characterise ambulance response to disrupters. Finally, we observed good potential for use of UAVs in traffic related studies and expect future improvements made to UAV technology, in terms of video quality/stability, coupled with advanced video processing software, may further enhance the suitability of UAVs.

In chapter 6, we shifted focus towards providing a solution to reduce time spent at the scene by paramedics. To achieve this objective, one method in use is via, en-route cannulation. Therefore, in a bid to train paramedics and study the feasibility of this procedure, we developed and tested a training system to simulate conditions during transport in the context of en-route venipuncture initiation. The IMU sensor board used was found to reveal acceleration fluctuations up to ± 0.4 g and ± 0.2 g in the x and y, as well as z axis on a vehicle during typical transport. This translated to swings in pitching and rolling of $\pm 10^\circ$ and $\pm 7.5^\circ$ respectively. When these distributions were input into the 6 DOF motion simulator, it was found that good replications in pitching and rolling of the platform could be achieved. The lack of some detail in the replications were attributed to the limited movement and recording responses of the platform and sensor respectively. Tests conducted found that acceleration measurements using the IMU sensor board and smartphone, when both were placed on a platform and subjected to identical lower frequency perturbations (<100 Hz), were highly correlated. In the preliminary test with participants, it was found that the simulated vibration affected the performances of participants trained and untrained in venipuncture procedures.

However, due to constraints regarding availability, participation of a real-life paramedic in the experiment was not possible, which otherwise would have added better context to the preliminary test results. Therefore, it is envisioned that a follow-on comprehensive study conducted with a more targeted group of participants will provide the data needed to address this issue more definitively. The architecture of this system can be extended to the training of other pre-hospital procedures that are done en-route. The simulator presented, may also be

applied to improve training for flight paramedics where the performance of more complex lifesaving skill sets such as endotracheal intubation and needle chest decompression may be necessary in the pre-hospital trauma setting. Furthermore, there is potential for developing this tool further to enhance the training of venipuncture procedures in a clinical skills laboratory setting.

The findings in this thesis are expected to advance technologies that assist in the effective use of ambulances and attendant services with ambulances.

Bibliography

- [1] C. Rockwood, C. Mann, J. Farrington, O. Hampton, and R. Motley, "History of emergency medical services in the United States.," *The Journal of Trauma*, vol. 16, no. 4. pp. 299–308, 1976.
- [2] J. D. Farrington, "The registry of ambulance attendants," *Emerg. Med. Today*, vol. 1, no. 1, 1972.
- [3] M. N. Shah, "PUBLIC HEALTH THEN AND NOW Emergency Medical Services Syste," *Public Heal. Then Now*, vol. 96, no. March, pp. 414–423, 2006.
- [4] A. Pollock, "Ambulance services in London and Great Britain from 1860 until today: A glimpse of history gleaned mainly from the pages of contemporary journals," *Emerg. Med. J.*, vol. 30, no. 3, pp. 218–222, 2013.
- [5] J. Peters and G. B. Hall, "Assessment of ambulance response performance using a geographic information system," *Soc. Sci. Med.*, vol. 49, pp. 1551–1566, 1999.
- [6] J. S. Sampalis, A. Lavoie, J. I. Williams, D. S. Mulder, and M. Kalina, "Impact of on-site care, prehospital time, and level of in-hospital care on survival in severely injured patients," *Journal of Trauma - Injury, Infection and Critical Care*, vol. 34, no. 2. p. 252, 1993.
- [7] P. Kivell and K. Mason, "Trauma systems and major injury centres for the 21st century: an option," *Health Place*, vol. 5, pp. 99–110, 1999.
- [8] A. M. K. Harmsen, G. F. Giannakopoulos, P. R. Moerbeek, E. P. Jansma, H. J. Bonjer, and F. W. Bloemers, "The influence of prehospital time on trauma patients outcome: A systematic review," *Injury*, vol. 46, no. 4, pp. 602–609, 2015.
- [9] J. B. Brown *et al.*, "Not all prehospital time is equal: Influence of scene time on mortality," *J. Trauma Acute Care Surg.*, vol. 81, no. 1, pp. 93–100, 2016.
- [10] L. Brotcorne, G. Laporte, and F. Semet, "Ambulance location and relocation models," *Eur. J. Oper. Res.*, vol. 147, no. 3, pp. 451–463, 2003.
- [11] C. Toregas, R. Swain, C. ReVelle, and L. Bergman, "The Location of Emergency Service Facilities," *Oper. Res.*, vol. 19, no. 6, pp. 1363–1373, 1971.
- [12] R. Church and C. ReVelle, "The maximal covering location problem," *Pap. Reg. Sci. Assoc.*, vol. 32, pp. 101–118, 1974.

- [13] D. Schilling, D. J. Elzinga, J. Cohon, R. Church, and D. Schilling, "The Team / Fleet Models for Simultaneous Facility and Equipment," *Transp. Sci.*, vol. 13, no. 2, pp. 163–175, 1979.
- [14] V. Marianov and C. Revelle, "The capacitated standard response fire protection siting problem: deterministic and probabilistic models," *Ann. Oper. Res.*, vol. 40, pp. 303–322, 1992.
- [15] M. S. Daskin and E. H. Stern, "A hierarchical objective set covering model for emergency medical service vehicle deployment," *Transp. Sci.*, vol. 15, no. 2, pp. 137–152, 1981.
- [16] K. Hogan and C. Revelle, "Concepts and applications of backup coverage," *Manage. Sci.*, vol. 32, no. 11, pp. 1434–1444, 1986.
- [17] M. S. Daskin, "A Maximum Expected Covering Location Model : Formulation, Properties and Heuristic Solution," *Transp. Sci.*, vol. 17, no. 1, pp. 48–70, 1983.
- [18] C. Revelle, K. Hogan, C. Revelle, and K. Hogan, "The Maximum Availability Location Problem," *Transp. Sci.*, vol. 23, no. 3, pp. 192–200, 1989.
- [19] M. Ball and F. L. Lin, "A Reliability Model Applied to Emergency Service Vehicle Location," *Oper. Res.*, vol. 41, no. 1, pp. 18–36, 1992.
- [20] M. B. Mandell, "Covering models for two-tiered emergency medical services systems," vol. 6, pp. 355–368, 1998.
- [21] M. Gendreau and G. Laporte, "A dynamic model and parallel tabu search heuristic for real-time ambulance relocation," vol. 27, 2001.
- [22] K. Peleg and J. S. Pliskin, "A geographic information system simulation model of EMS: Reducing ambulance response time," *Am. J. Emerg. Med.*, vol. 22, no. 3, pp. 164–170, 2004.
- [23] L. C. Nogueira, L. R. Pinto, and P. M. S. Silva, "Reducing Emergency Medical Service response time via the reallocation of ambulance bases," *Health Care Manag. Sci.*, vol. 19, no. 1, pp. 31–42, 2016.
- [24] S. Shibuya, T. Yoshida, Z. Yamashiro, and M. Miyawaki, "Fast emergency vehicle preemption systems," *Transp. Res. Rec. J. Transp. Res. Board*, vol. 1739, no. 1, pp. 44–50, 2000.
- [25] E. Kwon, S. Kim, and R. Betts, "Route-based dynamic preemption of traffic signals for emergency vehicles operations," *Proc. TRB Annu.*, vol. 9, pp. 1–18, 2003.
- [26] I. Yun, B. B. Park, C. K. Lee, and Y. T. Oh, "Comparison of Emergency Vehicle Preemption methods using a Hardware-In-The-Loop simulation," *KSCE J. Civ. Eng.*, vol. 16, no. 6, pp.

- 1057–1063, 2012.
- [27] J. Wang, M. Yun, W. Ma, and X. Yang, "Travel Time Estimation Model for Emergency Vehicles under Preemption Control," *Procedia - Soc. Behav. Sci.*, vol. 96, no. Cictp, pp. 2147–2158, 2013.
- [28] Y. Wang, Z. Wu, X. Yang, and L. Huang, "Design and implementation of an emergency vehicle signal preemption system based on cooperative vehicle-infrastructure technology," *Advances in Mechanical Engineering*, vol. 2013. 2013.
- [29] C. Louisell, J. Collura, D. Teodorovic, and S. Tignor, "Simple Worksheet Method to Evaluate Emergency Vehicle Preemption and Its Impacts on Safety," *Transp. Res. Rec. J. Transp. Res. Board*, vol. 1867, no. 1, pp. 151–162, 2004.
- [30] E. J. Nelson and D. Bullock, "Impact of Emergency Vehicle Preemption on Signalized Corridor Operation: An Evaluation," *Transp. Res. Rec. J. Transp. Res. Board*, vol. 1727, no. 1, pp. 1–11, 2000.
- [31] X. Qin and A. M. Khan, "Control strategies of traffic signal timing transition for emergency vehicle preemption," *Transp. Res. Part C Emerg. Technol.*, vol. 25, pp. 1–17, 2012.
- [32] I. M. Lockwood, "ITE traffic calming definition," *ITE J. (Institute Transp. Eng.)*, vol. 67, no. 7, pp. 22–24, 1997.
- [33] R. Ewing and C. Kooshian, "U.S. experience with traffic calming," *ITE J. (Institute Transp. Eng.)*, vol. 67, no. 8, pp. 28–33, 1997.
- [34] C. Atkins and M. Coleman, "The Influence of Traffic Calming on Emergency Response Times," *ITE J. (Institute Transp. Eng.)*, vol. 67, no. 8, pp. 42–46, 1997.
- [35] K. Ahn and H. Rakha, "A field evaluation case study of the environmental and energy impacts of traffic calming," *Transp. Res. Part D Transp. Environ.*, vol. 14, no. 6, pp. 411–424, 2009.
- [36] J. Gulden and R. Ewing, "New traffic calming device of choice," *ITE J. (Institute Transp. Eng.)*, vol. 79, no. 12, pp. 26–31, 2009.
- [37] A. García, A. T. Moreno, and M. A. Romero, "A new traffic-calming device: Speed kidney," *ITE J. (Institute Transp. Eng.)*, vol. 82, no. 12, pp. 28–33, 2012.
- [38] A. L. García, A. N. A. T. S. U. I. Moreno, M. A. Romero, and J. O. S. É. Perea, "Estimating the effect of traffic calming measures on ambulances," *Emergencias*, vol. 25, no. 1, pp. 285–288, 2013.

- [39] Catherine Berthod and Carole Leclerc, "Traffic Calming in Québec: Speed Humps and Speed Cushions," *J. Civ. Eng. Archit.*, vol. 7, no. 4, pp. 456–465, 2013.
- [40] "Ambulance Victoria," [Online]. Available: <https://www.ambulance.vic.gov.au/>, p. Retrieved, August 2018.
- [41] A. Rouse, "Do ambulance crews triage trauma patients?," *Emerg. Med. J.*, vol. 8, no. 3, pp. 185–191, 1991.
- [42] G. S. Johnson and H. R. Guly, "The effect of pre-hospital administration of intravenous nalbuphine on on-scene times," *J. Accid. Emerg. Med.*, vol. 12, no. 1, pp. 20–22, 1995.
- [43] M. Powar, J. Nguyen-Van-Tam, J. Pearson, and A. Dove, "Hidden impact of paramedic interventions," *Emerg. Med. J.*, vol. 13, no. 6, pp. 383–385, 1996.
- [44] C. F. Weston and M. J. McCabe, "Audit of an emergency ambulance service: impact of a paramedic system," *J R Coll Physicians L.*, vol. 26, no. 1, pp. 86–89, 1992.
- [45] U. M. Guly, R. G. Mitchell, R. Cook, D. J. Steedman, and C. E. Robertson, "Paramedics and technicians are equally successful at managing cardiac arrest outside hospital," *Bmj*, vol. 310, no. 6987, p. 1091, 1995.
- [46] D. C. Cone, S. J. Davidson, and Q. Nguyen, "A time-motion study of the emergency medical services turnaround interval," *Ann. Emerg. Med.*, vol. 31, no. 2, pp. 241–246, 1998.
- [47] J. R. Studnek, K. Staley, T. Blackwell, S. Vandeventer, J. S. Garrett, and S. R. Ward, "The Association Between Ambulance Hospital Turnaround Times and Patient Acuity, Destination Hospital, and Time of Day," *Prehospital Emerg. Care*, vol. 15, no. 3, pp. 366–370, 2011.
- [48] S. M. Isaacs *et al.*, "Facilitating EMS Turnaround Intervals at Hospitals in the Face of Receiving Facility Overcrowding," *Prehospital Emerg. Care*, vol. 9, no. 3, pp. 267–275, 2005.
- [49] R. F. Maio, "EMS systems: Opening the 'Black Box,'" *Ann. Emerg. Med.*, no. April, pp. 3–4, 1993.
- [50] J. R. Apodaca-Madrid and K. Newman, "Design and evaluation of a Green Ambulance," *2010 IEEE Green Technol. Conf.*, no. May, pp. 1–5, 2010.
- [51] K. Williamson, "Fuel cell auxiliary power proving efficient for Yorkshire emergency response vehicles," *Fuel Cells Bull.*, vol. 2011, no. 10, pp. 12–14, 2011.
- [52] A. Cook, "The road to electrification for specialty vehicles," *Proc. 2008 IEEE Int. Conf. Veh.*

- Electron. Safety, ICVES 2008*, pp. 103–107, 2008.
- [53] J. W. Chung and D. O. Meltzer, “Estimate of the carbon footprint of the US health care sector,” *Jama*, vol. 302, no. 18, pp. 1970–1972, 2009.
- [54] L. H. Brown, D. V. Canyon, P. G. Buettner, J. Mac Crawford, and J. Judd, “The carbon footprint of Australian ambulance operations,” *EMA - Emerg. Med. Australas.*, vol. 24, no. 6, pp. 657–662, 2012.
- [55] L. H. Brown, P. G. Buettner, D. V. Canyon, J. Mac Crawford, and J. Judd, “Estimating the life cycle greenhouse gas emissions of Australian ambulance services,” *J. Clean. Prod.*, vol. 37, pp. 135–141, 2012.
- [56] J. J. Hess and L. A. Greenberg, “Fuel use in a large, dynamically deployed emergency medical services system,” *Prehosp. Disaster Med.*, vol. 26, no. 5, pp. 394–398, 2011.
- [57] W. Baker, N. Mansfield, I. Storer, and S. Hignett, “Future electric vehicles for ambulances (FEVA),” *J. Paramed. Pract.*, vol. 5, no. 2, pp. 77–82, 2013.
- [58] N. Rauh, T. Franke, and J. F. Krems, “Understanding the Impact of Electric Vehicle Driving Experience on Range Anxiety,” *Hum. Factors J. Hum. Factors Ergon. Soc.*, vol. 57, no. 1, pp. 177–187, 2015.
- [59] O. Egbue and S. Long, “Barriers to widespread adoption of electric vehicles: An analysis of consumer attitudes and perceptions,” *Energy Policy*, vol. 48, no. March, pp. 717–729, 2012.
- [60] P. Denholm and W. Short, “An Evaluation of Utility System Impacts and Benefits of Optimally Dispatched Plug-In Hybrid Electric Vehicles,” *NREL Rep. noTP-620*, no. October, p. 41, 2006.
- [61] D. B. Richardson, “Electric vehicles and the electric grid: A review of modeling approaches, Impacts, and renewable energy integration,” *Renew. Sustain. Energy Rev.*, vol. 19, pp. 247–254, 2013.
- [62] G. A. Putrus, P. Suwanapingkarl, D. Johnston, E. C. Bentley, and M. Narayana, “Impact of electric vehicles on power distribution networks,” *IEEE Veh. Power Propuls. Conf.*, no. September, pp. 7–11, 2009.
- [63] S. Shao, M. Pipattanasomporn, and S. Rahman, “Challenges of PHEV penetration to the residential distribution network,” *2009 IEEE Power Energy Soc. Gen. Meet. PES '09*, pp. 1–8, 2009.
- [64] R. C. Green II, L. Wang, and M. Alam, “The impact of plug-in hybrid electric vehicles on

- distribution networks: A review and outlook," *Renew. Sustain. Energy Rev.*, vol. 15, no. 1, pp. 544–553, 2011.
- [65] K. . Chau and Y. . Wong, "Overview of power management in hybrid electric vehicles," *Energy Convers. Manag.*, vol. 43, pp. 1953–1968, 2002.
- [66] S. C. Hawkins, "The green machine. Development of a high-efficiency, low-pollution EMS response vehicle," *JEMS a J. Emerg. Med. Serv.*, vol. 33, no. 7, pp. 108–120, 2008.
- [67] a. Brahma, B. Glenn, Y. Guezennec, T. Miller, G. Rizzoni, and G. Washington, "Modeling, performance analysis and control design of a hybrid sport-utility vehicle," *Proc. 1999 IEEE Int. Conf. Control Appl. (Cat. No.99CH36328)*, vol. 1, pp. 448–453, 1999.
- [68] J. Won and R. Langari, "Fuzzy torque distribution control for a parallel hybrid vehicle," *Expert Syst.*, vol. 19, no. 1, pp. 4–10, 2002.
- [69] C.-C. Lin, H. Peng, and J. W. Grizzle, "A stochastic control strategy for hybrid electric vehicles," *Proc. 2004 Am. Control Conf.*, vol. 5, pp. 4710–4715, 2004.
- [70] J. W. Grizzle, "Power management strategy for a parallel hybrid electric truck," *IEEE Trans. Control Syst. Technol.*, vol. 11, no. 6, pp. 839–849, 2003.
- [71] L. V. Pérez, G. R. Bossio, D. Moitre, and G. O. García, "Optimization of power management in an hybrid electric vehicle using dynamic programming," *Math. Comput. Simul.*, vol. 73, no. 1–4 SPEC. ISS., pp. 244–254, 2006.
- [72] R. Wang, "Dynamic Programming Technique in Hybrid Electric Vehicle Optimization," *IEEE Int. Electr. Veh. Conf.*, pp. 1–8, 2012.
- [73] G. Paganelli, S. Delprat, T. M. Guerra, J. Rimaux, and J. J. Santin, "Equivalent consumption minimization strategy for parallel hybrid powertrains," *IEEE Veh. Technol. Conf.*, vol. 4, pp. 2076–2081, 2002.
- [74] A. Sciarretta, M. Back, and L. Guzzella, "Optimal control of parallel hybrid electric vehicles," *IEEE Trans. Control Syst. Technol.*, vol. 12, no. 3, pp. 352–363, 2004.
- [75] P. Rodatz, G. Paganelli, A. Sciarretta, and L. Guzzella, "Optimal power management of an experimental fuel cell/supercapacitor- powered hybrid vehicle," *Control Eng. Pract.*, vol. 13, no. 1, pp. 41–53, 2005.
- [76] C. Musardo, G. Rizzoni, Y. Guezennec, and B. Staccia, "A-ECMS: An Adaptive Algorithm for Hybrid Electric Vehicle Energy Management," *Eur. J. Control*, vol. 11, no. 4–5, pp. 509–524,

- 2005.
- [77] S. Delprat, T. M. Guerra, and J. Rimaux, "Optimal control of a parallel powertrain : From global optimization to real time control strategy," *2002 Veh. Technol. Conf.*, vol. 4, pp. 2082–2088, 2002.
- [78] M. J. Kim and H. Peng, "Power management and design optimization of fuel cell/battery hybrid vehicles," *J. Power Sources*, vol. 165, no. 2, pp. 819–832, 2007.
- [79] D. Assanis *et al.*, "Optimization Approach to Hybrid Electric Propulsion System Design*," *Mech. Struct. Mach.*, vol. 27, no. 4, pp. 393–421, 1999.
- [80] B. Zhang and Z. Chen, "Multi-objective parameter optimization of a series hybrid electric vehicle using evolutionary algorithms," *Veh. Power ...*, pp. 921–925, 2009.
- [81] X. Liu, Y. Wu, and J. Duan, "Optimal Sizing of a Series Hybrid Electric Vehicle Using a Hybrid Genetic Algorithm," *2007 IEEE Int. Conf. Autom. Logist.*, pp. 1125–1129, 2007.
- [82] W. Gao and S. K. Porandla, "Design optimization of a parallel hybrid electric powertrain," *2005 IEEE Veh. Power Propuls. Conf.*, p. 6 pp., 2005.
- [83] Z. Chen, C. C. Mi, B. Xia, and C. You, "Energy management of power-split plug-in hybrid electric vehicles based on simulated annealing and Pontryagin's minimum principle," *J. Power Sources*, vol. 272, pp. 160–168, 2014.
- [84] A. Sciarretta and L. Guzzella, "Control of hybrid electric vehicles," *IEEE Control Syst.*, vol. 27, no. 2, pp. 60–70, 2007.
- [85] V. Schwarzer and R. Ghorbani, "Drive cycle generation for design optimization of electric vehicles," *IEEE Trans. Veh. Technol.*, vol. 62, no. 1, pp. 89–97, 2013.
- [86] C. Lin, L. Zhao, X. Cheng, and W. Wang, "A DCT-Based Driving Cycle Generation Method and Its Application for Electric Vehicles," *Math. Probl. ...*, vol. 2015, 2015.
- [87] L. Ntziachristos and Z. Samaras, "Speed-dependent representative emission factors for catalyst passenger cars and influencing parameters," *Atmos. Environ.*, vol. 34, no. 27, pp. 4611–4619, 2000.
- [88] K. Ekberg, L. Eriksson, and M. Sivertsson, "Cycle Beating - An Analysis of the Boundaries During Vehicle Testing," *IFAC-PapersOnLine*, vol. 49, no. 11, pp. 657–664, 2016.
- [89] E. Tazelaar, J. Bruinsma, B. Veenhuizen, and P. van den Bosch, "Driving cycle characterization

- and generation, for design and control of fuel cell buses,” *World Electr. Veh. J.*, vol. 3, no. 1, 2009.
- [90] V. Schwarzer and R. Ghorbani, “New opportunities for large-scale design optimization of electric vehicles using GPU technology,” *2011 IEEE Veh. Power Propuls. Conf.*, pp. 1–6, 2011.
- [91] S. J. Moura, H. K. Fathy, D. S. Callaway, and J. L. Stein, “A Stochastic Optimal Control Approach for Power Management in Plug-In Hybrid Electric Vehicles,” *IEEE Trans. Control Syst. Technol.*, vol. 19, no. 3, pp. 545–555, 2011.
- [92] J. Lin and D. A. Niemeier, “Estimating Regional Air Quality Vehicle Emission Inventories: Constructing Robust Driving Cycles,” *Transp. Sci.*, vol. 37, no. 3, pp. 330–346, 2003.
- [93] F. Souffran, L. Miegerville, and P. Guerin, “Simulation of Real-World Vehicle Missions Using a Stochastic Markov Model for Optimal Design Purposes,” *Veh. Power Propuls. Conf.*, no. 1, 2011.
- [94] A. Ravey *et al.*, “Energy-Source-Sizing Methodology for Hybrid Fuel Cell Vehicles Based on Statistical Description of Driving Cycles,” *IEEE Trans. Veh. Technol.*, vol. 60, no. 9, pp. 4164–4174, 2015.
- [95] TechZiffy, “Ambulance Equipment Market data status, By Competitors, strategies benefits, Type (Offshore, Onshore), Region, Country and forecast to 2026,” [Online]. Available: <https://techziffy.com/ambulance-equipment-market-data-status-by-competitors-strategies-benefits-type-offshore-onshore-region-country-and-forecast-to-2026/9564/>, p. Retrieved, October 2018.
- [96] R. Farrington and J. Rugh, “Impact of Vehicle Air-Conditioning on Fuel Economy, Tailpipe Emissions, and Electric Vehicle Range,” *Earth Technol. Forum*, no. September, p. <http://www.nrel.gov/docs/fy00osti/28960.pdf>, 2000.
- [97] N. Kim and A. Rousseau, “Thermal impact on the control and the efficiency of the 2010 Toyota Prius hybrid electric vehicle,” *Proc. Inst. Mech. Eng. Part D J. Automob. Eng.*, vol. 230, no. 1, pp. 1–11, 2015.
- [98] B. Mebarki, B. Draoui, B. Allaou, L. Rahmani, and E. Benachour, “Impact of the air-conditioning system on the power consumption of an electric vehicle powered by lithium-ion battery,” *Model. Simul. Eng.*, vol. 2013, 2013.
- [99] M. F. Sukri, M. N. Musa, M. Y. Senawi, and H. Nasution, “Achieving a better energy-efficient automotive air-conditioning system: a review of potential technologies and strategies for

- vapor compression refrigeration cycle," *Energy Effic.*, vol. 8, no. 6, pp. 1201–1229, 2015.
- [100] Q. Zhang and M. Canova, "Mild hybrid technique using the automotive air-conditioning system," *Proc. Inst. Mech. Eng. Part D J. Automob. Eng.*, vol. 230, no. 10, pp. 1392–1402, 2016.
- [101] A. Alahmer, M. Abdelhamid, and M. Omar, "Design for thermal sensation and comfort states in vehicles cabins," *Appl. Therm. Eng.*, vol. 36, no. 1, pp. 126–140, 2012.
- [102] S. Miller, "Hybrid-Electric Vehicle Model in Simulink," (<https://www.mathworks.com/matlabcentral/fileexchange/28441>). *MATLAB Cent. File Exch.*, vol. Retrieved, no. April, 2017.
- [103] B. Kramer *et al.*, "ADVISOR: a systems analysis tool for advanced vehicle modeling," *J. Power Sources*, vol. 110, no. 2, pp. 255–266, 2002.
- [104] A. Same, A. Stipe, D. Grossman, and J. W. Park, "A study on optimization of hybrid drive train using Advanced Vehicle Simulator (ADVISOR)," *J. Power Sources*, vol. 195, no. 19, pp. 6954–6963, 2010.
- [105] E. G. Giakoumis and A. T. Zachiotis, "Investigation of a diesel-engined vehicle's performance and emissions during the WLTC driving cycle - Comparison with the NEDC," *Energies*, vol. 10, no. 2, p. 240, 2017.
- [106] P. Iodice and A. Senatore, "Exhaust emissions of new high-performance motorcycles in hot and cold conditions," *Int. J. Environ. Sci. Technol.*, vol. 12, no. 10, pp. 3133–3144, 2015.
- [107] Łoza and L. Sitnik, "The speed profile evaluation method in the vehicle operation," *IOP Conf. Ser. Mater. Sci. Eng.*, vol. 421, no. 2, 2018.
- [108] M. Gis, M. Bednarski, and P. Wiśniowski, "Comparative analysis of NEDC and WLTC homologation tests for vehicle tests on a chassis dynamometer," *J. KONES*, vol. 25, no. 3, 2018.
- [109] E. G. Giakoumis and A. Alysandratou, "Performance and Emissions of a Heavy-Duty Truck during the UDDS Driving Cycle: Simulation Analysis," *J. Energy Eng.*, vol. 142, no. 2, p. E4015011, 2015.
- [110] J. Ho and M. Lindquist, "Time saved with the use of emergency warning lights and siren while responding to requests for emergency medical aid in a rural environment," *Prehospital Emerg. Care*, vol. 5, no. 2, pp. 159–162, 2001.

- [111] J. Ho and B. Casey, "Time saved with use of emergency warning lights and sirens during response to requests for emergency medical aid in an urban environment," *Ann. Emerg. Med.*, vol. 32, no. 5, pp. 585–588, 1998.
- [112] J. Nicholl, J. West, S. Goodacre, and J. Turner, "The relationship between distance to hospital and patient mortality in emergencies: An observational study," *Emerg. Med. J.*, vol. 24, no. 9, pp. 665–668, 2007.
- [113] W. Hu, Q. Dong, and B. Huang, "Correlations between road crash mortality rate and distance to trauma centers," *J. Transp. Heal.*, vol. 6, no. November 2016, pp. 50–59, 2017.
- [114] B. Murray and R. Kue, "The Use of Emergency Lights and Sirens by Ambulances and Their Effect on Patient Outcomes and Public Safety: A Comprehensive Review of the Literature," *Prehosp. Disaster Med.*, vol. 32, no. 2, pp. 209–216, 2017.
- [115] P. Górski, "Occupational exposure to noise from authorized emergency vehicle sirens," *Int. J. Occup. Saf. Ergon.*, vol. 20, no. 3, pp. 407–420, 2014.
- [116] M. C. T. Hansen, J. H. Schmidt, A. C. Brøchner, J. K. Johansen, S. Zwisler, and S. Mikkelsen, "Noise exposure during prehospital emergency physicians work on Mobile Emergency Care Units and Helicopter Emergency Medical Services," *Scand. J. Trauma. Resusc. Emerg. Med.*, vol. 25, no. 1, pp. 1–9, 2017.
- [117] U. Weber *et al.*, "Emergency ambulance transport induces stress in patients with acute coronary syndrome," *Emerg. Med. J.*, vol. 26, no. 7, pp. 524–528, 2009.
- [118] A. R. Hodge, "Review of the 20 Mile/H Speed Zones. 1991.," *Traffic Eng. Control*, vol. 33, no. 10, pp. 545–547, 1992.
- [119] R. Ziolkowski, "Speed Profile as a Tool to Estimate Traffic Calming Measures Efficiency," *J. Civ. Eng. Archit.*, no. December 2014, 2014.
- [120] K. Schittkowski, "On the convergence of a generalized seduced gradient algorithm for nonlinear programming problems," *Optimization*, vol. 17, no. 6, pp. 731–755, 1986.
- [121] T. Tettamanti and I. Varga, "Development of road traffic control by using integrated VISSIM-MATLAB simulation environment," *Period. Polytech. Civ. Eng.*, vol. 56, no. 1, pp. 43–49, 2012.
- [122] R. Gray, "Looming auditory collision warnings for driving," *Hum. Factors*, vol. 53, no. 1, pp. 63–74, 2011.
- [123] H. S. Loeb, V. Kandadai, C. C. McDonald, and F. K. Winston, "Emergency Braking in Adults

- Versus Novice Teen Drivers: Response to simulated sudden driving events," *Transp. Res. Rec. J. Transp. Res. Board*, vol. 2516, pp. 8–14, 2015.
- [124] M. Morimoto, M. Yairi, K. Iida, and M. Itoh, "The role of low frequency components in median plane localization," *Acoust. Sci. Technol.*, vol. 24, no. 2, pp. 76–82, 2003.
- [125] A. Ben Jemaa, G. Irato, A. Zanela, A. Brescia, M. Turki, and M. Jaïdane, "Congruent auditory display and confusion in sound localization: Case of elderly drivers," *Transp. Res. Part F Traffic Psychol. Behav.*, vol. 59, no. 2018, pp. 524–534, 2018.
- [126] D. McMorran *et al.*, "Sensor and actuator simulation training system for en-route intravenous procedure," *Sensors Actuators A Phys.*, vol. 279, pp. 680–687, 2018.
- [127] K. Sagawa and H. Inooka, "Ride quality evaluation of an actively-controlled stretcher for an ambulance," *Proc. Inst. Mech. Eng. Part H J. Eng. Med.*, vol. 216, no. 4, pp. 247–256, 2002.
- [128] M. A. Khan, W. Ectors, T. Bellemans, D. Janssens, and G. Wets, "UAV-Based Traffic Analysis: A Universal Guiding Framework Based on Literature Survey," *Transp. Res. Procedia*, vol. 22, no. 2016, pp. 541–550, 2017.
- [129] B. Coifman, M. McCord, R. G. Mishalani, M. Iswalt, and Y. Ji, "Roadway traffic monitoring from an unmanned aerial vehicle," *IEE Proc. - Intell. Transp. Syst.*, vol. 153, no. 1, pp. 11–20, 2006.
- [130] A. Puri, "A Survey of Unmanned Aerial Vehicles (UAV) for Traffic Surveillance," *Dep. Comput. Sci. Eng. Univ. South Florida*, pp. 1–29, 2005.
- [131] K. Kanistras, G. Martins, M. J. Rutherford, and K. P. Valavanis, "A Survey of Unmanned Aerial Vehicles (UAVs) for Traffic Monitoring," *Handb. Unmanned Aer. Veh.*, pp. 2643–2666, 2015.
- [132] R. Ke, Z. Li, S. Kim, J. Ash, Z. Cui, and Y. Wang, "Real-Time Bidirectional Traffic Flow Parameter Estimation from Aerial Videos," *IEEE Trans. Intell. Transp. Syst.*, vol. 18, no. 4, pp. 890–901, 2017.
- [133] E. N. Barmponakis, E. I. Vlahogianni, and J. C. Golias, "Extracting kinematic characteristics from unmanned aerial vehicles," in *Transportation Research Board 95th Annual Meeting*, 2016, pp. 16–3429.
- [134] K. Choi, I. Lee, J. Hong, T. Oh, and S. W. Shin, "Developing a UAV-based rapid mapping system for emergency response," *Unmanned Syst. Technol. XI*, vol. 7332, no. April 2009, p. 733209, 2009.

- [135] B. Coifman, M. McCord, R. G. Mishalani, and K. Redmill, "Surface transportation surveillance from unmanned aerial vehicles," *Proc. 83rd Annu. Meet. Transp. Res. Board*, 2004.
- [136] C. M. Farmer, "Relationship of traffic fatality rates to maximum state speed limits," *Traffic Inj. Prev.*, vol. 18, no. 4, pp. 375–380, 2017.
- [137] L. S. Friedman, P. Barach, and E. D. Richter, "Raised speed limits, case fatality and road deaths: A six year follow-up using ARIMA models," *Injury Prevention*, vol. 13, no. 3, pp. 156–161, 2007.
- [138] L. Wu, Y. Ci, J. Chu, and H. Zhang, "The influence of intersections on fuel consumption in urban arterial road traffic: A single vehicle test in Harbin, China," *PLoS One*, vol. 10, no. 9, pp. 1–11, 2015.
- [139] T. Satiennam, A. Seedam, T. Radpukdee, W. Satiennam, W. Pasangtiyo, and Y. Hashino, "Development of on-road exhaust emission and fuel consumption models for motorcycles and application through traffic microsimulation," *J. Adv. Transp.*, vol. 2017, 2017.
- [140] R. Tay, "Speed Cameras Improving Safety or Raising Revenue?," *J. Transp. Econ. Policy*, vol. 44, no. 2, pp. 247–257, 2010.
- [141] A. Van Benthem, "What is the optimal speed limit on freeways?," *J. Public Econ.*, vol. 124, pp. 44–62, 2015.
- [142] L. Walter and J. Broughton, "Effectiveness of speed indicator devices: An observational study in South London," *Accid. Anal. Prev.*, vol. 43, no. 4, pp. 1355–1358, 2011.
- [143] Q. Xu, F. Shao, T. Guo, and L. Gong, "The Effects of Campus Bump on Drivers' Fixation Dispersion and Speed Reduction," *Math. Probl. Eng.*, vol. 2015, pp. 1–8, 2015.
- [144] Ambulance Service of NSW, "Vehicle and Stretcher Dimensions," 2017.
- [145] "2019 Toyota Hiace Slwb Automatic 3.0L 4D Van," [Online]. Available: <https://www.whichcar.com.au/detail/2019-toyota-hiace/55738>, p. Retrieved, March 2019.
- [146] "Vehicles - NSW Ambulance," [Online]. Available: <http://www.ambulance.nsw.gov.au/about-us/Vehicles.html>, p. Retrieved, March 2019.
- [147] "DJI Phantom 4 Pro," [Online]. Available: <https://www.dji.com/au/phantom-4-pro>, p. Retrieved, April 2019.
- [148] A. Walha, A. Wali, and A. M. Alimi, "Video Stabilization for Aerial Video Surveillance," *AASRI*

Procedia, vol. 4, pp. 72–77, 2013.

- [149] C. Huang, W. Chen, M. H. Ma, C. Lai, and F. Lin, “Ambulance utilization in metropolitan and rural areas in Taiwan,” *J. Formos. Med. Assoc.*, vol. 100, no. 9, pp. 581–586, 2001.
- [150] E. Seow, H. P. Wong, A. Phe, and T. Tock, “The pattern of ambulance arrivals in the emergency department of an acute care hospital in Singapore,” *Emerg. Med. J.*, vol. 18, no. 4, pp. 297–299, 2001.
- [151] P. T. Pons, E. E. Moore, J. M. Cusick, M. Brunko, B. Antuna, and L. Owens, “Prehospital venous access in an urban paramedic system—a prospective on-scene analysis,” *J. Trauma*, vol. 28, no. 10, pp. 1460–1463, 1988.
- [152] R. L. Wears and C. N. Winton, “Load and go versus stay and play: Analysis of prehospital IV fluid therapy by computer simulation,” *Ann. Emerg. Med.*, vol. 19, no. 2, pp. 163–168, 1990.
- [153] C. M. Slovis, E. W. Herr, D. Londorf, T. D. Little, B. R. Alexander, and R. J. Guthmann, “Success rates for initiation of intravenous therapy en route by prehospital care providers,” *Am. J. Emerg. Med.*, vol. 8, no. 4, pp. 305–307, 1990.
- [154] S. E. Jones, T. P. Nesper, and E. Alcouloumre, “Prehospital intravenous line placement: A prospective study,” *Ann. Emerg. Med.*, vol. 18, no. 3, pp. 244–246, 1989.
- [155] C. McGuire-Wolfe, “A previously unidentified risk of needlestick injury in the emergency medical services setting,” *Am. J. Infect. Control*, vol. 42, no. 3, p. 325, 2014.
- [156] M. Lynagh, R. Burton, and R. Sanson-Fisher, “A systematic review of medical skills laboratory training: Where to from here?,” *Med. Educ.*, vol. 41, no. 9, pp. 879–887, 2007.
- [157] F. Lund *et al.*, “Effectiveness of IV cannulation skills laboratory training and its transfer into clinical practice: A randomized, controlled trial,” *PLoS One*, vol. 7, no. 3, 2012.
- [158] R. S. Jones, A. Simmons, G. L. Boykin, D. Stamper, and J. C. Thompson, “Measuring Intravenous Cannulation Skills of Practical Nursing Students Using Rubber Mannequin Intravenous Training Arms,” *Mil. Med.*, vol. 179, no. 11, pp. 1361–1367, 2014.
- [159] A. Macnab, Y. Chen, F. Gagnon, B. Bora, and C. Laszlo, “Vibration and noise in paediatric emergency transport vehicles: a potential cause of morbidity?,” *Aviat. Space. Environ. Med.*, vol. 66, pp. 212–219, 1995.
- [160] X. Sun, S. Byrns, I. Cheng, B. Zheng, and A. Basu, “Smart Sensor-Based Motion Detection System for Hand Movement Training in Open Surgery,” *J. Med. Syst.*, vol. 41, no. 2, 2017.

- [161] B. Song *et al.*, “Feasibility Study of a Sensor-Based Autonomous Load Control Exercise Training System for COPD Patients,” *J. Med. Syst.*, vol. 39, no. 1, 2015.
- [162] C. Bernad, A. Laspalas, D. González, J. L. Núñez, and F. Buil, “Transport Vibration Laboratory Simulation: On the Necessity of Multiaxis Testing,” *Packag. Technol. Sci.*, vol. 24, no. 1, pp. 1–14, 2011.
- [163] F. Xu, C. Li, and T. Jiang, “On the Shaker Simulation of Wind-Induced Non-Gaussian Random Vibration,” *Shock Vib.*, vol. 2016, pp. 1–10, 2016.
- [164] M. Garcia-Romeu-Martinez, S. P. Singh, and V. Cloquell-Ballester, “Measurement and analysis of vibration levels for truck transport in Spain as a function of payload, suspension and speed,” *Packag. Technol. Sci.*, vol. 21, pp. 439–451, 2008.
- [165] P. Böröcz, Á. Mojzes, and P. Csavajda, “Measuring and Analysing the Effect of Openings and Vibration on Reusable Pharmaceutical Insulated Boxes with Daily Distribution,” *J. Appl. Packag. Res.*, vol. 7, no. 2, pp. 32–44, 2015.
- [166] E. Levenberg, “Estimating vehicle speed with embedded inertial sensors,” *Transp. Res. Part C Emerg. Technol.*, vol. 46, pp. 300–308, 2014.
- [167] X. Zhao *et al.*, “Displacement monitoring technique using a smartphone based on the laser projection-sensing method,” *Sensors Actuators, A Phys.*, vol. 246, pp. 35–47, 2016.
- [168] A. Depari, A. Flammini, S. Rinaldi, and A. Vezzoli, “Multi-sensor system with Bluetooth connectivity for non-invasive measurements of human body physical parameters,” *Sensors Actuators, A Phys.*, vol. 202, pp. 147–154, 2013.
- [169] M. Covarrubias, M. Bordegoni, and U. Cugini, “A hand gestural interaction system for handling a desktop haptic strip for shape rendering,” *Sensors Actuators, A Phys.*, vol. 233, pp. 500–511, 2015.
- [170] A. Ferraz, V. Carvalho, J. Machado, and J. Brito, “Mechatronic system for performing blood pre-transfusion tests,” *Sensors Actuators, A Phys.*, vol. 246, pp. 81–90, 2016.
- [171] D. McMorran, D. C. K. Chung, J. Li, M. Muradoglu, O. W. Liew, and T. W. Ng, “Adapting a Low-Cost Selective Compliant Articulated Robotic Arm for Spillage Avoidance,” *J. Lab. Autom.*, vol. 21, no. 6, pp. 799–805, 2016.
- [172] U. Eryilmaz, H. Sancar Tokmak, K. Cagiltay, V. Isler, and N. O. Eryilmaz, “A novel classification method for driving simulators based on existing flight simulator classification standards,”

- Transp. Res. Part C Emerg. Technol.*, vol. 42, pp. 132–146, 2014.
- [173] F. E. Grubbs, “Sample Criteria for Testing Outlying Observations,” *Ann. Math. Stat.*, vol. 21, no. 1, pp. 27–58, 2007.
- [174] S. Ballesteros-Peña, G. Vallejo-De la Hoz, and I. Fernández-Aedo, “Pain scores for venipuncture among ED patients,” *Am. J. Emerg. Med.*, vol. 35, no. 4, pp. 653–654, 2017.
- [175] G. Wulf, C. Shea, and R. Lewthwaite, “Motor skill learning and performance: A review of influential factors,” *Med. Educ.*, vol. 44, no. 1, pp. 75–84, 2010.
- [176] W. C. McGaghie, S. B. Issenberg, E. R. Petrusa, and R. J. Scalese, “Effect of practice on standardised learning outcomes in simulation-based medical education,” *Med. Educ.*, vol. 40, no. 8, pp. 792–797, 2006.
- [177] L. N. Petz *et al.*, “Prehospital and En Route Analgesic Use in the Combat Setting: A Prospectively Designed, Multicenter, Observational Study,” *Mil. Med.*, vol. 180, no. 3S, pp. 14–18, 2015.
- [178] V. A. Reva, T. M. Hörer, A. I. Makhnovskiy, M. V. Sokhranov, I. M. Samokhvalov, and J. J. DuBose, “Field and en route resuscitative endovascular occlusion of the aorta,” *J. Trauma Acute Care Surg.*, vol. 83, no. 1, pp. S170–S176, 2017.
- [179] M. J. El Sayed and E. Zaghrini, “Prehospital Emergency Ultrasound: A Review of Current Clinical Applications, Challenges, and Future Implications,” *Emerg. Med. Int.*, vol. 2013, pp. 1–6, 2013.